

**CIRCADIAN LIGHT EVALUATION OF A SPACE EQUIPPED WITH CLEAR GLASS WINDOW AND OPTIMIZED SHADE VERSUS LOW-E GLASS WINDOW WITHOUT SHADE**

**BY**

**Habib Arjmand Mazidi**

Submitted to the graduate degree program in Architectural Engineering and the Graduate Faculty of the University of Kansas in partial fulfillment of the requirements for the degree of Master of Science.

---

Chairperson Dr. Hongyi Cai

---

Dr. Mario A. Medina

---

Dr. Brian Rock

Date Defended:

The Thesis Committee for Habib Arjmand Mazidi

Certifies that this is the approved version of the following thesis:

**CIRCADIAN LIGHT EVALUATION OF A SPACE EQUIPPED WITH CLEAR GLASS WINDOW AND OPTIMIZED SHADE VERSUS LOW-E GLASS WINDOW WITHOUT SHADE**

---

Chairperson Dr. Hongyi Cai

Date approved:

## ABSTRACT

The aim of this research was investigating the effect of (i) Low-E glazing window and (ii) clear glass window equipped with optimized shade on the circadian light distribution across an interior space. To that end, computer simulations were conducted in the Grasshopper® for Rhino® plugins to evaluate the circadian light of a simulated office space located in Topeka, KS. For this purpose, five cases were studied: a clear glass window (89% visible light transmittance (VT)) with optimized shade (the baseline case), three different low-E glass windows (65%, 53%, and 39% VTs) all without shade (test cases), and a clear glass window (89% VT) without shade (the reference case). The simulations were conducted on four different days (March 20, June 21, September 20, and December 21) at three times per day (10 a.m., 1 p.m., and 5 p.m.) for four orientations (south, east, north, and west) and under two sky conditions. The circadian light data were converted to the circadian stimulus (CS) [1] and evaluated based on the total and Useful Circadian Light Frequency (UCLF).

In contrast to total circadian light, the UCLF evaluation indicated that, on average, the optimized shade cases contributed to higher UCLF than Low-E glazing window cases at north and west orientations under clear sky condition (49.9% and 41.5.1% of maximum 66%) and south and north orientations under overcast sky condition (39.3% and 39.1% of maximum 65%) respectively.

In conclusion, this study supports the favorable design of optimized shades for the clear glass window in both south and north orientations for their contributions to the interior circadian light in comparison with the Low-E glazing windows with VTs below 65%.

## **ACKNOWLEDGEMENTS**

Undoubtedly, this master's thesis would not be possible without help and support of several people and sectors. I would like to express my great appreciation to Dr. Hongyi Cai who knowledgeable and constantly advised me during my master's thesis and provided several lighting courses as foundations for this study. I appreciate the committee members, Dr. Mario Medina and Dr. Brian Rock, for their time and attention. Thanks to Ms. Farzaneh Mahlab, a PhD student, who helped me in some parts of my study with some worthwhile discussions.

I should also acknowledge the Environmental Studies Program (under the Department of Geography) for providing me a teaching position, which financially supported my entire master's program.

To my family, and my wife who gave me the ultimate motivation to pursue this master's program with a sincere dedication.

# TABLE OF CONTENTS

ABSTRACT.....	III
ACKNOWLEDGEMENTS.....	IV
TABLE OF CONTENTS.....	V
LIST OF FIGURES .....	VII
LIST OF TABLES.....	XII
TERMINOLOGY .....	XIII
CHAPTER 1: INTRODUCTION.....	1
CHAPTER 2: BACKGROUND.....	4
2.1    INDOOR ENVIRONMENTAL QUALITIES (IEQ).....	4
2.2    PHOTOBIOLOGY AND DAYLIGHT IN INTERIOR SPACE.....	4
2.2.1    Visual aspect of daylight.....	5
2.2.2    Non-visual aspect of daylight; circadian light .....	8
2.3    CIRCADIAN LIGHT AND DAYLIGHTING STRATEGIES .....	20
2.3.1    Shading design.....	20
2.3.1    Fenestration system.....	22
2.4    MODELLING PHOTOPIC AND CIRCADIAN ILLUMINANCE.....	25
2.4.1    Current daylight simulation software.....	26
2.4.2    Material reflectance.....	29
2.4.3    Glazing system.....	30
CHAPTER 3: METHODOLOGY.....	34
3.1    THE SPACE INFORMATION .....	34
3.1.1    Architectural elements and dimensions .....	34
3.1.2    Surface materials.....	35
3.1.3    Glazing materials .....	35
3.2    WINDOW-TO-WALL RATIO (WWR).....	40
3.3    OPTIMIZED SHADING DESIGN BASED ON THERMAL DEMAND .....	40

3.3.1	Geographical location and climate data .....	40
3.3.2	Shading Zone .....	41
3.4	CIRCADIAN LIGHT COMPUTER SIMULATION METHOD .....	64
3.4.1	Lark® characteristics .....	65
3.4.2	Simulation input.....	67
3.4.3	Running the simulations.....	70
3.4.4	Simulation output.....	71
3.5	CIRCADIAN LIGHT CONVERSION .....	71
3.6	USEFUL CIRCADIAN LIGHT FREQUENCY (UCLF).....	72
3.6.1	UCLF equation development .....	74
CHAPTER 4: RESULTS AND DISCUSSIONS .....		76
4.1	RESULTS .....	76
4.1.1	Circadian illuminance for points 1 & 3.....	76
4.1.2	Useful Circadian Light Frequency (UCLF) .....	85
4.3	Circadian light availability based on the distance from window .....	87
4.2	DISCUSSIONS .....	96
4.2.1	Total circadian light received at Point 1 and 3.....	96
4.2.2	Circadian light distribution across the space.....	98
4.2.3	The effect of distance from window .....	100
4.2.4	Linear regression analysis and uniformity .....	100
CHAPTER 5: CONCLUSIONS AND RECOMMENDATIONS .....		105
5.1	CONCLUSIONS .....	105
5.2	RECOMMENDATIONS .....	106
REFERENCES .....		107
APPENDIX A: SURFACE MATERIALS' REFLECTANCE INFORMATION .....		113
APPENDIX B: UCLF DATA TABLES.....		119

## LIST OF FIGURES

<b>Figure 1:</b> Electromagnetic spectrum showing visible light. Image courtesy of <a href="http://www.luxes.es">www.luxes.es</a> .....	5
<b>Figure 2:</b> The scotopic ( $S\lambda$ ) (related to dim light vision) and the photopic ( $V\lambda$ ) curves of spectral luminous efficacy (non-normalized values). Image courtesy of 2018 Webvision: The Organization of the Retina and Visual System. ....	6
<b>Figure 3:</b> A simplified illustration of the retino-hypothalamic tract. Image source Uthayan Thurairajah; <a href="http://monsoonjournal.com">http://monsoonjournal.com</a> .....	9
<b>Figure 4:</b> Melanopic spectral sensitivity curve [28]. ....	11
<b>Figure 5:</b> Proposed circadian light sensitivity curve [1]. ....	11
<b>Figure 6:</b> The spectral sensitivity of the human circadian system at two light levels, (a) 300 scotopic lux at the cornea (left) and (b) 300,000 scotopic lux (right) [1]. ....	13
<b>Figure 7:</b> Nocturnal melatonin suppression for different narrowband spectra plotted as a function of $\log_{10}$ CLA (equation (2)) [1]. ....	14
<b>Figure 8:</b> Normalized spectral irradiance profiles for the unfiltered Xe-arc and 480-nm monochromatic stimuli used in an experiment for the Melanopic illuminance evaluation [4]. ....	15
<b>Figure 9:</b> Stimulus response functions for the consensual pupil light reflex elicited by the unfiltered Xe-arc source and a monochromatic 480-nm stimulus [4]. ....	16
<b>Figure 10:</b> Averaged circadian action function $C\lambda$ [5]. ....	17
<b>Figure 11:</b> Normalized efficiency functions for photopic curve (CIE) and circadian curves from Rea et al. and Lucas et al. The vertical red lines demonstrate the Three channels RGB intervals in Radiance, and grey lines demonstrate further divisions for 9 channels (reproduced from [31]) .....	19
<b>Figure 12:</b> Psychometric chart, and the relative comfort zone. Image source: <a href="https://soa.utexas.edu/sites/default/disk/urban_ecosystems/urban_ecosystems/09_03_fa_ferguson_on_raish_ml.pdf">https://soa.utexas.edu/sites/default/disk/urban_ecosystems/urban_ecosystems/09_03_fa_ferguson_on_raish_ml.pdf</a> .....	21
<b>Figure 13:</b> An example of overheated period and further projection on the sun path chart. Image source: <a href="https://slideplayer.com/slide/4282815/">https://slideplayer.com/slide/4282815/</a> .....	21
<b>Figure 14:</b> different regular shading devices and their shading mask projected on sun path chart. ( <a href="http://www.nzeb.in/knowledge-centre/passive-design/shading/">http://www.nzeb.in/knowledge-centre/passive-design/shading/</a> ).....	22
<b>Figure 15:</b> Annual lighting energy consumption in different cases [46]. ....	24
<b>Figure 16:</b> Spectral Transmittance of Selected Tinted Glazing [49]. ....	25
<b>Figure 17:</b> Photopic illuminance (a) and Circadian light (b) measured in two different locations and orientations for four glazing scenarios [49]. ....	25

<b>Figure 18:</b> Graphical definition of a daylight coefficient $DC\alpha(x)$ for point $x$ . Adapted from [52].	27
<b>Figure 19:</b> Backward raytracing. Adapted from [54].	28
<b>Figure 20:</b> Reflectance graphics. Image courtesy of the University of Waikato ( <a href="https://www.sciencelearn.org.nz/images/45-types-of-reflection">https://www.sciencelearn.org.nz/images/45-types-of-reflection</a> ).	30
<b>Figure 21:</b> Transmittance. Graphic credits to Jurohi ( <a href="https://measuretruecolor.hunterlab.com/2013/10/15/bsdf-brdf-btdf/">https://measuretruecolor.hunterlab.com/2013/10/15/bsdf-brdf-btdf/</a> ).	31
<b>Figure 22:</b> Plan view of the space and measurement points.	34
<b>Figure 23:</b> ASHRAE USA climate zones (Image source: <a href="http://www.iaqsource.com/article.php/ashrae-climate-zone-map/?id=194">http://www.iaqsource.com/article.php/ashrae-climate-zone-map/?id=194</a> ).	36
<b>Figure 24:</b> Low-transmittance Low-E glazing, LoE 340 (Produced by the author based on the glazing [56], Rea et. al. C $\lambda$ [34], and CIE V $\lambda$ [58] spectral data).	38
<b>Figure 25:</b> Medium-transmittance Low-E (53%) glazing with CG5323 coating- Produced by the author based on the glazing [56], Rea et. al. C $\lambda$ [34], and CIE V $\lambda$ [58] spectral data.	38
<b>Figure 26:</b> High-transmittance Low-E (65%) glazing with LoE 366 coating- Produced by the author based on the glazing [56], Rea et. al. C $\lambda$ [34], and CIE V $\lambda$ [58] spectral data.	39
<b>Figure 27:</b> Clear (89%) glass with LoE i89 coating- Produced by the author based on the glazing [56], Rea et. al. C $\lambda$ [34], and CIE V $\lambda$ [58] spectral data.	39
<b>Figure 28:</b> Daily temperature history of Topeka, Kansas, 1981-2010 [60].	41
<b>Figure 29:</b> Daily temperature history of Topeka, Kansas, 1980-2016 [63].	42
<b>Figure 30:</b> Hourly May 11 Average temperature history of Topeka, Kansas, 1980-2016 (as an example of derived data) [63].	44
<b>Figure 31:</b> Overheat area of a year, on 12-month schedule (a) and 6-month schedule (b) (matched with sun path chart), based on hourly average temperature history of Topeka, Kansas (1980-2016)	45
<b>Figure 32:</b> Shading zones, highlighted on sun path diagram (the base sun path chart for 38°N is produced through the University of Oregon, Solar Radiation Monitoring Laboratory webpage [64]).	46
<b>Figure 33:</b> The dry-bulb (a), Universal Thermal Climate index (UTCI) (b), and the Effective Temperature (TE) (c) schedules based on the weather file. (Produced through Ladybug® plugin on Grasshopper®).	48
<b>Figure 34:</b> Shading zone from Dec 21 to June 21 (a) and June 21 to Dec 21 (b) based on UTCI, Topeka, KS.	49
<b>Figure 35:</b> Shading zone from Dec 21 to June 21 (a) and Jun 21 to Dec 21 (b) based on TE, Topeka, KS.	50



<b>Figure 36:</b> Shading masks for four orientations; (a) south, (b) east, (c) north, and (d) west. ....	53
<b>Figure 37:</b> Optimized shades for the four orientations; south (a), east (b), north (c), and west (d). ....	55
<b>Figure 38:</b> South orientation illuminance (lux) evaluation; Useful Daylight Illuminance (UDI, 100-2000 lux) for optimized shade case (a), Low-E 65% (b), Low-E 39% (c), and Low-E 53% (d). ....	56
<b>Figure 39:</b> South orientation illuminance (lux) evaluation; Point-in-time (8/01 @ 9:00 am) illuminance for optimized shade case (a), Low-E 65% (b), Low-E 39% (c), and Low-E 53% (d).....	57
<b>Figure 40:</b> East orientation illuminance (lux) evaluation; Useful Daylight Illuminance (UDI, 100-2000 lux) for optimized shade case (a), Low-E 65% (b), Low-E 39% (c), and Low-E 53% (d). ....	58
<b>Figure 41:</b> East orientation illuminance (lux) evaluation; Point-in-time (8/01 @ 8:30 am) illuminance for optimized shade case (a), Low-E 65% (b), Low-E 39% (c), and Low-E 53% (d). ....	59
<b>Figure 42:</b> North orientation illuminance (lux) evaluation; Useful Daylight Illuminance (UDI, 100-2000 lux) for optimized shade case (a), Low-E 65% (b), Low-E 39% (c), and Low-E 53% (d). ....	60
<b>Figure 43:</b> North orientation illuminance (lux) evaluation; Point-in-time (8/01 @ 5:00 pm) illuminance for optimized shade case (a), Low-E 65% (b), Low-E 39% (c), and Low-E 53% (d).....	61
<b>Figure 44:</b> West orientation illuminance (lux) evaluation; Useful Daylight Illuminance (UDI, 100-2000 lux) for optimized shade case (a), Low-E 65% (b), Low-E 39% (c), and Low-E 53% (d). ....	62
<b>Figure 45:</b> West orientation illuminance (lux) evaluation; Point-in-time (8/01 @ 3:00 pm) illuminance for optimized shade case (a), Low-E 65% (b), Low-E 39% (c), and Low-E 53% (d).....	63
<b>Figure 46:</b> Simulation process .....	64
<b>Figure 47:</b> Sky file without (top) and with (bottom) color information. Image adapted from [48]. ....	66
<b>Figure 48:</b> CIE D65 and D95 skies SPD curves. (Produced by the author through Daylight Series excel sheet [69]).....	68
<b>Figure 49:</b> Study Points and direction of views.....	69
<b>Figure 50:</b> An example of extracted 9-channel RGB Radiance material. In contrast with the regular RGB channels, in LARK method, Inanici et al. have arranged the 9-channel from blue (B) channels to red (R) channels, B1, B2, B3, G1, G2, G3, R1, R2, R3. ....	69
<b>Figure 51:</b> Simulation scenarios .....	70
<b>Figure 52:</b> Simulation quality set.....	71
<b>Figure 53:</b> CLA curve based on CS values with highlighted 30% and 60% threshold [1]. ....	72
<b>Figure 54:</b> Circadian illuminance reached to the two office workers locations (points 1 & 3) for 4 study dates from south under clear sky condition. ....	77
<b>Figure 55:</b> Circadian illuminance reached to the two office workers locations (points 1 & 3) for 4 study dates from south under overcast sky condition.....	78

<b>Figure 56:</b> Circadian illuminance reached to the two office workers locations (points 1 & 3) for 4 study dates from east under clear sky condition. ....	79
<b>Figure 57:</b> Circadian illuminance reached to the two office workers locations (points 1 & 3) for 4 study dates from east under overcast sky condition. ....	80
<b>Figure 58:</b> Circadian illuminance reached to the two office workers locations (points 1 & 3) for 4 study dates from North under clear sky condition. ....	81
<b>Figure 59:</b> Circadian illuminance reached to the two office workers locations (points 1 & 3) for 4 study dates from North under overcast sky condition. ....	82
<b>Figure 60:</b> Circadian illuminance reached to the two office workers locations (points 1 & 3) for 4 study dates from west under clear sky condition. ....	83
<b>Figure 61:</b> Circadian illuminance reached to the two office workers locations (points 1 & 3) for 4 study dates from west under overcast sky condition. ....	84
<b>Figure 62:</b> Useful Circadian Light Frequency (UCLF) for south orientation and two sky conditions, clear sky (a) and overcast sky (b) .....	85
<b>Figure 63:</b> Useful Circadian Light Frequency (UCLF) for south orientation and two sky conditions, clear sky (a) and overcast sky (b) .....	86
<b>Figure 64:</b> Useful Circadian Light Frequency (UCLF) for North orientation and two sky conditions, clear sky (a) and overcast sky (b) .....	86
<b>Figure 65:</b> Useful Circadian Light Frequency (UCLF) for west orientation and two sky conditions, clear sky (a) and overcast sky (b) .....	87
<b>Figure 66:</b> Total circadian light availability for south orientation-clear sky condition in three distances from window and two directions of view, window direction (right) and front wall direction (left). The shaded area represents the useful circadian light, 30% to 66%.....	88
<b>Figure 67:</b> Total circadian light availability for south orientation-overcast sky condition in three distances from window and two directions of view, window direction (right) and front wall direction (left). The shaded area represents the useful circadian light, 30% to 65%. ....	89
<b>Figure 68:</b> Total circadian light availability for east orientation-clear sky condition in three distances from window and two directions of view, window direction (right) and front wall direction (left). The shaded area represents the useful circadian light, 30% to 66%.....	90
<b>Figure 69:</b> Total circadian light availability for east orientation-overcast sky condition in three distances from window and two directions of view, window direction (right) and front wall direction (left). The shaded area represents the useful circadian light, 30% to 65%.....	91

<b>Figure 70:</b> Total circadian light availability for north orientation-clear sky condition in three distances from window and two directions of view, window direction (right) and front wall direction (left). The shaded area represents the useful circadian light, 30% to 66%.....	92
<b>Figure 71:</b> Total circadian light availability for north orientation-overcast sky condition in three distances from window and two directions of view, window direction (right) and front wall direction (left). The shaded area represents the useful circadian light, 30% to 65%. ....	93
<b>Figure 72:</b> Total circadian light availability for west orientation-clear sky condition in three distances from window and two directions of view, window direction (right) and front wall direction (left). The shaded area represents the useful circadian light, 30% to 66%.....	94
<b>Figure 73:</b> Total circadian light availability for west orientation-overcast sky condition in three distances from window and two directions of view, window direction (right) and front wall direction (left). The shaded area represents the useful circadian light, 30% to 65%.....	95
<b>Figure 74:</b> Average total circadian light for point 1 and 3, the locations of two office workers.....	98
<b>Figure 75:</b> Average of total circadian light available in the space in different times and conditions. ....	99
<b>Figure 76:</b> Linear regression relation between the case study; (a) optimized shade, (b) Low-E 39%, (c) Low-E 53%, (d) Low-E 65%; and the reference case (clear glass with no shade) at south orientation and under overcast sky condition.....	101
<b>Figure 77:</b> Linear regression relation between the case study; (a) optimized shade, (b) (b) Low-E 39%, (c) Low-E 53%, (d) Low-E 65%; and the reference case (clear glass with no shade) at east orientation and under overcast sky condition.....	102
<b>Figure 78:</b> Linear regression relation between the case study; (a) optimized shade, (b) (b) Low-E 39%, (c) Low-E 53%, (d) Low-E 65%; and the reference case (clear glass with no shade) at north orientation and under overcast sky condition.....	103
<b>Figure 79:</b> Linear regression relation between the case study; (a) optimized shade, (b) (b) Low-E 39%, (c) Low-E 53%, (d) Low-E 65%; and the reference case (clear glass with no shade) at west orientation and under overcast sky condition.....	104
<b>Figure 80:</b> Reflectance information for floor material; Dark Grey Tiles .....	113
<b>Figure 81:</b> Reflectance information for wall material; White Painted Gypsum .....	114
<b>Figure 82:</b> Reflectance information for ceiling material; White Painted Gypsum .....	115
<b>Figure 83:</b> Reflectance information for table material; Wood.....	116
<b>Figure 84:</b> Reflectance information for door material; Brown Wood.....	117
<b>Figure 85:</b> Reflectance information for shading material; Green Aluminum.....	118

## LIST OF TABLES

<b>Table 1:</b> Action factors acv of different light sources [5].....	17
<b>Table 2:</b> Coefficients for Photopic and Circadian Response Functions [31].....	19
<b>Table 3:</b> Reflectance specifications of the space surfaces.....	35
<b>Table 4:</b> ASHRAE 90.1-2016 Prescriptive Fenestration Requirements [47]. ....	36
<b>Table 5:</b> Technical specification of the studied glazing materials.....	37
<b>Table 6:</b> Glazing photopic and circadian efficiencies based on equations 23 and 24. ....	40
<b>Table 7:</b> Average daily maximum temperature normal ( $F^\circ$ ) of Topeka, Kansas [60].....	43
<b>Table 8:</b> Simulation schedule.....	67
<b>Table 9:</b> The relationship between Inanici et al. CL [31] used in this study, Rea et al. CLA and CS [1], and photopic lux based on D95 clear sky (a) and D65 overcast sky (b). ....	73
<b>Table 10:</b> Circadian light frequency scales based on Rea et al. CLA and CS [1], and photopic lux in this study, (a) D65 overcast sky and (b) D95 clear sky.....	74
<b>Table 11:</b> Circadian light differences between point 1 and point 3, the locations of two office workers. The greater negative numbers show the greater differences. ....	97
<b>Table 12:</b> Circadian light uniformity (avg/min) for all scenarios in two sky conditions and different orientations.....	100
<b>Table 13:</b> South orientation useful melatonin suppression for the whole space, and total melatonin suppression for point 1 & 3 under clear sky condition.....	120
<b>Table 14:</b> South orientation useful melatonin suppression for the whole space, and total melatonin suppression for point 1 & 3 under overcast sky condition. ....	121
<b>Table 15:</b> East orientation useful melatonin suppression for the whole space, and total melatonin suppression for point 1 & 3 under clear sky condition.....	122
<b>Table 16:</b> East orientation useful melatonin suppression for the whole space, and total melatonin suppression for point 1 & 3 under overcast sky condition. ....	123
<b>Table 17:</b> North orientation useful melatonin suppression for the whole space, and total melatonin suppression for point 1 & 3 under clear sky condition.....	124
<b>Table 18:</b> North orientation useful melatonin suppression for the whole space, and total melatonin suppression for point 1 & 3 under Overcast sky condition. ....	125
<b>Table 19:</b> West orientation useful melatonin suppression for the whole space, and total melatonin suppression for point 1 & 3 under clear sky condition.....	126
<b>Table 20:</b> West orientation useful melatonin suppression for the whole space, and total melatonin suppression for point 1 & 3 under Overcast sky condition. ....	127

## TERMINOLOGY

<b><i>Circadian Action Factor (<math>\alpha_{cv}</math>):</i></b>	A metric developed to describe the circadian efficiency of the colors of light
<b><i>Circadian Efficiency (<math>C_e</math>):</i></b>	The ratio of transmitted circadian light of a glazing material to the total circadian light
<b><i>Circadian Light (CL), (<math>CL_A</math>):</i></b>	The range of light peak at blue light and responsible for melatonin suppression
<b><i>Circadian Stimulus (CS):</i></b>	A metric proposed by Rea et al. adjusted to melatonin suppression percentage
<b><i>Circadian Transmittance (<math>C_\tau</math>):</i></b>	The fraction of Circadian light transmitted through the window
<b><i>Continuous Daylight Autonomy (CDA):</i></b>	Daylight Autonomy with partial credits for values lower than the minimum illuminance target
<b><i>Correlated Color Temperature (CCT):</i></b>	A method to define light source color appearance
<b><i>Daylight Autonomy (DA):</i></b>	The percentage of a year when minimum illuminance target is met by daylight
<b><i>Daylight Factor (DF):</i></b>	The ratio of internal illuminance to unobstructed horizontal illuminance
<b><i>Illuminance (<math>lm/m^2</math>):</i></b>	Weighted irradiance, or radiant flux incident on a surface area
<b><i>Indoor Environmental Qualities (IEQ):</i></b>	Sets of qualities lead to overall human comfort
<b><i>Intrinsically Photosensitive Retinal Ganglion Cells (ipRGCs):</i></b>	Non-image forming photoreceptors in mammalian eyes system
<b><i>Luminance (<math>cd/m^2</math>):</i></b>	Weighted radiance, or luminous intensity per unit area of a surface
<b><i>Luminous Intensity (cd):</i></b>	Weighted radiant intensity, or radiant flux within a solid angle
<b><i>Melanopic Illuminance (EML):</i></b>	A metric developed by Lucas et al. to evaluate the circadian light
<b><i>Photopic Efficiency (<math>ph_e</math>):</i></b>	The ratio of transmitted photopic light of a glazing material to the total photopic light
<b><i>Photopic Luminous Intensity (<math>V_\lambda</math>):</i></b>	Human spectral response under photopic conditions

<b><i>Photopic Transmittance (<math>Ph_{\tau}</math>):</i></b>	The fraction of Photopic light transmitted through the window.
<b><i>Psychrometric Chart:</i></b>	A graphical representation of the psychrometric processes of air.
<b><i>Reflectance:</i></b>	The ratio of reflected radiant power to incident radiant power
<b><i>Shading Mask:</i></b>	A representation of the sky as viewed from a reference point
<b><i>SHGC:</i></b>	Solar Heat Gain Coefficient
<b><i>Spatial Daylight Autonomy (SDA):</i></b>	A percentage of floor area that exceeds a specified
<b><i>Suprachiasmatic Nuclei (SCN):</i></b>	The master clock in mammals
<b><i>U-factor:</i></b>	The rate of heat loss
<b><i>Useful Circadian Light Frequency (UCLF):</i></b>	A method to define frequent circadian light associated with bearable light
<b><i>Useful Daylight Illuminance (UDI):</i></b>	Climate-based daylight metric predicts annual time-series of absolute illuminance values based on realistic skies
<b><i>Visible Light Transmittance (VT):</i></b>	An optical property that indicates the fraction of visible light transmitted through the window.
<b><i>Visible Light:</i></b>	The visible portion of light spectrum in the range of 380 nm to 780 nm

# CHAPTER 1

## INTRODUCTION

Built environment has an important role in modern human's life. People spend around 87 percent of their life indoors [2]. Furthermore, building energy and indoor environmental qualities (IEQ) are among topics that have drawn more attentions than before. While IEQs (temperature, ventilation, and lighting) are some key factors in building energy consumption, they also affect occupants' health, productivity, and comfort [3].

For decades, human visual perception, which is connected to the visible light spectrum, has been the baseline in lighting specifications. However, some recent discoveries on human non-visual system have introduced circadian light in lighting performance as another aspect of visible light. Human circadian system is most sensitive to shorter wavelengths in the range of blue band. Although there is still no concrete peak wavelength such as what was agreed for photopic light (555 nm), nearly all researchers in this area proposed a wavelength between 450 nm to 490 nm [4, 5, 6].

Daylight as a white light source contains a full range of visible wavelengths and satisfies both photopic and circadian light. This quality encourages architects and lighting designers to harvest daylight in interior spaces. While daylight is a very good source, it is associated with thermal discomfort and glare due to direct sunlight. Consequently, exterior shading and interior blinds have been employed to control undesired sunlight. With developments in glazing materials, Low-E coating has been widely used to supplement or even replace shading system since this kind of material is capable in blocking infrared (IR) wavelengths (responsible for heat gain) and ultraviolet (UV) wavelengths (which can damage interior materials as well as human body tissues).

Undoubtedly, by meeting the ASHRAE 90.1 codes, Low-E glazing reduces the concern of over-exposure of solar heat gain (SHGC), heat loss (U-factor), and UV in the interior space. However, depending on the overall visible light transmittance (VT) of the glazing medium, glare may still be a concern leading to the supplemental use of shading. To prevent glare, glare-control coating material with lower VT is developed to provide a nearly glare-free space. Yet, another concern arises whether the low VT, which is associated with this material, affects annual photopic and circadian light levels in the interior space especially under an overcast sky condition. This issue needs to be clarified when the deployment of low-E glazing window is compared to alternatives such as exterior shading or interior blinds.

Due to characteristics of ever-changing solar position, designing a fixed shade for the entire year, which blocks undesired sunlight, is impossible. Overhang period calculation and shading mask (developed more than six decades ago) are still effective ways to design an optimized shade for buildings especially for the south orientation.

In this thesis, we investigated the impact of different window configurations including clear glass equipped with an optimized shade, clear glass with no shade, and Low-E glass without shade on interior circadian light distribution, for a small virtual office space located in Topeka, KS. The optimized shades are designed based on the thermal need for four different orientations (south-east, south-west, north-west, and north-east) based on the desired building orientation (20° south-east). Three Low-E glazing materials with high, medium, and low VTs were chosen for this study. Circadian measurement is based on computer simulations using Radiance®-based plugins on Grasshopper® for Rhino® in addition to Lark® components [7]. Simulations in this study are conducted on four representative days (solar equinoxes and solar solstices) and three times per day (10 am, 1 p.m., and 5 p.m.) under clear sky and overcast sky conditions. The results were then



converted to the circadian stimulus (CS) metric [1] for further data treatments. The blind schedule was excluded from this study to concentrate on the analysis of Useful Circadian Light Frequency (UCLF).

Going forward, in the chapter 2, the science and literature of the photopic and circadian light, shading, glazing materials, and daylight computer simulation software will be reviewed. The methodology of the study including the simulated space, surface and glazing material choices, optimized shading design process, circadian light computer simulation, and circadian light conversion method will be covered in the chapter 3. The circadian light results from computer simulations based on the four different data treatments followed by the discussions will be presented in the chapter 4. The last chapter will be allocated to the conclusions and recommendations.

## **CHAPTER 2**

### **BACKGROUND**

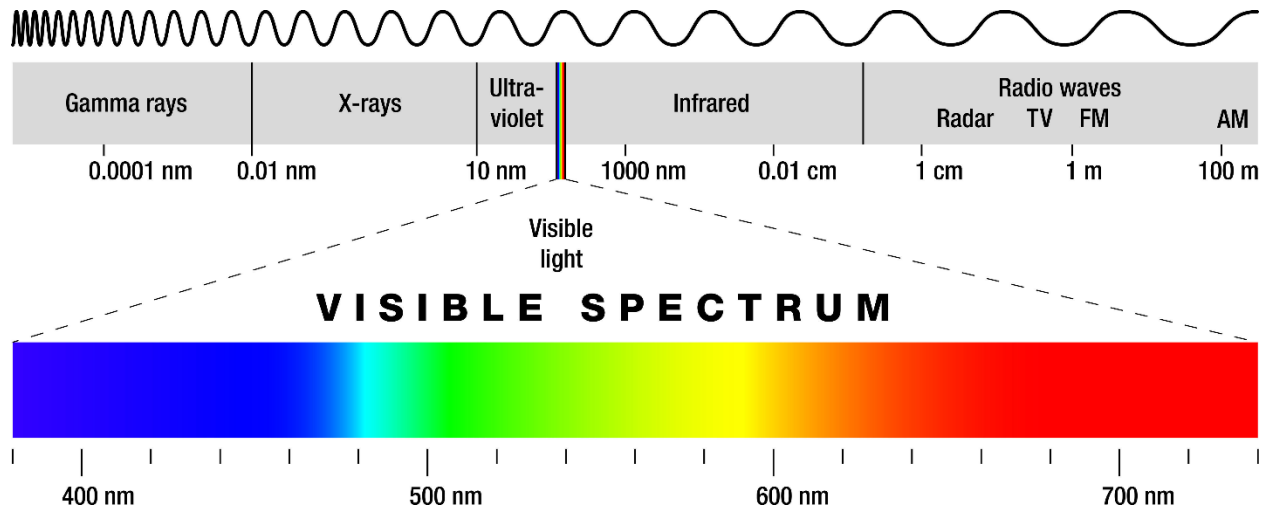
#### **2.1 Indoor Environmental Qualities (IEQ)**

Human performance in an indoor environment is connected to the range of comforts that they experience. Indoor environmental qualities (IEQs) - thermal comfort (temperature), indoor air quality (ventilation), visual comfort (view/lighting), and aural comfort (privacy/acoustic) [8], [9], [10] - propose the main factors in indoor human satisfaction. Human comfort results in both human well-being [11] [12] [13] and human work-productivity [14] [15]. Notwithstanding, human comfort has a complex relationship with the IEQs, and it is difficult to connect them linearly [16]. Each quality can affect the overall human satisfaction differently in each space [10]. Visual comfort is a noticeable aspect of IEQ after thermal and air quality [17] [9]. Humans prefer sitting near windows for some possible reasons such as linking to outside views and/or accessing to natural light with full spectrum [18].

#### **2.2 Photobiology and daylight in interior space**

Daylight and light-dark cycle have had important roles in human's evolution, from skin and hairs pigmentation (to protect human kind from harmful daylight radiation) to visual developments and sensitivities, and recently-discovered circadian rhythm [6]. Daylight available on the earth's surface is based on the solar radiation in the range of 100-4000 nm- visible and none visible to human eyes. The visible portion of the full spectrum, which is known as light, includes electromagnetic radiation in the range of 380 nm to 780 nm. The wavelengths from 100 nm to 400

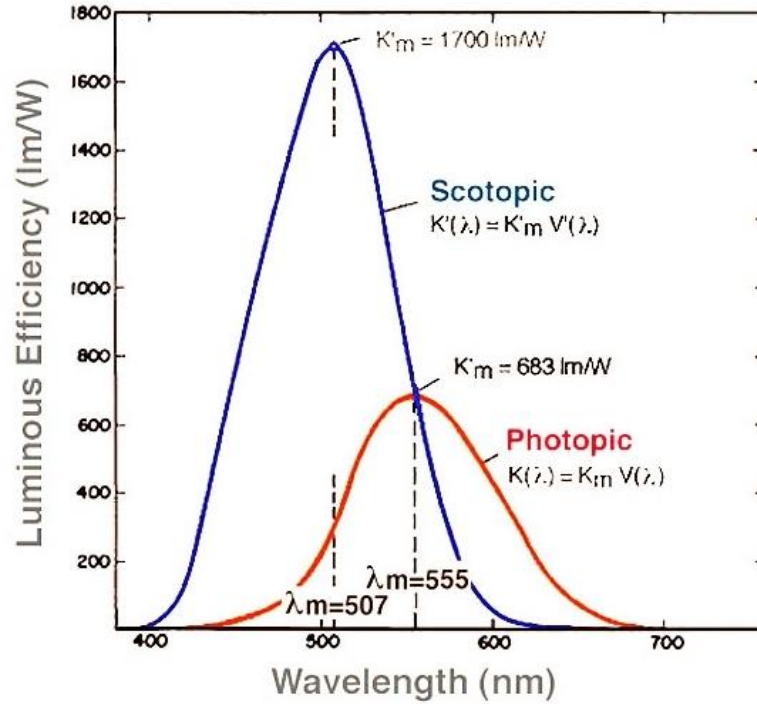
nm are generally called ultraviolet (UV) and are divided to three ranges; UV-C (200-280 nm), UV-B (280-315 nm), and UV-A (315-400 nm). Infrared (IR) radiation is also referred to the wavelengths between 780 nm and 1000 nm [18].



*Figure 1: Electromagnetic spectrum showing visible light. Image courtesy of [www.luxes.es](http://www.luxes.es)*

### 2.2.1 Visual aspect of daylight

By studying the human vision sensitivity (subjective experiments) and converting the results to a Spectral Power Distribution (SPD) curve, Photopic Luminous Intensity ( $V_\lambda$ ) was introduced as a fundamental baseline for luminous intensity, luminance, and illuminance [19]. Through these fundamentals, some daylight metrics have developed as useful tools for architects, engineers, lighting designers, and commissioners. Single-point-in-time Illuminance (SPT), Daylight Factor (DF), Daylight Autonomy (DA), Continuous Daylight Autonomy (CDA), Spatial Daylight Autonomy (SDA), Useful Daylight Illuminance (UDI), Daylight Uniformity, and Daylight Glare Index (DGI) are among commonly used daylight metrics.



**Figure 2:** The scotopic ( $S_{\lambda}$ ) (related to dim light vision) and the photopic ( $V_{\lambda}$ ) curves of spectral luminous efficacy (non-normalized values). Image courtesy of 2018 Webvision: The Organization of the Retina and Visual System.

An example for calculating the photopic lux is as follows:

$$P_{\phi} = 683 \int_{380nm}^{780nm} P_{\lambda} \cdot V_{\lambda} d\lambda \quad (1)$$

Where:

$P_{\phi}$ : Illuminance in lux

683: Photopic luminous efficacy (lm/watt)

$V_{\lambda}$ : photopic spectral sensitivity function

$P_{\lambda}$ : Spectral power (irradiance) ( $W/m^2/nm$ )

### 2.2.1.1 Daylight Factor (DF)

Proposed over 50 years ago, the Daylight Factor (DF) is the ratio of the internal illuminance to the unobstructed horizontal illuminance under CIE overcast sky conditions that is usually shown as a percentage [20]. The DF gives a general report of a daylight conditions in a space. however,

in cases of high illuminance in direct sunlight or sunny sky conditions, the DF cannot be a good factor. In other words, the DF is most useful for locations with overcast skies [21]. Current LEED® (Leadership in Energy and Environmental Design) criteria for the DF in buildings is minimum %2 [20].

#### **2.2.1.2 Daylight Autonomy (DA) and Continuous Daylight Autonomy (CDA)**

The Daylight Autonomy (DA) at a specified work plane location, is expressed as a percentage of a year when the minimum illuminance target is met by the daylight. This factor requires an annual simulation, and this calculation method is classified under dynamic daylight metrics. The minimum illuminance can be derived from the IESNA (Illuminating Engineering Society of North America) recommendation for each task. Early DA metric use dates to a Swiss standard, circa 1989. Variations of the original DA are developed and Continuous DA (CDA) methods such as incremental summing and continuous summing are used to predict daylight performance [21].

#### **2.2.1.3 Spatial Daylight Autonomy (SDA)**

The Spatial Daylight Autonomy (SDA) introduced by IESNA is a daylight illuminance sufficiency for a given space area. It defines a percentage of floor area that exceeds a specified illuminance for a specified percentage of the analysis period (THRESHOLD/N%) [22]. For example, 300 lux/50% means that at least 300 lux daylight must be achieved at least 50% of the occupied hours to consider a space adequately daylit. This can then be reported as daylit area or a percentage of floor area that is daylit [23].

#### **2.2.1.4 Useful Daylight Illuminance (UDI)**

This climate-based daylight metric predicts annual time-series of absolute illuminance values based on realistic skies generated from available climate database. Achieved UDI is then defined as an annual occurrence of illuminances across the work plane for all the illuminances that are in the range of 100 lux to 2000 lux. This range is derived from the reports of occupant preferences and behaviors in daylight offices with user-operated shading devices, and expressed in more details as follow:

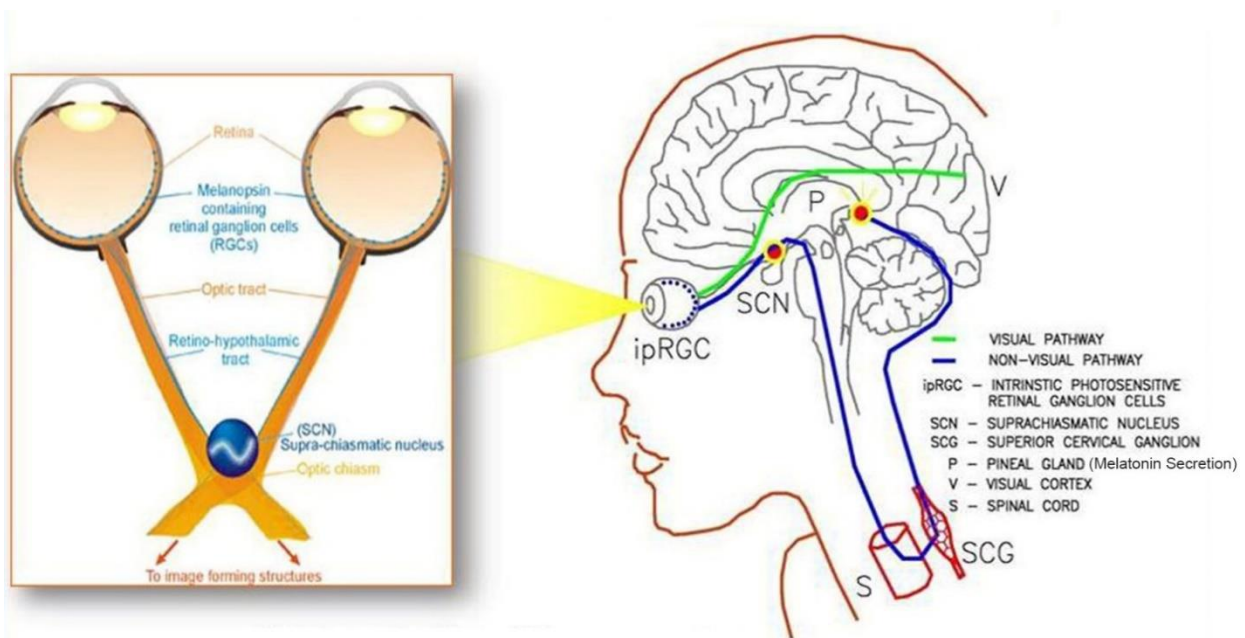
- daylight < 100 lux: Daylight illuminance less than 100 lux is generally considered insufficient since it cannot contribute to a significant lighting condition.
- 100 lux < daylight < 500 lux: Daylight illuminance in the range of 100 lux and 500 lux is considered effective, and it can have a role of primary source of illumination or in conjunction with electrical lighting.
- 500 lux < daylight < 2000 lux: Daylight illuminance between 500 lux and 2000 lux is usually perceived as desirable or at least tolerable.
- daylight > 2000 lux: Daylight illuminance above 2000 lux is likely to produce visual discomfort [24].

Daylight availability and level vary based on the building orientation, window to wall ratio (WWR), shading, glazing material, surface reflectance, etc. Hence, designers evaluate the space daylight through mentioned factors in accordance with the space function, occupancy, aesthetics, energy codes and requirements.

### **2.2.2 Non-visual aspect of daylight; circadian light**

Circadian rhythm in human is a cycle length close to 24 hours even in the absence of periodic environmental stimuli such as light. It is believed that this system is responsible to adapt

physiological and behavioral functions of the human body to the environmental cycles associated with earth's rotation. However, since the timing period of the system is close to, but not exactly, 24 hours, the circadian system must be entrained by external stimuli to the regular basis. Like most organisms, this entrainment occurs in human kind through light-dark (day-night) exposure [25]. Observations of sleep patterns of totally blind people further the idea of human circadian entrainment. Many of blind people complain about cyclic sleep disorder. It means they can sleep through the night and wake up at a time for some time, but after some days or weeks, their sleep patterns are disrupted and not matched with day-night cycle [26].



**Figure 3:** A simplified illustration of the retino-hypothalamic tract. Image source Uthayan Thuraiirajah; <http://monsoonjournal.com>

The effect of light on human circadian system is driven through a non-image-forming system that starts from a newly discovered photoreceptors called retinal ganglion cells (ipRGC). The photopigment in the ipRGC (melanopsin) has a maximum absorption at 480 nm wavelength. The ipRGCs send signals to the suprachiasmatic nuclei (SCN) - the master clock in mammals - of

hypothalamus of the brain (Figure 3). The SCN contribute to synchronizing the timing of different physiological mechanisms in human body such as DNA repair and hormone production. Furthermore, the SCN are connected to the circadian timing system and the awakening system parts in the brain [27].

The human circadian system is comprised of three divisions: internal (endogenous) oscillator located in the SCN; external (exogenous) oscillator located in SCN; and melatonin hormone, which transmits the internal darkness message to all the organisms through the blood. In the lack of light, the internal oscillator still operates, however, with a period of slightly different from the 24-hour cycle. Hence, to entrain the SCN and adjust the sleep-wake to a daily time and all seasons, external stimuli are necessary [27].

Natural light-dark cycle is a potential external stimulus for circadian entrainment shifting either forward or backward. This process occurs through the melatonin suppression. The amount of light required to suppress the melatonin is still being researched by several scientists. Notwithstanding, latest studies proposed peak wavelength in the range of 460 nm [1] (Figure 4) and 480 nm [28] (Figure 5).



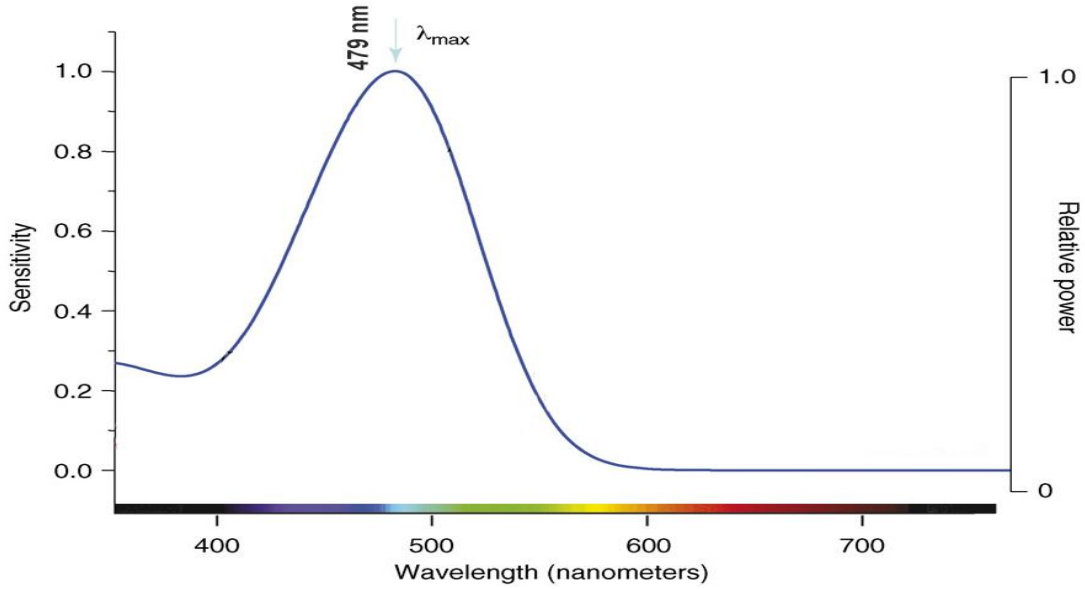


Figure 4: Melanopic spectral sensitivity curve [28].

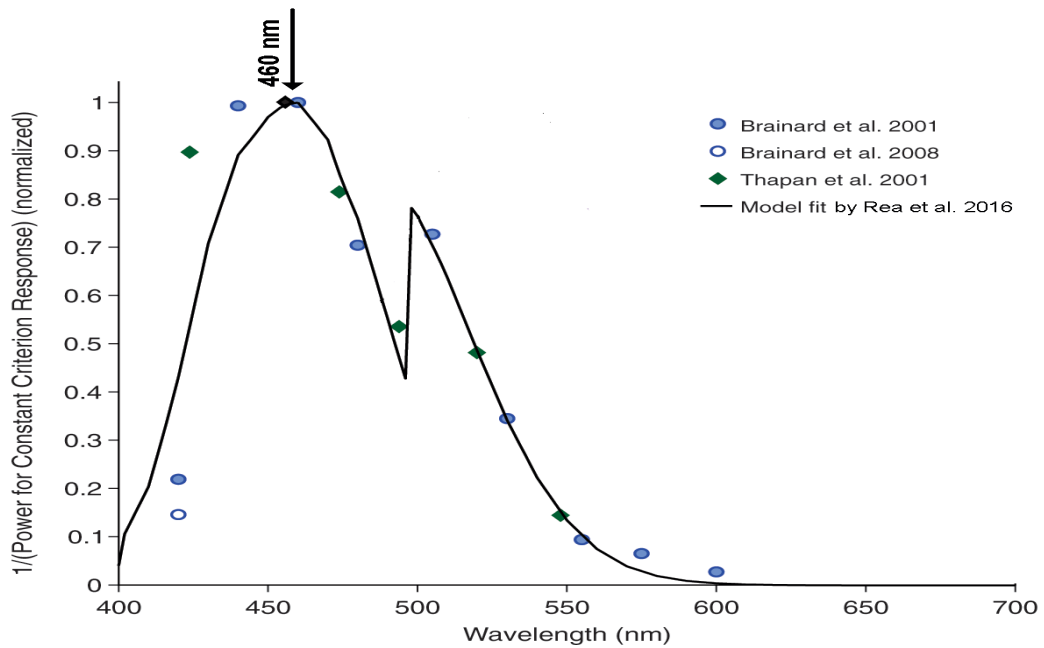


Figure 5: Proposed circadian light sensitivity curve [1].

### 2.2.2.1 Circadian light calculation

By the development in circadian light phenomenon, several scientists accomplished [6, 1, 29, 4, 30, 31, 5] to breakthrough some metrics for estimation of either the effectiveness or the availability of circadian light in a lit space.

## 2.2.2.1 Circadian Light ( $CL_A$ ) and Circadian Stimulus (CS)

These metrics were originally introduced as a model of human circadian phototransduction by Rea et al. [29] based on Brainard et al. [32] and Thapan et al. [33] findings. The Circadian light ( $CL_A$ ) incorporated all the previously-known photoreceptors [rods, L, M, and short-wavelength (S) cones] and ipRGCs into a comprehensive model that accounts for both the spectral sensitivity and the relatively high-threshold response to white light [29]. This model considers the amount of incident light on the retina. The spectral sensitivity is generated to have a stimulus-response function.

$$CL_A = \begin{cases} 1548 \left[ \int Mc_\lambda E_\lambda d\lambda + \left( a_{b-y} \left( \int \frac{S_\lambda}{mp_\lambda} E_\lambda d\lambda - k \int \frac{V_\lambda}{mp_\lambda} E_\lambda d\lambda \right) - a_{rod} \left( 1 - e^{-\frac{\int V'_\lambda E_\lambda d\lambda}{RodSat}} \right) \right) \right] \\ \quad \text{if } \int \frac{S_\lambda}{mp_\lambda} E_\lambda d\lambda - k \int \frac{V_\lambda}{mp_\lambda} E_\lambda d\lambda > 0 \\ 1548 \int Mc_\lambda E_\lambda d\lambda \quad \text{if } \int \frac{S_\lambda}{mp_\lambda} E_\lambda d\lambda - k \int \frac{V_\lambda}{mp_\lambda} E_\lambda d\lambda \leq 0 \end{cases} \quad (2)$$

Where:

$CL_A$ : circadian light. The constant, 1548, sets the normalization of  $CL_A$  so that 2856K blackbody radiation at 1000 lux has a  $CL_A$  value of 1000.

$E_\lambda$ : light source spectral irradiance distribution

$Mc_\lambda$ : melanopsin (corrected for crystalline lens transmittance)

$S_\lambda$ : S-cone fundamental

$mp_\lambda$ : macular pigment transmittance

$V_\lambda$ : photopic luminous efficiency function

$V'_\lambda$ : scotopic luminous efficiency function

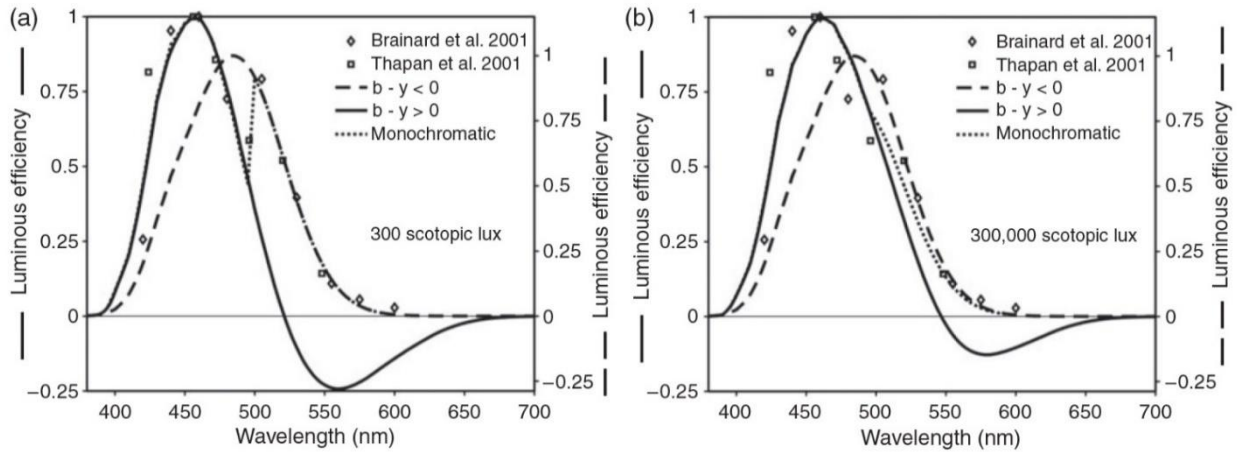
$RodSat$ : half-saturation constant for bleaching rods/46.5W/m<sup>2</sup>

$K = 0.2616$

$a_{b-y} = 0.7000$

$a_{rod} = 3.3000$

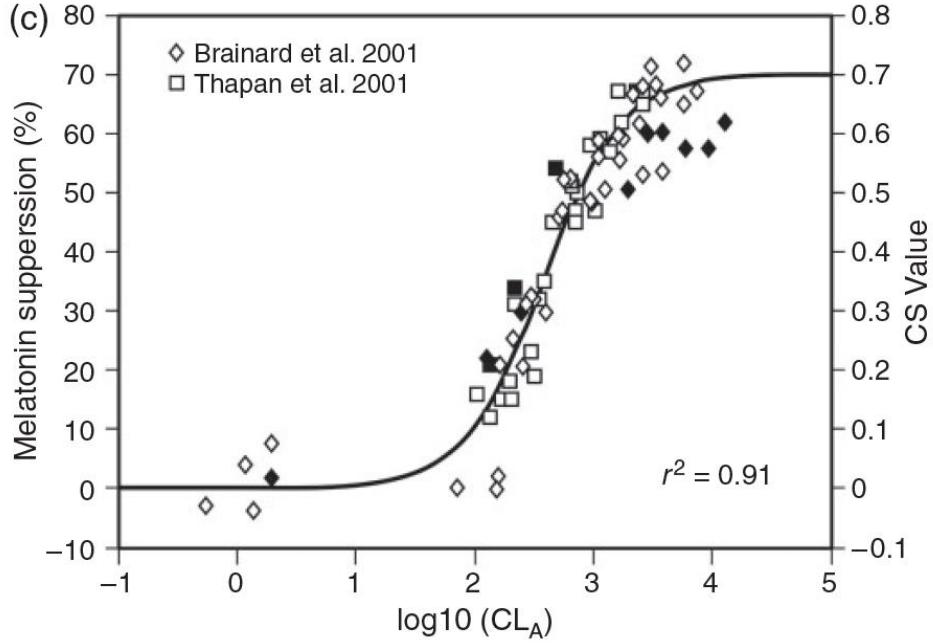
Equation (2) defines the spectral sensitivity of the human circadian system. Circadian light ( $CL_A$ ) advanced from the previous studies [6, 29] by the same authors, is measured in spectrally weighted flux per unit area. Figure 6 shows the spectral sensitivity of the human circadian system for two different light sources - narrowband, ‘cool’ ( $b-y < 0$ ) and ‘warm’ ( $b-y > 0$ ) - for 300 scotopic lux (Figure 6a) and much higher level 300,000 scotopic lux (Figure 6b). Since the rods control absolute sensitivity of the cones, the modelled spectral sensitivity changes with the level of rod saturation; higher light levels result in a change in the overall spectral sensitivity [1].



**Figure 6:** The spectral sensitivity of the human circadian system at two light levels, (a) 300 scotopic lux at the cornea (left) and (b) 300,000 scotopic lux (right) [1].

By plotting the nocturnal melatonin suppression data for  $\log_{10} CL_A$  (Figure 7), circadian stimulus (CS) is introduced through equation (3), which provides a functional way to evaluate the circadian effectiveness of a light source [1].

$$CS = 0.7 - \frac{0.7}{1 + \left(\frac{CL_A}{355.7}\right)^{1.1026}} \quad (3)$$



**Figure 7:** Nocturnal melatonin suppression for different narrowband spectra plotted as a function of  $\log_{10} CL_A$  (equation (2)) [1].

### 2.2.2.1.2 Melanopic illuminance

This method is based on ipRGCs photoreceptors' maximum sensitivity of 480 nm originally conducted and developed by Lucas et al. [28]. By modifying the equation (4) (derived from photopic lux equation (1)), Melanopic illuminance ( $M\phi$ ) was introduced [4].

$$\phi = 5.03 \times 10^{15} \int P_{\lambda} \cdot V_{\lambda} d\lambda \quad (4)$$

Where:

$\phi$ : Photon flux (photons/ $cm^2$ /sec)

P: power ( $W/cm^2/nm$ )

$\lambda$ : wavelength (nm)

$$M\phi = 4557 \int P_{\lambda} \cdot V^z_{\lambda} d\lambda \quad (5)$$

Where:

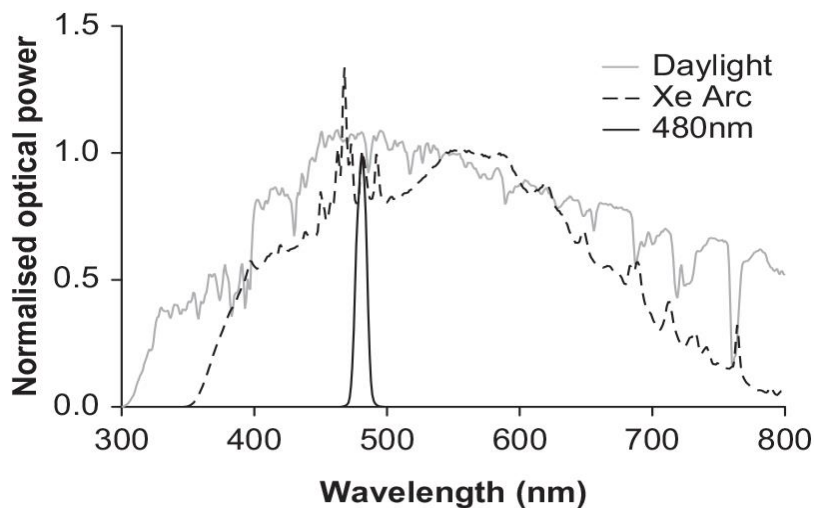
$M\phi$ : Melanopic illuminance

$P_{\lambda}$ : power ( $W/cm^2/nm$ )

$V^z_{\lambda}$ : Melanopic spectral efficiency function

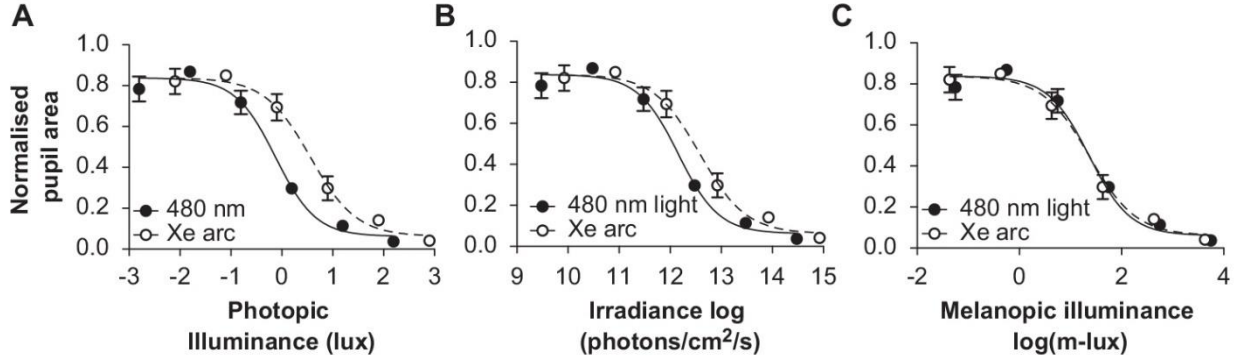
The corrected spectral sensitivity function used as  $V^z_\lambda$  is available online, at <http://lucasgroup.lab.lis.manchester.ac.uk/research/measuringmelanopicillumination/>

The constant (4557) is to ensure that for irradiance at 555 nm, 1 Melanopic lux equals to 1 photopic lux for a normal observer [4].



**Figure 8:** Normalized spectral irradiance profiles for the unfiltered Xe-arc and 480-nm monochromatic stimuli used in an experiment for the Melanopic illuminance evaluation [4].

The Melanopic illuminance was evaluated by projecting two light sources; Xe-arc, a close spectral distribution to mid-day daylight, and a monochromatic 480 nm light (Figure 8); to mice lacking in rods and cones. The results shown in Figure 9 are equally suitable for predicting the ability of these 2 light sources to elicit circadian phase shifts [4].



**Figure 9:** Stimulus response functions for the consensual pupil light reflex elicited by the unfiltered Xe-arc source and a monochromatic 480-nm stimulus [4].

There has been further advancement in Melanopic illuminance [30], which resulted to a well-used metric, Equivalent Melanopic Lux (EML) [30]. An associated Excel sheet for the EML calculation is available at

<http://personalpages.manchester.ac.uk/staff/robert.lucas/Lucas%20et%20al%202014%20workbook.xls>

### 2.2.2.1.3 Circadian Action Factor $a_{cv}$

By the definition of circadian action function  $C_\lambda$  (Figure 10), a simplified metric was developed to describe the circadian efficiency of the colors of light. The circadian radiation quantity  $X_{ec}$  is calculated according to  $C_\lambda$ :

$$X_{ec} = K \int X_{e\lambda} C_\lambda d\lambda \quad (6)$$

Where:

$X_{ec}$  : circadian radiation quantity

$K = 1$

The ratio from the integrals of the circadian and the photometric quantities is called the circadian action factor  $a_{cv}$  [5]:

$$a_{cv} = \frac{\int X_{e\lambda} C_\lambda d\lambda}{\int X_{e\lambda} V_\lambda d\lambda} \quad (7)$$

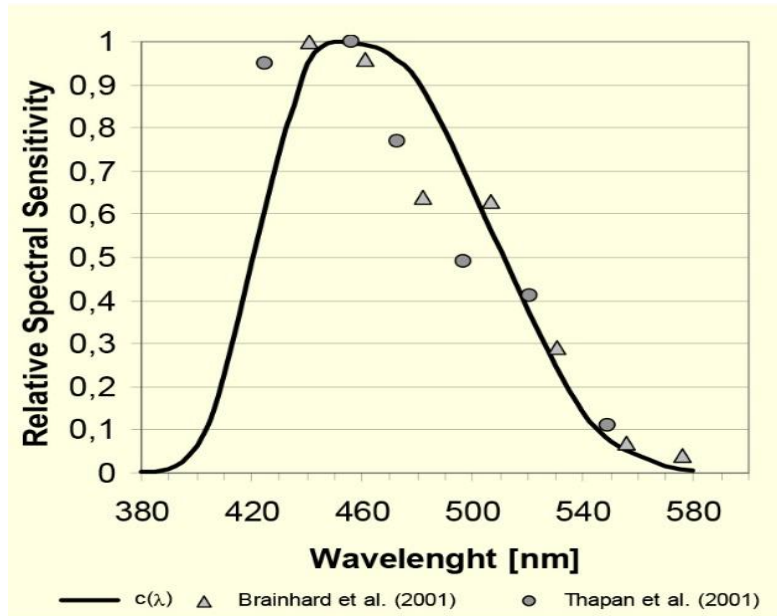


Figure 10: Averaged circadian action function  $C_\lambda$  [5].

Table 1: Action factors  $a_{cv}$  of different light sources [5].

Light Sources	$a_{cv}$ -Value
direct sun 5081 K	0,76
blue sky 19963 K	1,49
cloudy sky 5924 K	0,88
incandescent lamp 2800 K	0,35
HMI 3640 K neutral white, ceramics	0,39
high-pressure sodium lamp 2770 K	0,28
<b>Fluorescent Lamps</b>	
warm white 2827 K	0,31
neutral white 3678 K	0,52
Basic DAYLIGHT 765 6750 K	0,85
LUMILUX DAYLIGHT 865 6400 K	0,80
DELUXE BIOLUX 965 6500 K	0,94
LUMILUX SKYWHITE 880 8000 K	1,00
“Truelite” 5600 K	0,76
<b>Light-Emitting Diodes</b>	
LED blue $\lambda_{max}= 468 \text{ nm}$	6,9
LED white	1,05 .. 2
Maximum (monochromatic 460 nm)	26,3

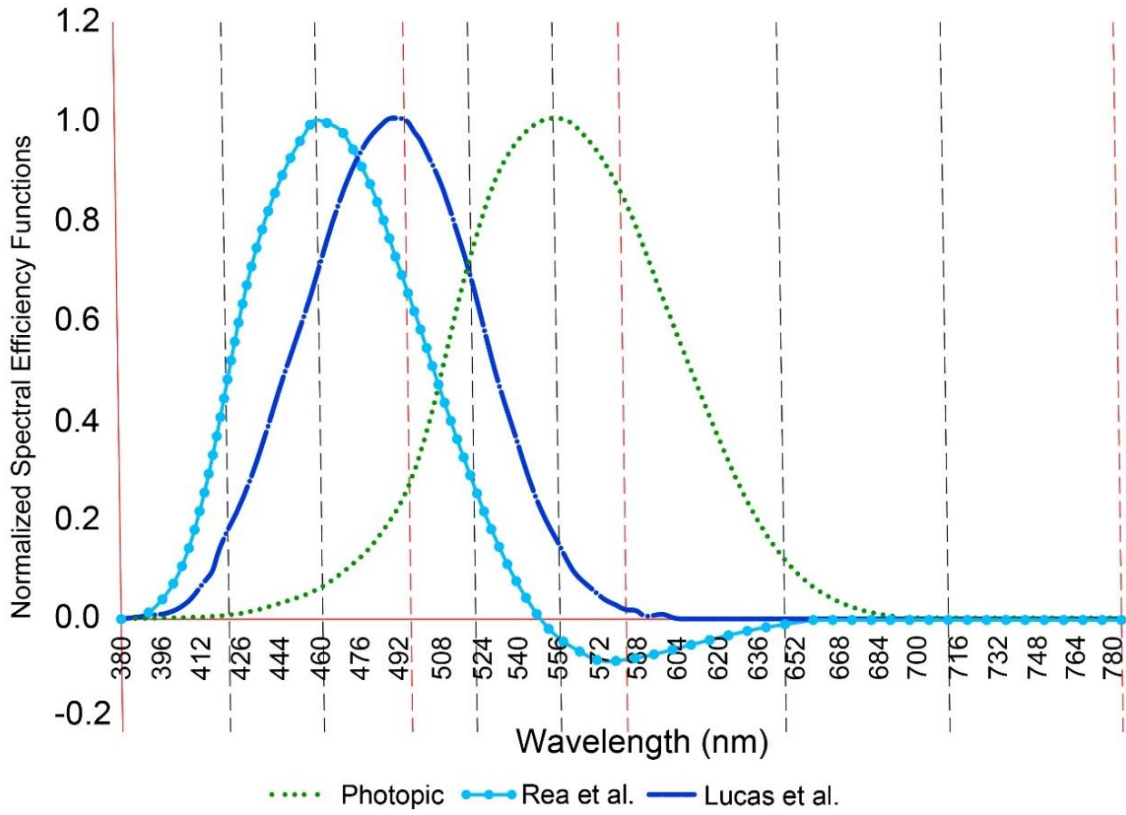
#### 2.2.2.1.4 Circadian illuminance

In this model, which is mainly used for computer simulation, the light source is divided to the Radiance® RGB channels. For each channel, a circadian coefficient is introduced based on Rea et al. [34] and Lucas et al. [30] circadian function curves  $C_\lambda$  (Figure 11). The Equation 8 for luminance and illuminance is then used to calculate circadian illuminance through replacing photopic coefficients by circadian coefficients.

$$L=179*(0.2651*R+0.670*G+0.065*B) \quad (8)$$

The wavelength intervals for a standard three-channel (RGB) in Radiance® are as 380-498 (B), 498-586 (G), and 586-780 nm (R). By dividing each of these primary channels into 3 channels, 9 channel bins are achieved (Figure 11 & Table 2). Having derived further circadian and photopic coefficients for the new 9 channels, it is now possible to calculate photopic-lux and circadian illuminance more accurately (Equations 9 & 10) [31]. The constant value of 179 (lumens/watt) is the standard luminous efficacy of equal energy of white light that is defined and used by Radiance® specifically for this conversion [35]. The luminous efficacy coefficient is further calculated as 130 for the Rea et al. [34] curve and 148 for the Lucas et al. [28] curve [31].





**Figure 11:** Normalized efficiency functions for photopic curve (CIE) and circadian curves from Rea et al. and Lucas et al. The vertical red lines demonstrate the Three channels RGB intervals in Radiance, and grey lines demonstrate further divisions for 9 channels (reproduced from [31])

**Table 2:** Coefficients for Photopic and Circadian Response Functions [31].

	Wavelength	Photopic	Rea et al.	Lucas et al.
B1	380-422	0.0004	0.0669	0.0166
B2	422-460	0.0095	0.394	0.1819
B3	460-498	0.0522	0.4264	0.3973
G1	498-524	0.1288	0.1464	0.2468
G2	524-550	0.2231	0.0362	0.1204
G3	550-586	0.3174	-0.0294	0.0351
R1	586-650	0.2521	-0.038	0.0018
R2	650-714	0.0162	-0.0026	0
R3	714-780	0.0002	0	0

$$\text{Photopic } L=179(0.0004 * B1 + 0.0095 * B2 + 0.0522 * B3 + 0.1288 * G1 + 0.2231 * G2 + 0.3174 * G3 + 0.2521 * R1 + 0.0162 * R2 + 0.0002 * R3) \quad (9)$$

$$\text{Circadian } L=130(0.0669 * B1 + 0.394 * B2 + 0.4264 * B3 + 0.1464 * G1 + 0.0362 * G2 + (-0.0294) * G3 + (-0.038) * R1 + (-0.0026) * R2 + 0 * R3) \quad (10)$$

## 2.3 Circadian light and daylighting strategies

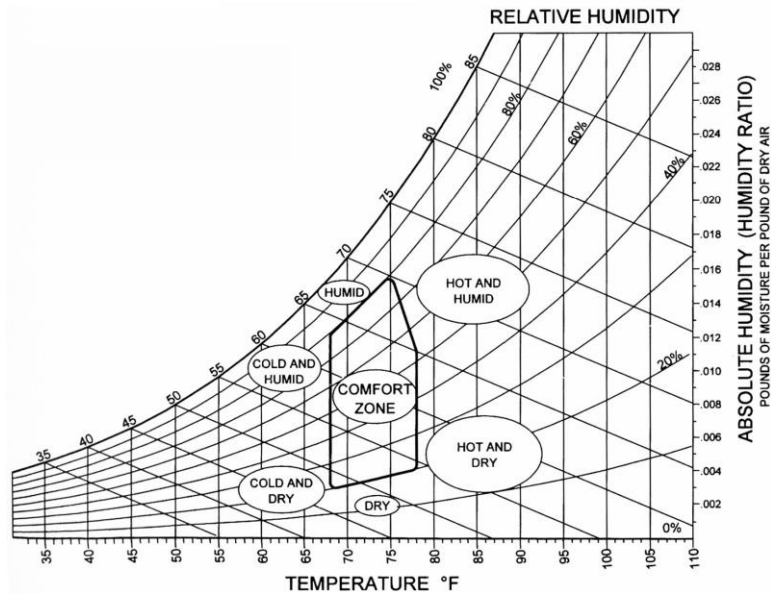
Based on several studies mentioned in this chapter, circadian light is an accepted fact now. Designers and increasing number of clients tend to consider the circadian light in either lighting/daylighting design or lighting commissioning. Recently, International WELL© Building Institute [36] was launched focused on building health and wellness. The WELL© certification has considered the circadian light as one of the requirements in building lighting design. Daylight strategies, including window and shading design, can play an important role in providing a WELL© environment.

### 2.3.1 Shading design

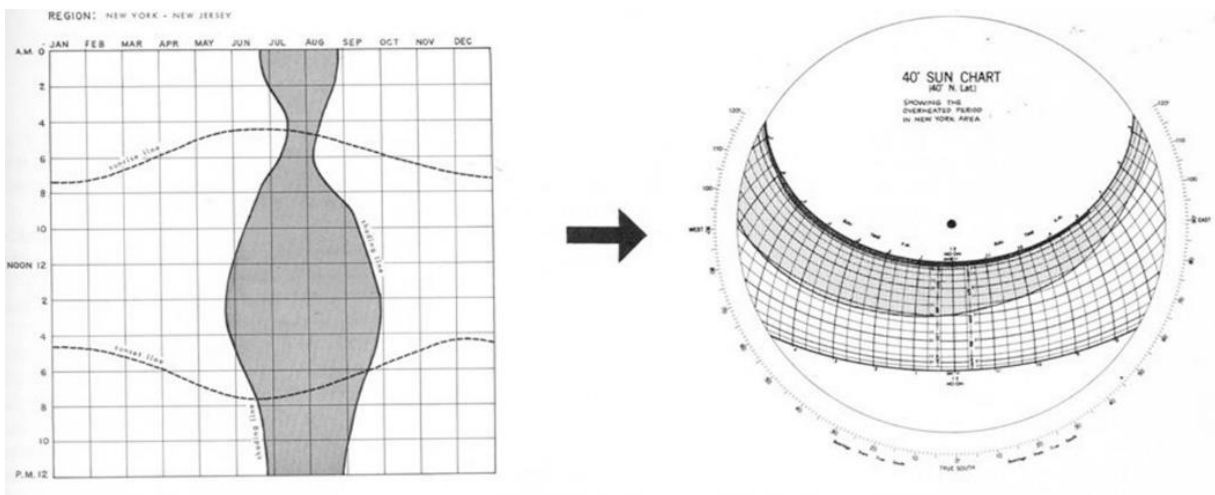
The importance of shading design in interior thermal and lighting control is undeniable according to several studies [37, 38, 39]. Despite accomplishments in shading design, and due to complexities, such as; geographical location, latitude, climate, surrounding environment and buildings, materials, façade design, space occupancy and function, etc., there is still no concrete shading solution for a building. Furthermore, shading properties are not usually provided by manufactures and are estimated using some experimental techniques or advance software [37].

One effective shading design technique is based on shading mask strategy primarily developed by Olgyay [40]. Through Psychrometric Chart (Figure 12), comfort zone for each location is derived as a target. The climate data is then evaluated in courtesy of comfort zone to

produce shading period (overheated period) of which is further projected on the sun path chart as a desired shading mask (Figure 13) [40]. This shading design method is manually doable and has been used by building designers for more than five decades. More recently, some software and tools were developed to ease the procedures of Olgyay shading design method [41] [42].

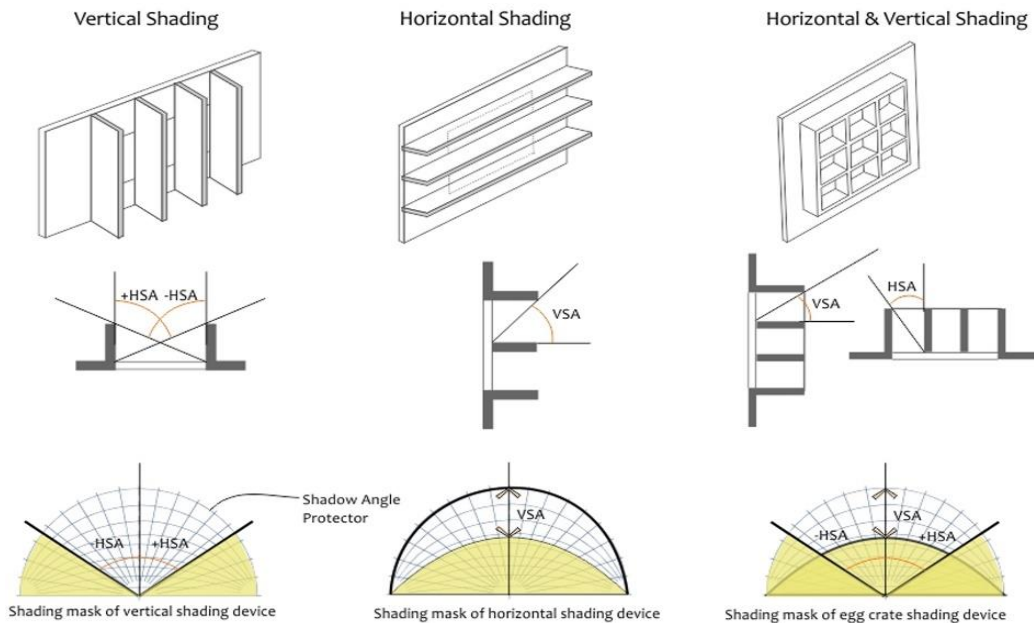


**Figure 12:** Psychrometric chart, and the relative comfort zone. Image source: [https://soa.utexas.edu/sites/default/disk/urban\\_ecosystems/urban\\_ecosystems/09\\_03\\_fa\\_ferguson\\_raish\\_ml.pdf](https://soa.utexas.edu/sites/default/disk/urban_ecosystems/urban_ecosystems/09_03_fa_ferguson_raish_ml.pdf)



**Figure 13:** An example of overheated period and further projection on the sun path chart. Image source: <https://slideplayer.com/slide/4282815/>

Coming to the relationship between shading design and circadian light, there are very few studies [43] that have considered circadian light as one factor among the other daylight metrics.



**Figure 14:** different regular shading devices and their shading mask projected on sun path chart. (<http://www.nzeb.in/knowledge-centre/passive-design/shading/>).

### 2.3.1 Fenestration system

According to the U.S. Energy Information Administration; space heating, ventilation, cooling, and lighting energy in commercial buildings (2012) and residential buildings (2015) in the U.S. account for 54% and 42% (electricity) of total energy consumption respectively [44, 45]. Window, as the main part of building fenestration system, which provides connection to the outside, plays an important role in thermal and illumination level adjustment. Based on the characteristics of glazing materials such as VT, U-factor (the rate of heat loss), and SHGC (solar heat gain coefficient), thermal performance and glare are always some challenging topics in window design [46]. Building geographical latitude (annual solar positions), climate (thermal need

and annual average solar resource), and surrounding environment and buildings (microclimate and shading obstacles) have direct relationship with window design. Solar control glazing materials released by manufactures with different qualities of VT, U-factor, SHGC, and in some cases UV control rate, are to adjust the indoor environmental conditions with the least mechanical and electrical energy consumption. These concerns led to some building codes and recommendations by some national and international organizations such as ASHRAE 90.1 [47] and IESNA Lighting Handbook [48].

The most common-used solar control glazing material is Low-E glass. Although its coating technology is being improved and some manufactures introduced higher VT Low-E glass, yet it has lower VT than clear glass. It also blocks a wide range of IR (infrared) rays (Figures 24-27), which is useful for heating-dominant climates.

#### **2.3.1.1 Low-E glazing vs overhang shading**

Daylighting design (window and possible shading) is a multifactor process and there is no concrete solution for a single space. Nonetheless, some studies have evaluated optimal shading design [39] and glazing performance [46] in buildings in terms of lighting and energy saving. Compared to no-shade and no-solar-control glazing conditions, shading in general contributes to more uniform lighting condition [39]. In case of Low-E glazing window (74% VT without shading), heat gain reduction is about 50%, while this quality is estimated 35-40% for regular overhang application. However, the daylighting performance (lighting energy consumption) of regular overhang shading is similar to that of the Low-E glazing scenario in cooling-dominant regions. It is noticeable that the interior blind does not have consistent results in the four simulated regions in the referred study (Figure 15) [46].

In absolute condition, spectral characteristics of glazing material can have a notable effect on photopic and circadian light level of interior space. A physical model case study by Hartman et al. [49] clearly represents the role of glazing SPDs in interior lighting condition (Figure 16 & 17). The VTs for the four glazing scenarios in this study ranged from 0.57 to 0.90. It is recognizable that despite higher rate in VT, the glazing with stronger spectral in blue light band shows greater circadian light level (Figure 17).

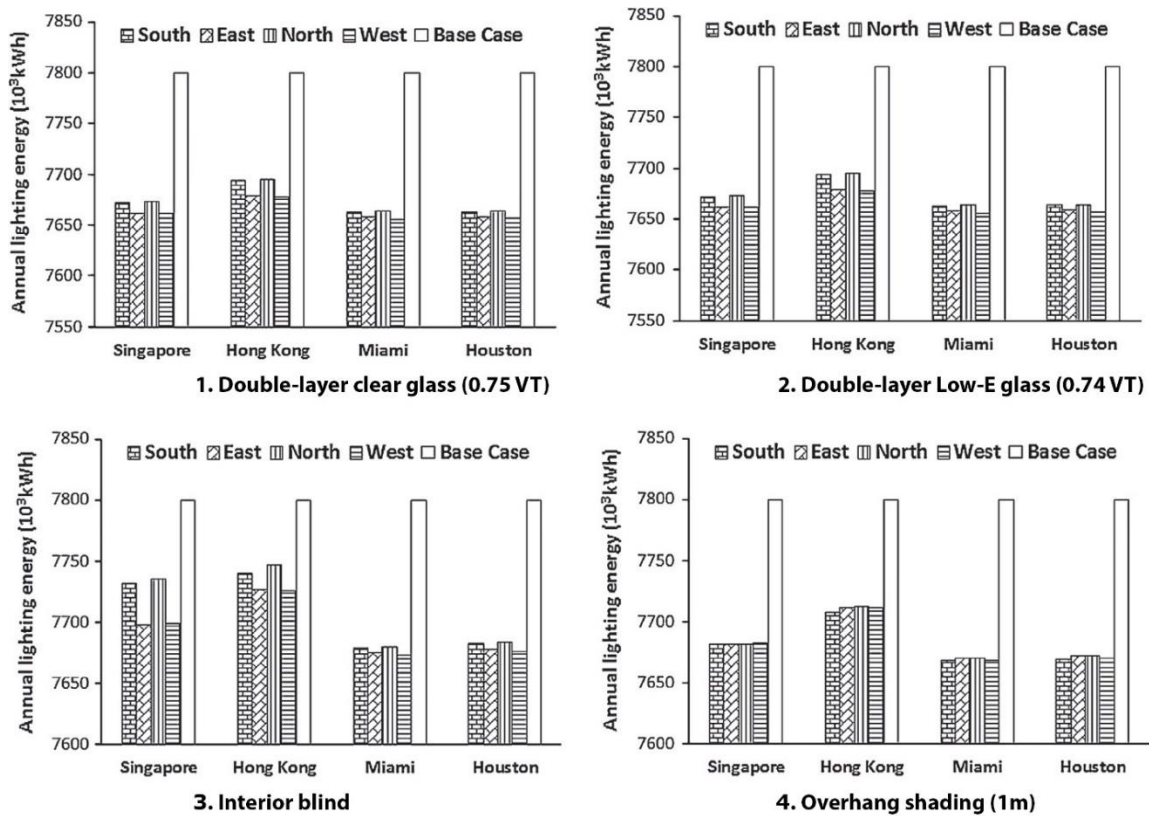
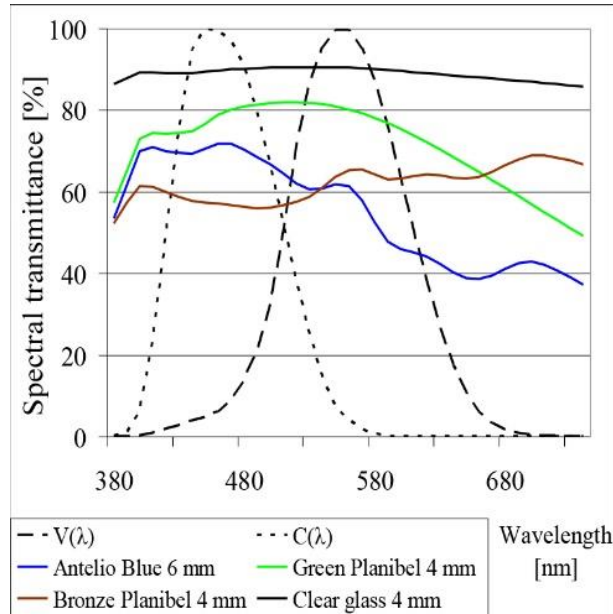
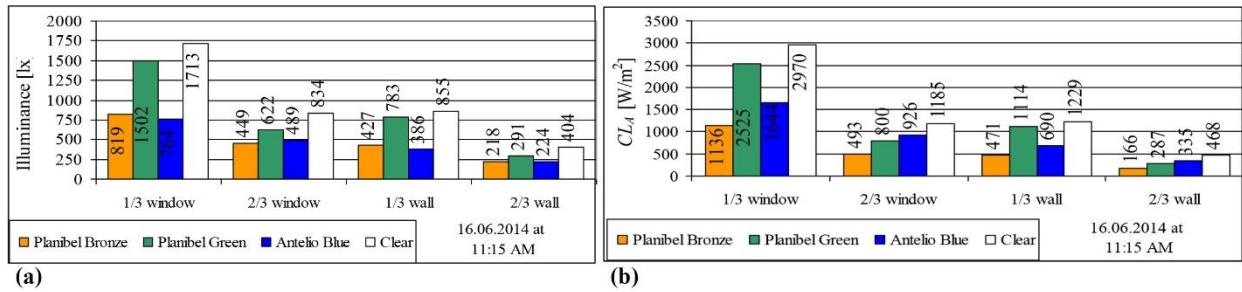


Figure 15: Annual lighting energy consumption in different cases [46].



**Figure 16:** Spectral Transmittance of Selected Tinted Glazing [49].



**Figure 17:** Photopic illuminance (a) and Circadian light (b) measured in two different locations and orientations for four glazing scenarios [49].

## 2.4 Modelling photopic and circadian illuminance

The aim of this thesis has not been developing a new circadian light simulation tool but rather to examine the effect of shading and glazing materials on circadian light distribution. Furthermore, the limitation of the most common software is explained in terms of circadian light

calculation. The Lark® plugin on Grasshopper® as one of the first attempts in circadian light computer simulation [7] and as a baseline for this study is introduced here.

### 2.4.1 Current daylight simulation software

There are several software tools developed for daylight simulation in buildings. Using complex ‘raytracing’ mechanism, the tools implement ‘daylight coefficient method’, and usually are based on the Radiance® engine. The daylight coefficient is a Radiance®-based method originally proposed by Tregenza and Waters [50] and is associated with climate-based sky model developed by Perez et al. [51]. This method is to speed up the calculation of year-round daylight by using a matrix of numbers representing relations between each sky segment and the interior or outside points [52].

#### 2.4.1.1 Dasim® daylight coefficient

Dasim® is a Radiance®-based daylight simulation tool, which works based on the daylight coefficient method. For point  $x$ , daylight coefficient  $DC_\alpha(x)$  is the ratio of the illuminance  $E_\alpha(x)$  of sky segment  $S_\alpha(x)$  to luminance  $L_\alpha$  and the angular size  $\Delta S_\alpha$  (Figure 18).

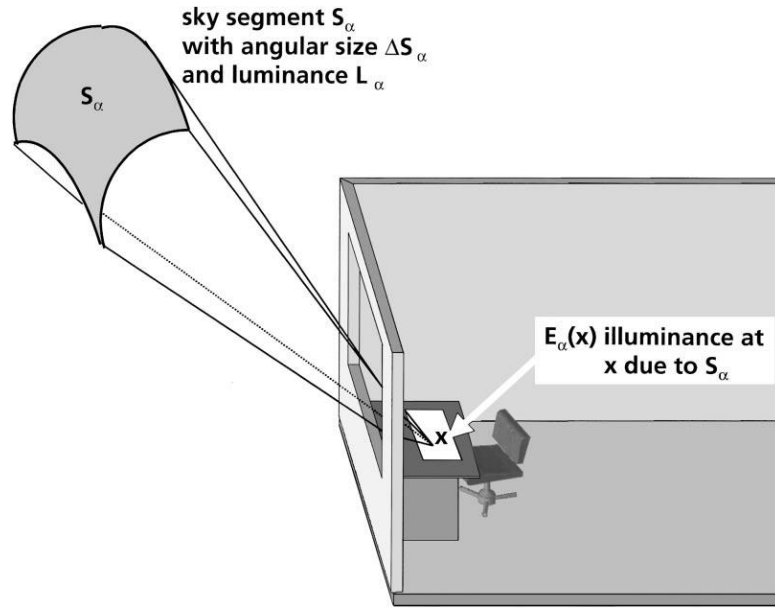
$$DC_\alpha(x) = \frac{E_\alpha(x)}{L_\alpha \Delta S_\alpha} \quad (11)$$

To calculate the total illuminance  $E(x)$  for the point  $x$ , a complete set of daylight coefficients should be added up with an arbitrary sky luminance distribution  $L_\alpha$  ( $\alpha=1, \dots, N$ ) through a simple linear superposition.

$$E(x) = \sum_{\alpha=1}^N DC_\alpha(x) L_\alpha \Delta S_\alpha \quad (12)$$



The Dasim® divides daylight sources to the diffuse daylight, ground reflections, and direct sunlight (Equation 13). The celestial hemisphere is divided to 145 sky segments for the diffuse daylight coefficient, and three ground segments for the ground daylight coefficients. The direct sunlight coefficients are location-based [52].



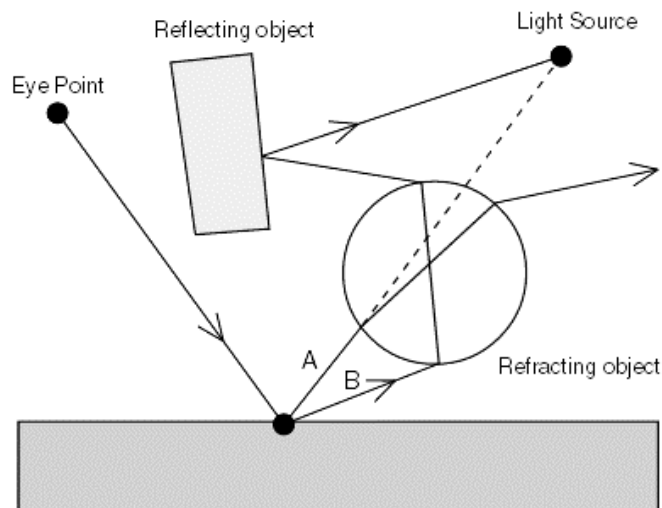
**Figure 18:** Graphical definition of a daylight coefficient  $DC_{\alpha}(x)$  for point  $x$ . Adapted from [52].

$$\begin{aligned}
 E(x) = & \sum_{\alpha=1}^{145} DC_{\alpha}^{diffuse}(x) L_{\alpha}^{diffuse} \Delta S_{\alpha}^{diffuse} \\
 & + \sum_{\alpha=1}^3 DC_{\alpha}^{ground}(x) L_{\alpha}^{ground} \Delta S_{\alpha}^{ground} \\
 & + \sum_{\alpha=1}^{65} DC_{\alpha}^{direct}(x) L_{\alpha}^{direct} \Delta S_{\alpha}^{direct} \quad (13)
 \end{aligned}$$

#### 2.4.1.2 Radiance® raytracing

Backward ‘raytracing’ is a method that the Radiance® uses in light calculation [53]. It depends on sending rays from the analysis position/s to the surrounding environment until it

reaches the light source/s directly or through surfaces' reflection. The Figure 19 shows a simplified diagram of how ray A is deflected away from the light source, while ray B reaches the source but through a complicated path [54].



*Figure 19: Backward raytracing. Adapted from [54].*

### **2.4.1.3 Current software limitation in circadian light simulation**

Current Radiance®-based software tools channelize materials in a simplified RGB channels and does not include spectral sky information in the daylight simulation. Through Dasim®, the sky luminance is calculated and processed into grayscale. As one of the three light sources in the Dasim®, spectral characteristic of the diffuse sky is necessary to calculate the circadian light specially when the analysis point does not receive direct sunlight.

The Lark® components in combination with other plugins, introduce 3-channel and 9-channel spectral sky and material for raytracing. This proposed quality enables raytracing to simulate spectral irradiance.

## 2.4.2 Material reflectance

Reflectance (Figure 20) is defined by the ratio of reflected radiant power to incident radiant power. For a certain area element  $dA$  of reflecting surface, incident radiant power is calculated by surface's irradiance  $E_e$ , multiplied with the size of the surface [55].

$$d\phi_{e,incident} = E_e \cdot dA \quad (14)$$

Reflected radiant power is given by the exitance  $M_e$ , multiplied with the size of the surface.

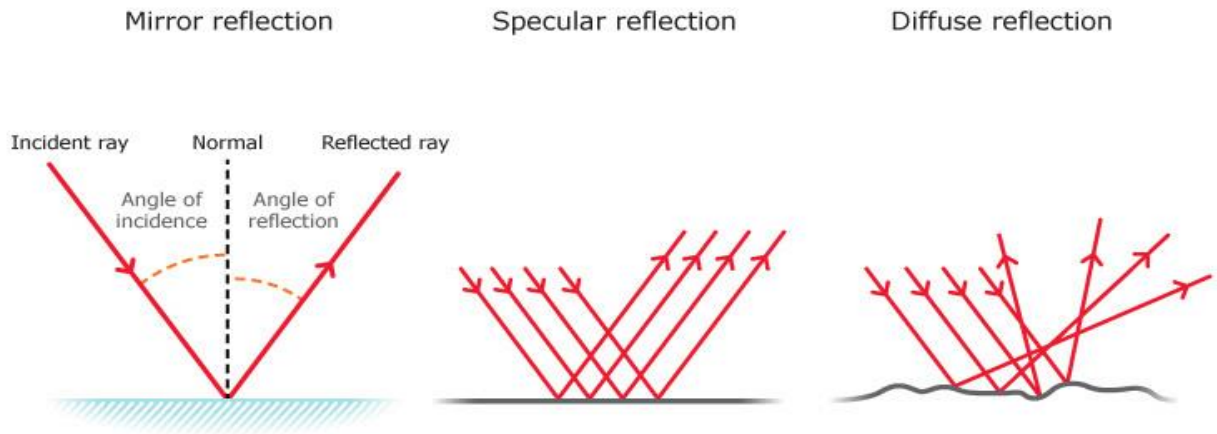
$$d\phi_{e,reflected} = M_e \cdot dA \quad (15)$$

Thus,

$$\rho = \frac{d\phi_{e,reflected}}{d\phi_{e,incident}} = \frac{M_e \cdot dA}{E_e \cdot dA} = \frac{M_e}{E_e} \quad (16)$$

or

$$M_e = \rho E_e \quad (17)$$



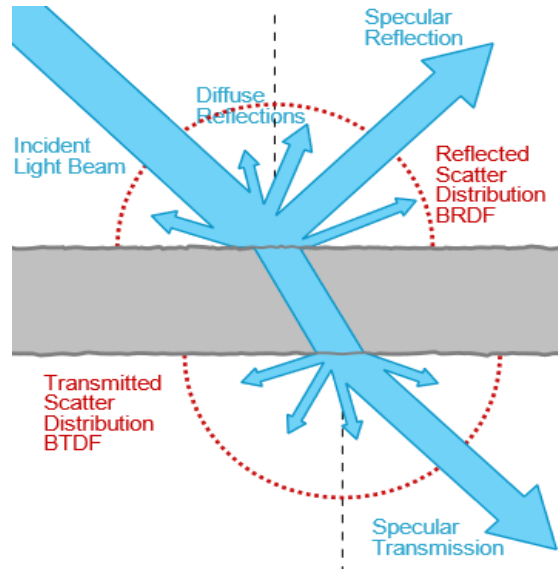
**Figure 20:** Reflectance graphics. Image courtesy of the University of Waikato (<https://www.sciencelearn.org.nz/images/45-types-of-reflection>)

Total reflectance is comprised of the regular reflectance  $\rho_r$  and the diffuse reflectance  $\rho_d$  (the ratio of the specularly plus diffusely reflected radiant powers to incident radiant power) [55].

$$\rho = \rho_r + \rho_d \quad , \quad 0 \leq \rho \leq 1 \quad (18)$$

### 2.4.3 Glazing system

Like reflectance, glazing medium transmittance is defined by the ratio of the transmitted radiant power to the incident radiant power. The transmitted radiant power is given by the exitance  $T_e$ , multiplied with the size of the surface.



**Figure 21: Transmittance.** Graphic credits to Jurohi  
 (<https://measuretruecolor.hunterlab.com/2013/10/15/bsdf-brdf-btdf/>)

$$d\phi_{e,transmitted} = T_e \cdot dA \quad (19)$$

Thus,

$$\tau = \frac{d\phi_{e,transmitted}}{d\phi_{e,incident}} = \frac{T_e \cdot dA}{E_e \cdot dA} = \frac{T_e}{E_e} \quad (20)$$

or

$$T_e = \tau E_e \quad (21)$$

Total transmittance  $\tau$  is subdivided to the regular transmittance  $\tau_r$ , and the diffuse transmittance  $\tau_d$ .

$$\tau = \tau_r + \tau_d \quad (22)$$

Two transmittance ratios, visible light transmittance VT and photopic light transmittance  $Ph_{\tau}$ , are needed to evaluate a glazing medium daylight applicability. The VT is included in the International Glazing Database through Optics6® software developed by Lawrence Berkeley National Laboratory [56] as  $T_{vis}$ . The VT is different from the proposed photopic transmittance  $\rho_{h_{\tau}}$  (Equation 20) and is the ratio of total light in the range of 380 nm to 780 nm wavelengths penetrated through the glazing material to the incident light. Whereas the  $Ph_{\tau}$  is the ratio of transmitted light under  $V_{\lambda}$  curve to the incident photopic light under the same curve.

Based on each wavelength's photopic and circadian light coefficient, the photopic and circadian efficiency (Equations 23 and 24), which can be specifically calculated for each glazing material, are developed here.

The photopic efficiency ratio,  $Ph_e$ , is defined as below:

$$Ph_e = \frac{\int_{380}^{780} Vis_{\lambda} \cdot V_{\lambda}}{\int_{380}^{780} V_{\lambda}} \quad (23)$$

Where,

$Vis_{\lambda}$  is transmitted visible light through glazing material.

Circadian efficiency ratio,  $C_e$ , is also defined with a same strategy:

$$C_e = \frac{\int_{380}^{780} Vis_{\lambda} \cdot C_{\lambda}}{\int_{380}^{780} C_{\lambda}} \quad (24)$$

What we discussed in this chapter intended to expand the knowledge of the reader in terms of daylight and furthermore circadian light in a built environment. The importance of circadian light in human sleep-wake cycle was also highlighted here. In addition, the most common daylight simulation software tools were introduced as a means for this thesis. In the next chapter, the methodology that employed in this thesis will be explained. The simulated space information (dimensions, surface and glazing materials), optimized shading design strategies, computer simulation software tools as well as their inputs and outputs, and lastly, the circadian light analysis methods will be included in the chapter 3.

## CHAPTER 3

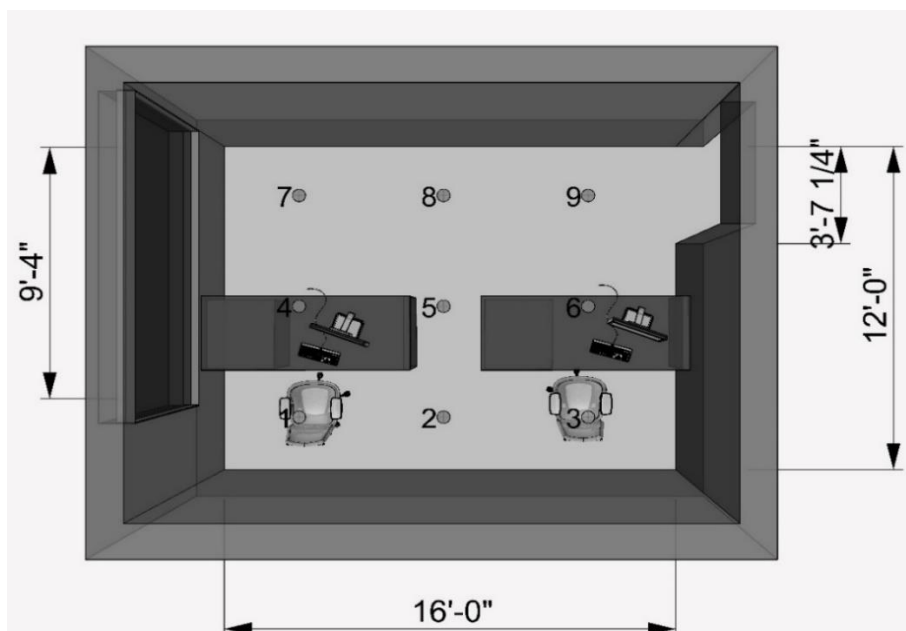
### METHODOLOGY

This thesis is examining a virtual simple office room in Topeka, Kansas, USA with latitude of  $39^\circ$  and longitude of  $-95.7^\circ$ . The circadian rhythm potential of the space was evaluated through computer simulations using the Honeybee®, Ladybug®, and Lark® plugins for Grasshopper® on Rhino®.

### 3.1 The space information

#### 3.1.1 Architectural elements and dimensions

The simulated office is a 12ft \* 16ft \* 10ft (w \* l \* h) room with a 9.3ft \* 5.7ft (l \* h) window on the shorter side (Figure 22). Nine grid points at eye level (two of them are considered the locations of two office workers) are used for the measurement of the circadian light distribution across the space (Figure 22).



*Figure 22: Plan view of the space and measurement points.*



### 3.1.2 Surface materials

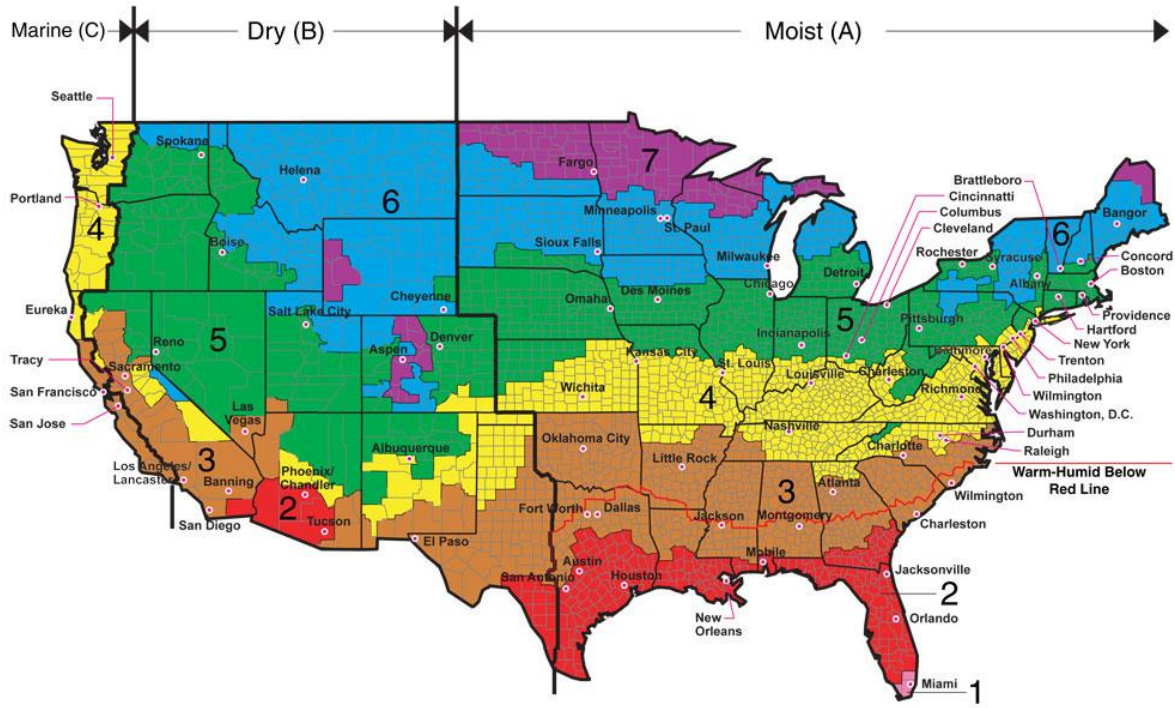
To simulate the office space, the surfaces' reflectance is set in the ranges of 0.2-0.3 for floor, 0.6-0.7 for walls, 0.7-0.8 for ceiling, 0.2-0.3 for furniture, 0.2-0.3 for shading material, and 0.2 for outdoor ground surface. The Lighting Materials for Simulation database [57] developed by Singapore University of Technology and Design was searched and the following materials as well as their reflectance distribution data were employed in this study (Table 3). The full information of the selected materials is available in appendix A.

*Table 3: Reflectance specifications of the space surfaces*

Space surface	Material	R-Reflectance	G-Reflectance	B-Reflectance	Total Reflectance
<b>Floor</b>	Dark grey tiles	20.15%	18.79%	17.16%	20.06%
<b>Wall</b>	White painted gypsum	81.43%	79.84%	71.50%	79.80%
<b>Ceiling</b>	White painted gypsum	84.62%	82.06%	72.63%	82.20%
<b>Tables</b>	Wood	46.28%	26.18%	10.43%	31.87%
<b>Door</b>	Brown wood	52.35%	38.15%	19.30%	41.88%
<b>Shading</b>	Green aluminum	22.78%	29.95%	4.83%	27.96%

### 3.1.3 Glazing materials

Four double-layer glazing materials - three solar heat-control Low-E glazing and one interior-thermal-control glazing with high VT - were chosen for this study. The three Low-E glasses (one low-transmittance (0.39% VT), one medium-transmittance (0.53% VT) , and one high-transmittance (0.65% VT)) met the requirements for maximum SHGC and U-factor of ASHRAE 90.1 standards (Figure 23 & Table 4) for Topeka, KS (zone 4A) [47].



All of Alaska in Zone 7 except for the following Boroughs in Zone 8: Bethel, Dellingham, Fairbanks, N. Star, Nome North Slope, Northwest Arctic, Southeast Fairbanks, Wade Hampton, and Yukon-Koyukuk  
 Zone 1 includes: Hawaii, Guam, Puerto Rico, and the Virgin Islands

Figure 23: ASHRAE USA climate zones (Image source: <http://www.iaqsource.com/article.php/ashrae-climate-zone-map/?id=194>)

Table 4: ASHRAE 90.1-2016 Prescriptive Fenestration Requirements [47].

ASHRAE 90.1-2016 Prescriptive Fenestration Requirements								
Climate Zone	1	2	3	4	5	6	7	8
<b>Vertical Fenestration (0-40% of wall)</b>								
<b>Maximum U-factor</b>								
Non-metal frame	0.5	0.37	0.33	0.31	0.31	0.3	0.28	0.25
Metal frame, fixed	0.57	0.54	0.45	0.38	0.38	0.36	0.33	0.29
Metal frame, operable	0.65	0.65	0.6	0.46	0.46	0.45	0.4	0.35
Metal frame, entrance door	1.1	0.83	0.77	0.68	0.68	0.68	0.68	0.68
<b>Maximum SHGC</b>								
All vertical fenestration	0.25	0.25	0.25	0.36	0.38	0.4	0.45	0.45
<b>Minimum Assembly VT/SHGC</b>								
All vertical fenestration	1.1	1.1	1.1	1.1	1.1	1.1	1.1	1.1
<b>Skylights (0-3% of roof)</b>								
<b>Maximum U-factor</b>								
all skylights	0.75	0.65	0.55	0.5	0.5	0.5	0.5	0.41
<b>Maximum SHGC</b>								
all skylights	0.35	0.35	0.35	0.4	0.4	0.4	NR	NR
<b>Minimum Assembly VT/SHGC</b>								
All skylights	NR	NR	NR	NR	NR	NR	NR	NR

All the glazing cases and their technical information were chosen from the International Glazing Database [56]. The list of final glazing materials are shown in the table 5, obtained from the factories spec-sheets.

*Table 5: Technical specification of the studied glazing materials*

Glazing Type	Glazing Factory	Trade Name	SHGC	U-factor		Visible Light Transmittance	UV Light Transmittance
				Air Fill	Argon Fill		
<b>Low-E 39%</b>	Cardinal Glass	LoE 340	0.18	0.29	0.25	39%	20%
<b>Low-E 53%</b>	Guardian Glass	CG5323	0.23	0.24	0.2	53%	11%
<b>Low-E 65%</b>	Cardinal Glass	LoE 366	0.27	0.29	0.24	65%	5%
<b>Clear glass 89%</b>	Cardinal Glass	LoE i89	0.78	0.48	-	89%	58%

Based on the current climate zone, not all Low-E glazing materials chosen for this study are commonly used in practice. For example, LoE 340 (Low-E 39%) (Figure 24) with SHGC 0.18 is a solar and glare control glass best matched with zone 2 and 3. However, this comparison between low-VT glazing and high-VT glazing can give a better sense of glazing effect.

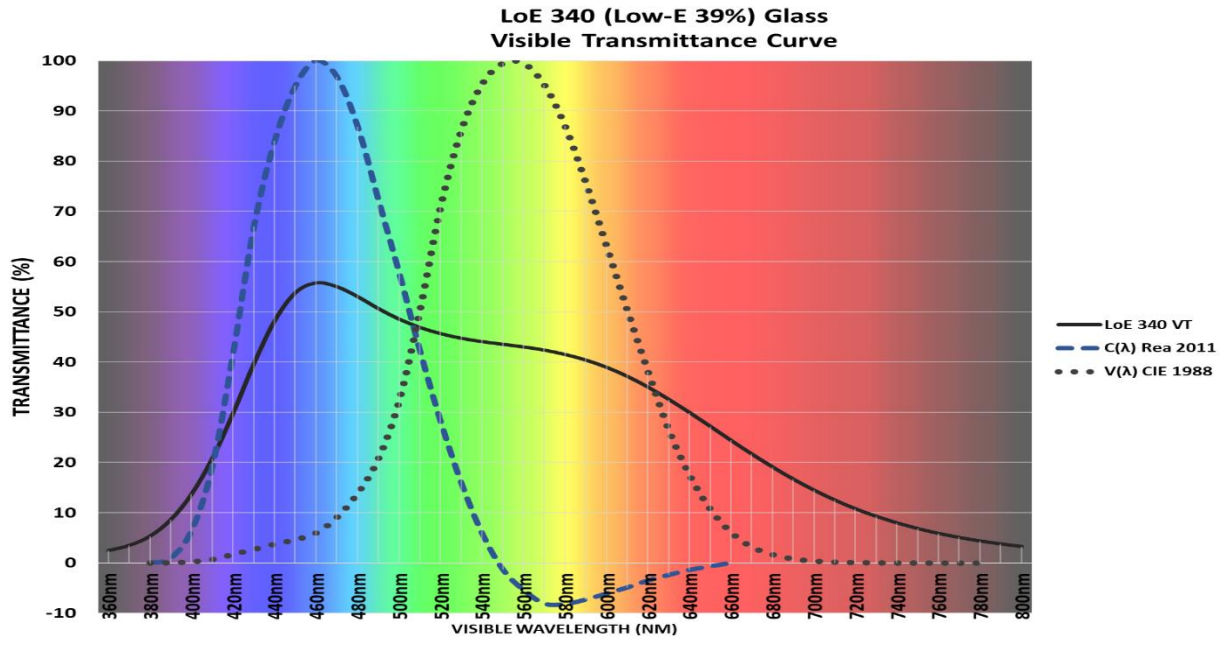


Figure 24: Low-transmittance Low-E glazing, LoE 340 (Produced by the author based on the glazing [56], Rea et. al.  $C_\lambda$  [34], and CIE  $V_\lambda$  [58] spectral data).

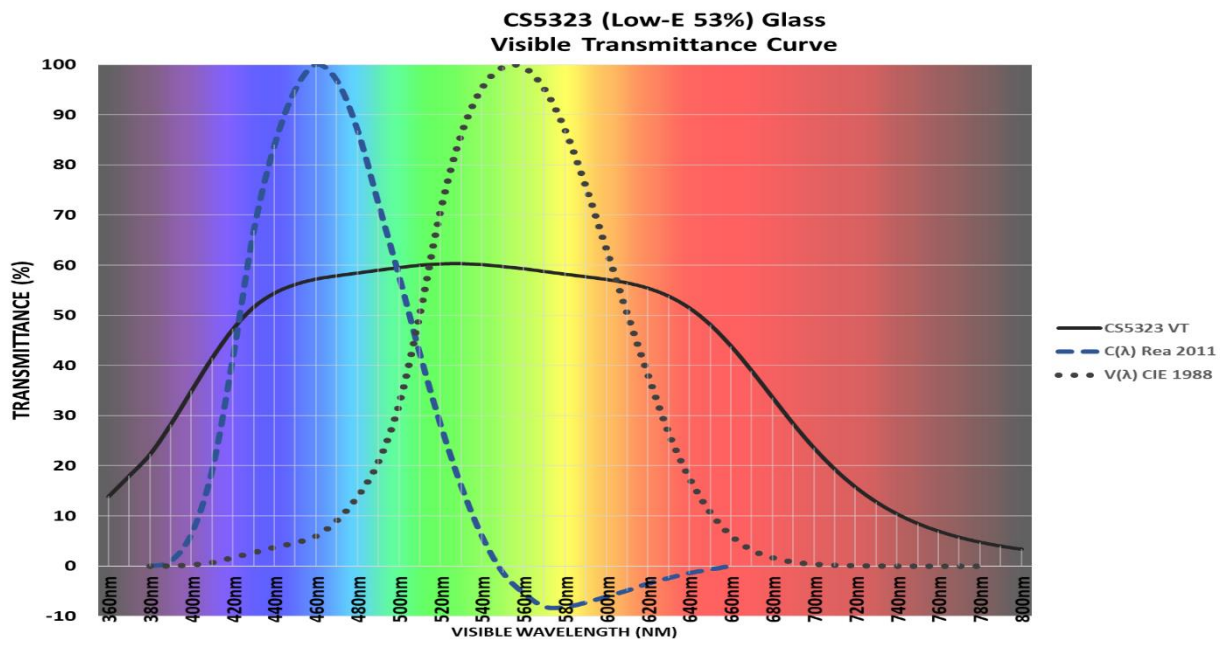


Figure 25: Medium-transmittance Low-E (53%) glazing with CG5323 coating- Produced by the author based on the glazing [56], Rea et. al.  $C_\lambda$  [34], and CIE  $V_\lambda$  [58] spectral data.

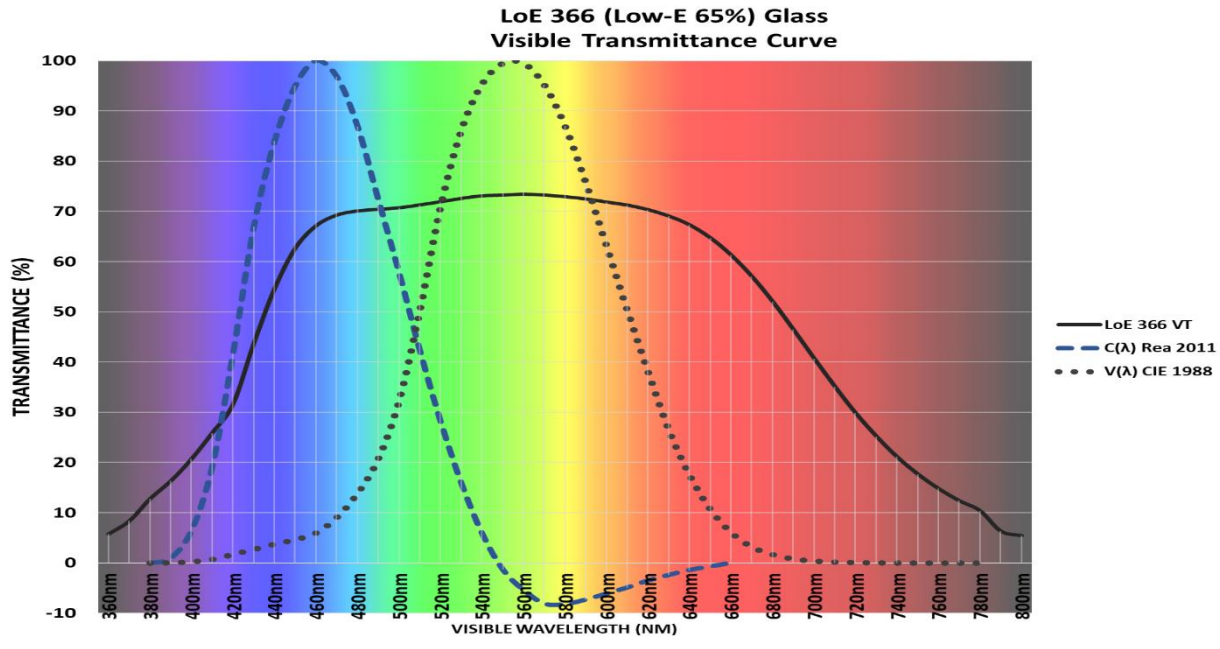


Figure 26: High-transmittance Low-E (65%) glazing with LoE 366 coating- Produced by the author based on the glazing [56], Rea et. al.  $C_{\lambda}$  [34], and CIE  $V_{\lambda}$  [58] spectral data.

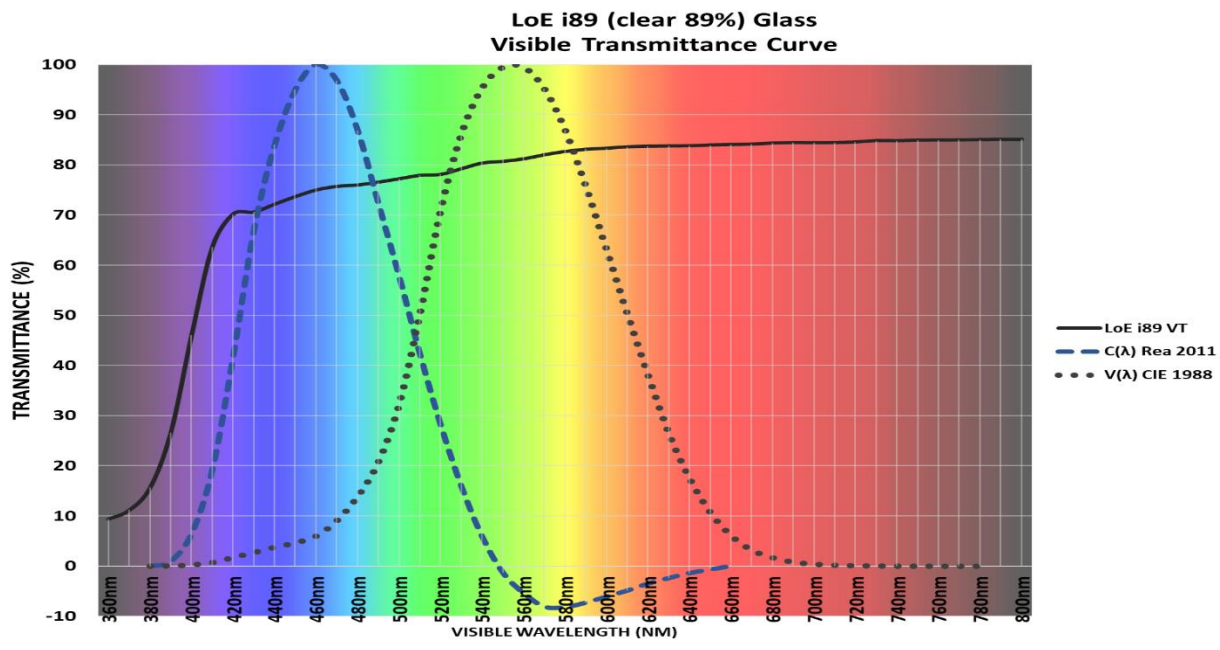


Figure 27: Clear (89%) glass with LoE i89 coating- Produced by the author based on the glazing [56], Rea et. al.  $C_{\lambda}$  [34], and CIE  $V_{\lambda}$  [58] spectral data.

Table 6 represents the differences between visible, photopic, and circadian light efficiencies of the selected glazing materials based on the developed equations 23 and 24. Noteworthy, the photopic and circadian light efficacy of the selected glazing materials are different than their nominal VTs (0.89).

*Table 6: Glazing photopic and circadian efficiencies based on equations 23 and 24.*

Glazing Type	Trade Name	Visible light Transmittance (VT)	Photopic Light Efficiency ( $Ph_e$ )	Circadian Light Efficiency ( $C_e$ )
Low-E 39%	LoE 340	0.39	0.43	0.49
Low-E 53%	CG5323	0.53	0.59	0.56
Low-E 65%	LoE 366	0.65	0.72	0.61
Clear Glass 89%	LoE i89	0.89	0.81	0.74

### 3.2 Window-to-wall ratio (WWR)

According to a study, recommended maximum Window-to-Wall ratio for zone 4A category is 27.55–48.9 percent [59]. The proposed WWR for this space is 44%, which has not exceeded the maximum recommended number.

### 3.3 Optimized Shading Design based on thermal demand

#### 3.3.1 Geographical location and climate data

Topeka, Kansas was chosen as the primary location of the space to design the window and shades and evaluate the space lighting conditions. The closest national weather station in Topeka, Kansas was used to obtain the weather data [60] and file [61]. Two sets of climate data - numerical daily and hourly temperature normal (Figure 28 & Table 7) and the \*.epw weather file (Figures 33(a)-33(c)) - are employed to pinpoint the times when the average temperature exceeds human thermal comfort. This zone is considered as the geographical shading period.

## Daily Climate Normals (1981–2010) – Topeka Area, KS (ThreadEx)



Click and drag to zoom to a shorter time interval

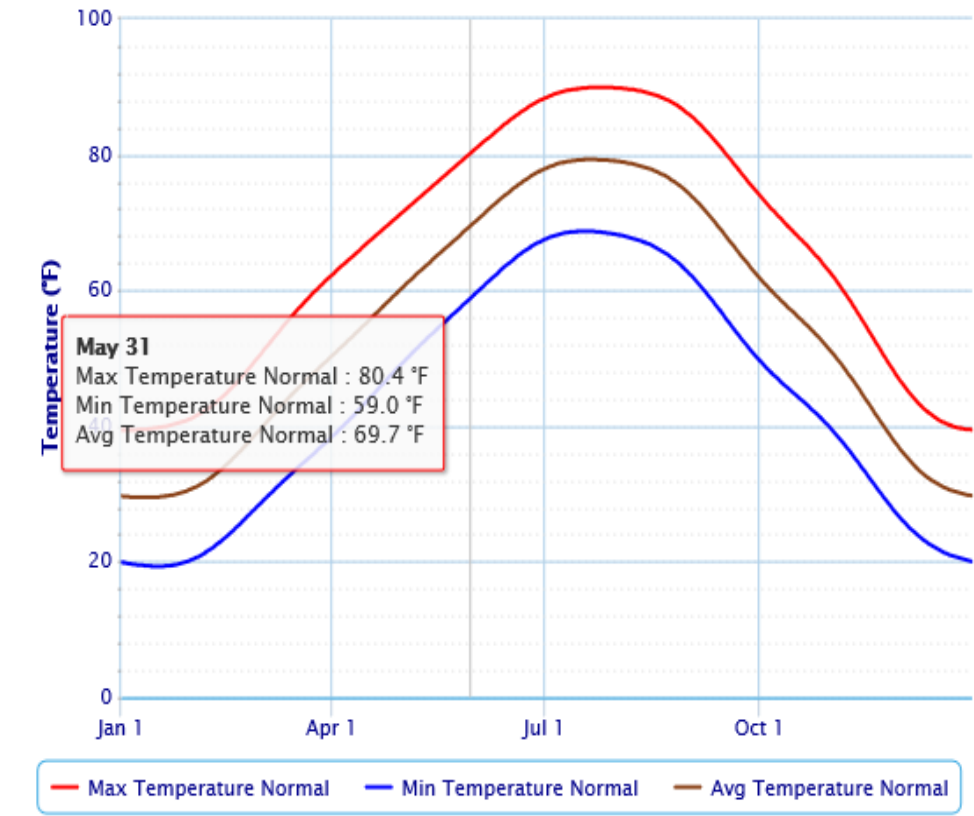


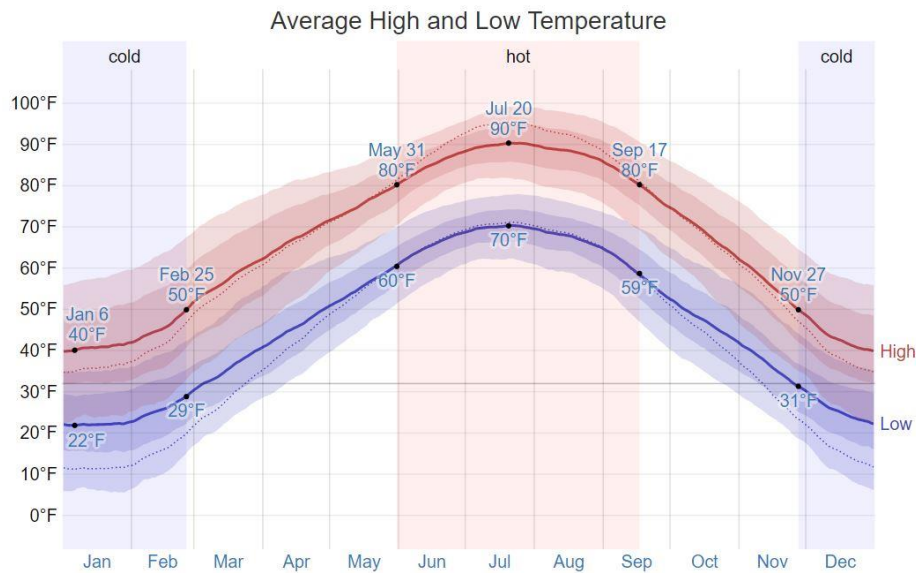
Figure 28: Daily temperature history of Topeka, Kansas, 1981-2010 [60].

### 3.3.2 Shading Zone

#### 3.3.2.1 Manually-drawn shading zone based on dry-bulb Temperature

To achieve more accurate results, I evaluated the numeric data (Table 7) based on 20° C (68° F) threshold temperature. The threshold was derived from the median minimum thermal comfort temperature [62]. Numbers marked in the Table 7 are maximum daily dry bulb temperature, and they do not consider other thermal comfort factors. On the other hand, the Table does not specify average hourly temperature, which is necessary for daily shading time border.

Hence, a set of hourly data [63] were needed to discover the shading time border (Figure 30). From the hourly data, all the times above 68° F were found and transferred on a time chart to produce an accurate shading period (Figure 31(a)). As it can be seen from the shading period, the shading time is not symmetrical around a year. If the chart is folded on 21<sup>st</sup> of June, the middle of the chart and the start time of a sun path chart, there are some unmatched times (figure 31(b)). Consequently, the solar gain that is desirable for some time in the first half of a year, by contrast for the other half (and during the same period) is not favorable. This is the most limitation of the fixed shading design.

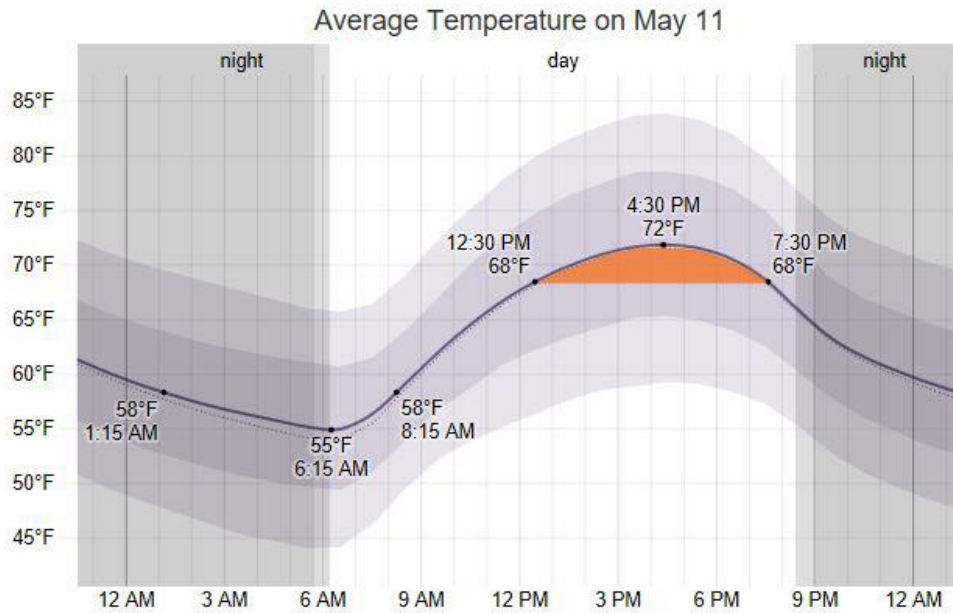


**Figure 29:** Daily temperature history of Topeka, Kansas, 1980-2016 [63].



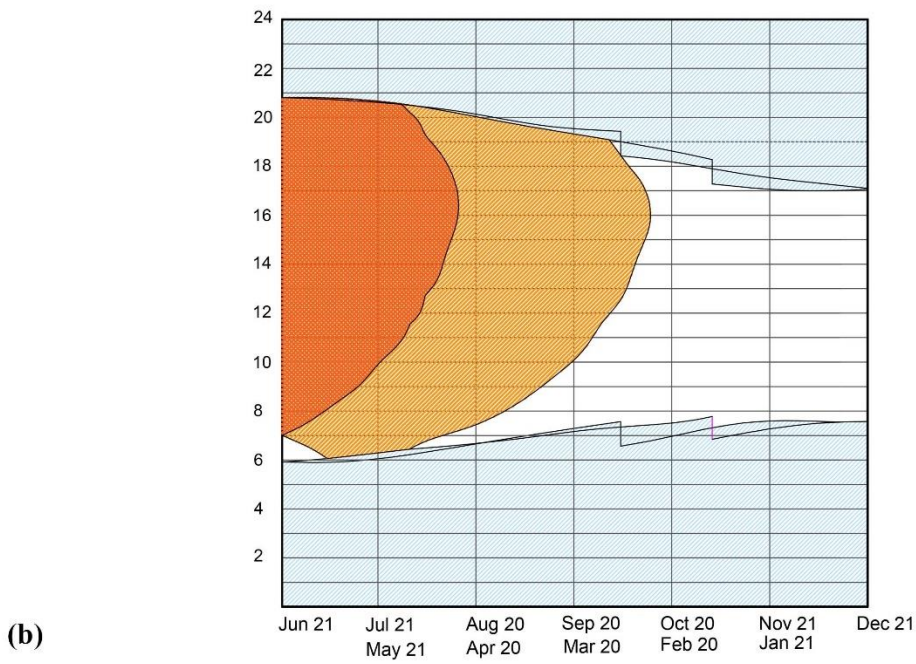
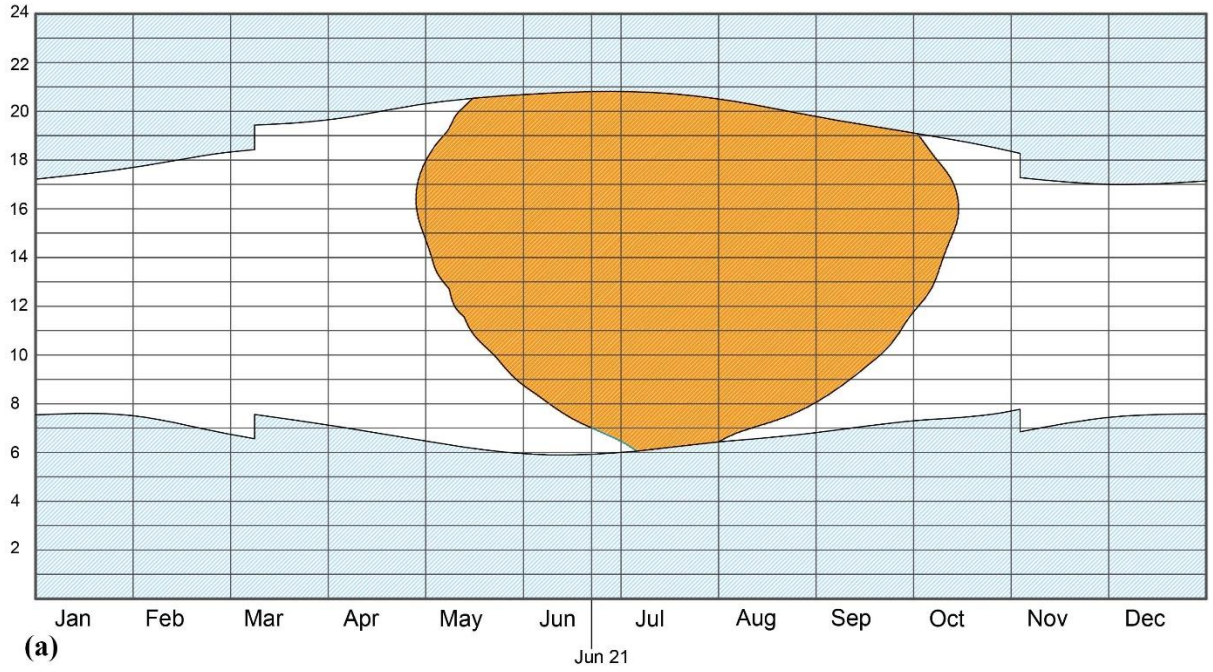
**Table 7:** Average daily maximum temperature normal (F°) of Topeka, Kansas [60].

Day	Jan	Feb	Mar	Apr	May	Jun	Jul	Aug	Sep	Oct	Nov	Dec
1	39	41	50	62	71	81	88	90	86	74	62	46
2	39	42	51	63	72	81	88	90	86	74	62	46
3	39	42	51	63	72	81	89	90	85	73	61	45
4	39	42	52	63	72	82	89	90	85	73	61	45
5	39	42	52	64	73	82	89	90	85	72	60	45
6	39	42	52	64	73	82	89	90	84	72	60	44
7	39	43	53	64	73	82	89	90	84	72	59	44
8	39	43	53	64	74	83	89	90	84	71	59	43
9	40	43	54	65	74	83	89	90	83	71	58	43
10	40	43	54	65	74	83	89	89	83	71	58	43
11	40	44	55	65	74	84	90	89	82	70	57	42
12	40	44	55	66	75	84	90	89	82	70	57	42
13	40	44	55	66	75	84	90	89	82	70	56	42
14	40	45	56	66	75	85	90	89	81	69	56	42
15	40	45	56	67	76	85	90	89	81	69	55	41
16	40	45	57	67	76	85	90	89	80	68	54	41
17	40	46	57	67	76	85	90	89	80	68	54	41
18	40	46	57	68	77	86	90	89	80	68	53	41
19	40	46	58	68	77	86	90	89	79	67	53	41
20	40	47	58	68	77	86	90	88	79	67	52	40
21	40	47	59	68	77	86	90	88	78	67	52	40
22	40	47	59	69	78	87	90	88	78	66	51	40
23	40	48	59	69	78	87	90	88	77	66	50	40
24	40	48	60	69	78	87	90	88	77	66	50	40
25	40	49	60	70	79	87	90	88	77	65	49	40
26	41	49	60	70	79	87	90	87	76	65	49	40
27	41	50	61	70	79	88	90	87	76	64	48	40
28	41	50	61	71	80	88	90	87	75	64	48	40
29	41	-	61	71	80	88	90	87	75	64	47	40
30	41	-	62	71	80	88	90	86	74	63	47	40
31	41	-	62	-	80	-	90	86	-	63	-	39

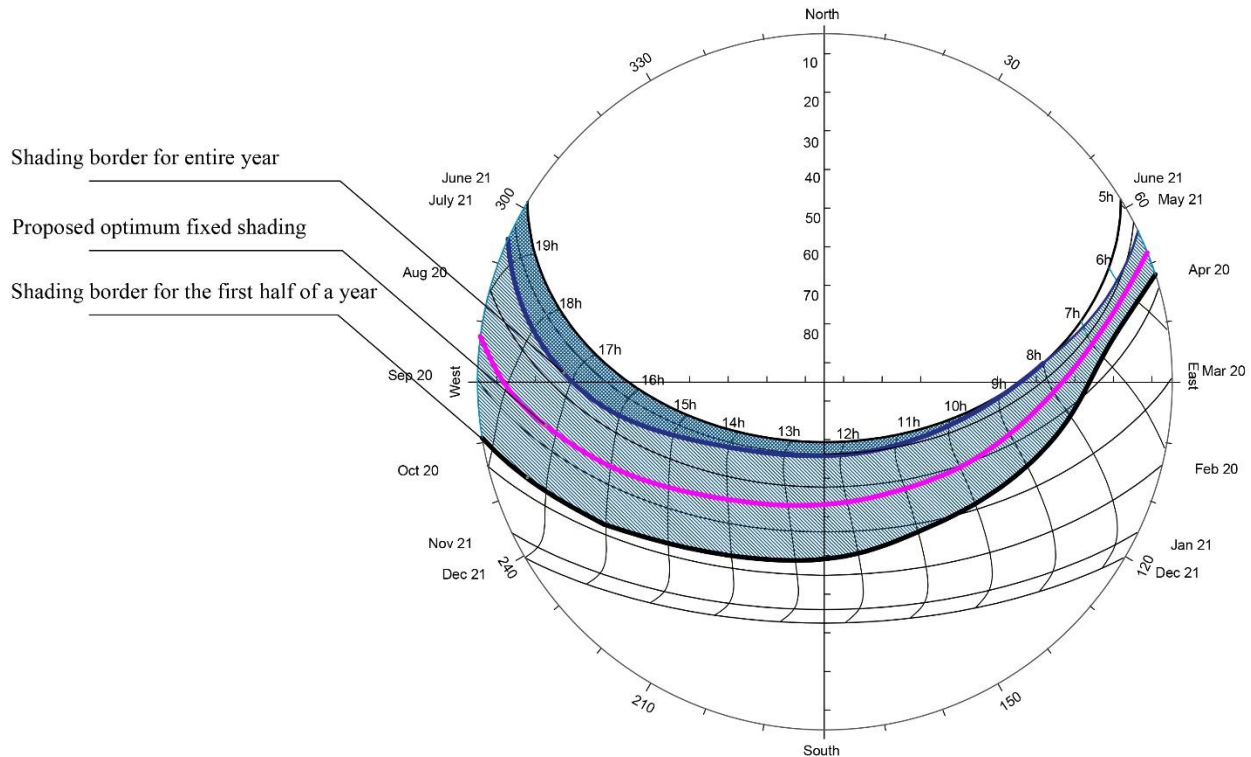


**Figure 30:** Hourly May 11 Average temperature history of Topeka, Kansas, 1980-2016 (as an example of derived data) [63].

To produce a shading schedule on the represented sun path chart, the shading period was transferred to the equivalent points. Based on the two different shading schedules for the first and second halves of a year on the sun path chart, two main border lines are highlighted (Figure 32). The first line is covered by a larger shading area. Taking the larger shading area would sacrifice the desired solar gain for the first half of a year. Whereas, considering the smaller shading area lets unfavorable sun light penetrate inside in the second half of a year. To satisfy both scenarios, an optimum line between the border of first and second shading areas is drawn (Figure 32). This is the baseline for optimized shading design of Topeka, Kansas.



**Figure 31:** Overheat area of a year, on 12-month schedule (a) and 6-month schedule (b) (matched with sun path chart), based on hourly average temperature history of Topeka, Kansas (1980-2016)



**Figure 32:** Shading zones, highlighted on sun path diagram (the base sun path chart for 38°N is produced through the University of Oregon, Solar Radiation Monitoring Laboratory webpage [64]).

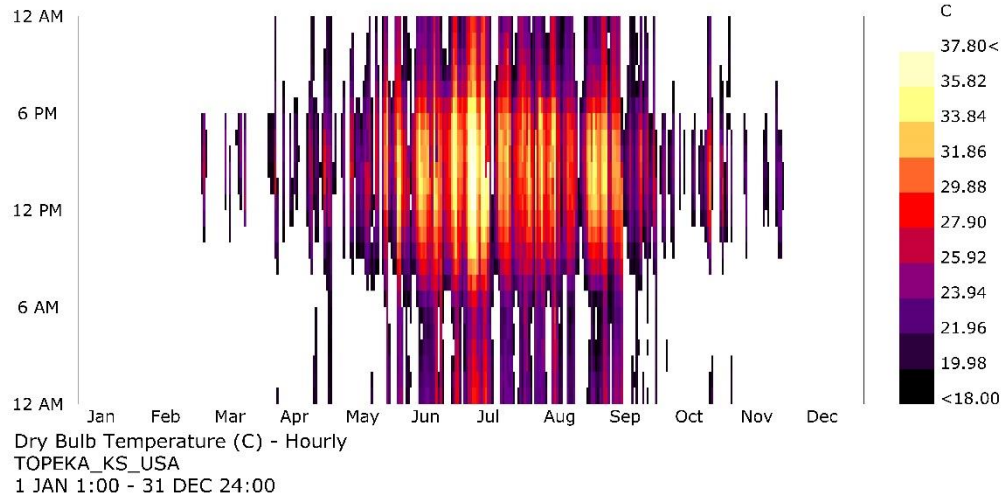
### 3.3.2.2 Software-simulated shading zone based on Dry Bulb, Universal Thermal Climate Index (UTCI) and Effective Temperature (TE)

The Ladybug® Plugin [42] developed for Grasshopper® on Rhino® is capable to calculate and produce the dry-bulb, Universal Thermal Climate index (UTCI), and the Effective Temperature (TE) schedules, all based on the weather file. The UTCI index, which is a combination of dry-bulb temperature, relative humidity, wind speed, and radiation, is a comprehensive thermal comfort zone based on the psychrometric chart [65]. The TE is a part of another component in Ladybug® in which the comfort temperature zone is categorized to very cold (<1°C), cold (1°-9°C), cool (9°-17°C), fresh (17°-21°C), comfortable (21°-23°C), warm (23°-

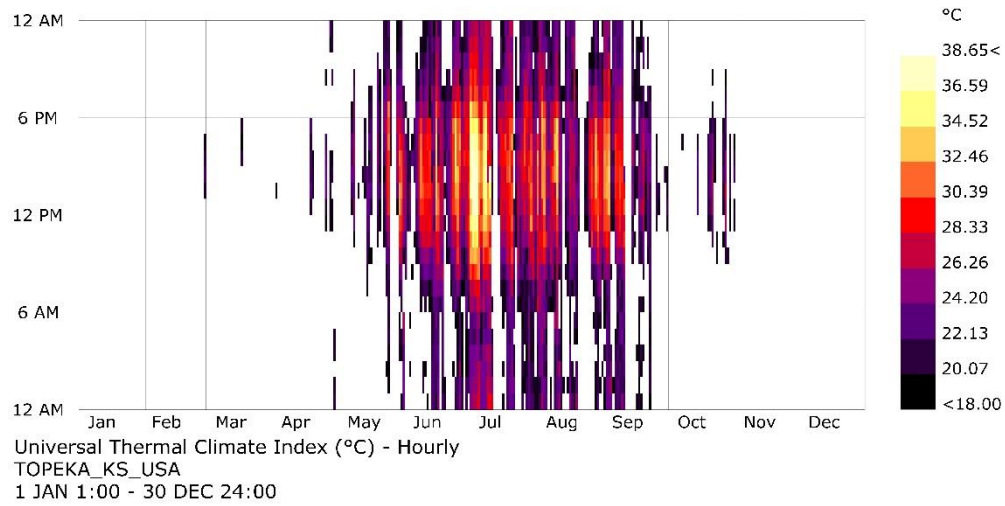
27°C), and hot (>27°C). To evaluate the overheat area, the shading schedule were produced based on the three methods - dry-bulb, UTCI, and TE - for Topeka, Kansas.

The produced UTCI schedule (Figure 33(b)) is an hourly thermal chart, which would be used for investigating the desired shading zone. Any temperature above 20°C (68°F) for the UTCI and above maximum fresh temperature (21°C (70°F)) would be considered shading-needed. By transferring the shading period from the UTCI and TE on the sun path charts, the same story as the manual process for the dry-bulb temperature happens (Figure 34(a) & (b), and Figure 35(a) & (b)). The shading zones for the two timeframes are not identical. Furthermore, an optimum shading zone should be investigated.

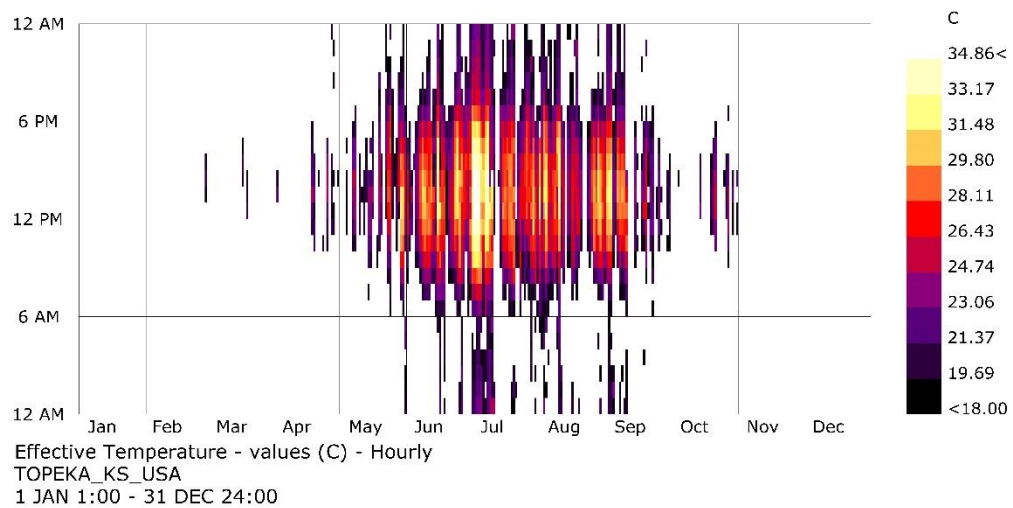
(a)



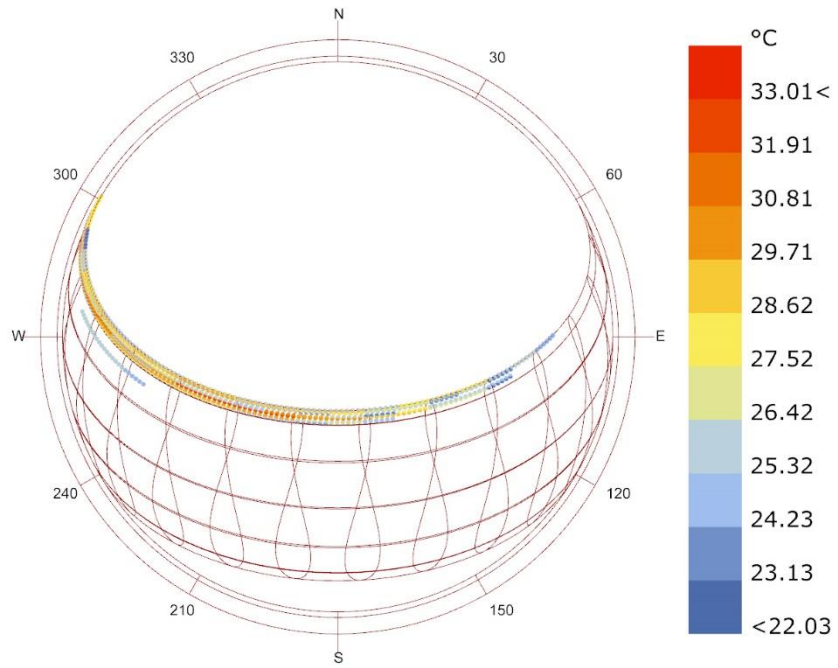
(b)



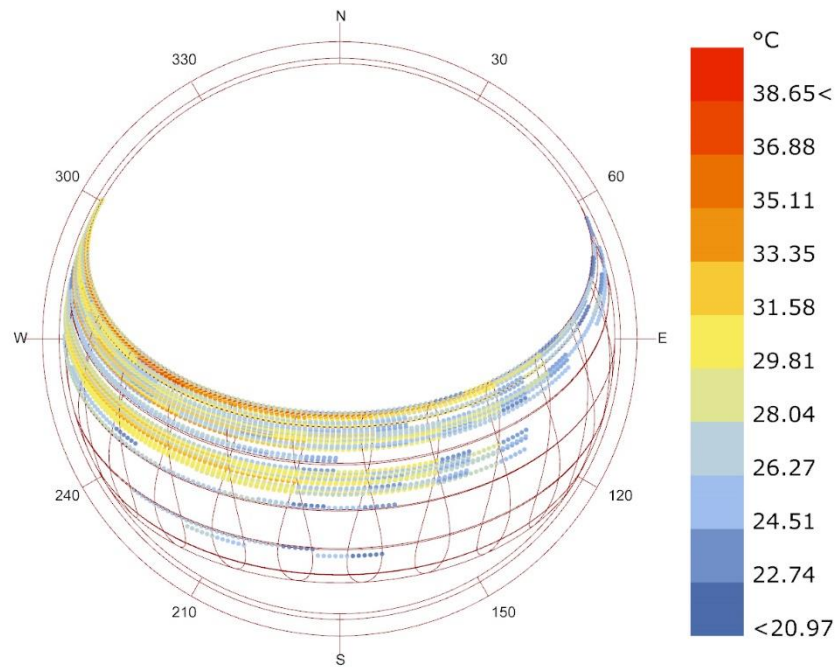
(c)



**Figure 33:** The dry-bulb (a), Universal Thermal Climate index (UTCI) (b), and the Effective Temperature (TE) (c) schedules based on the weather file. (Produced through Ladybug® plugin on Grasshopper®)

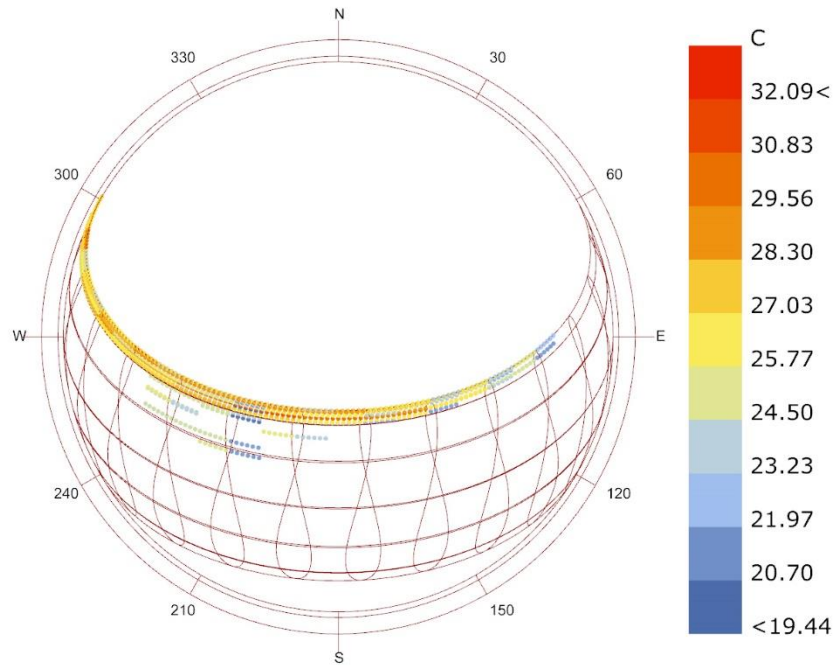


(a)

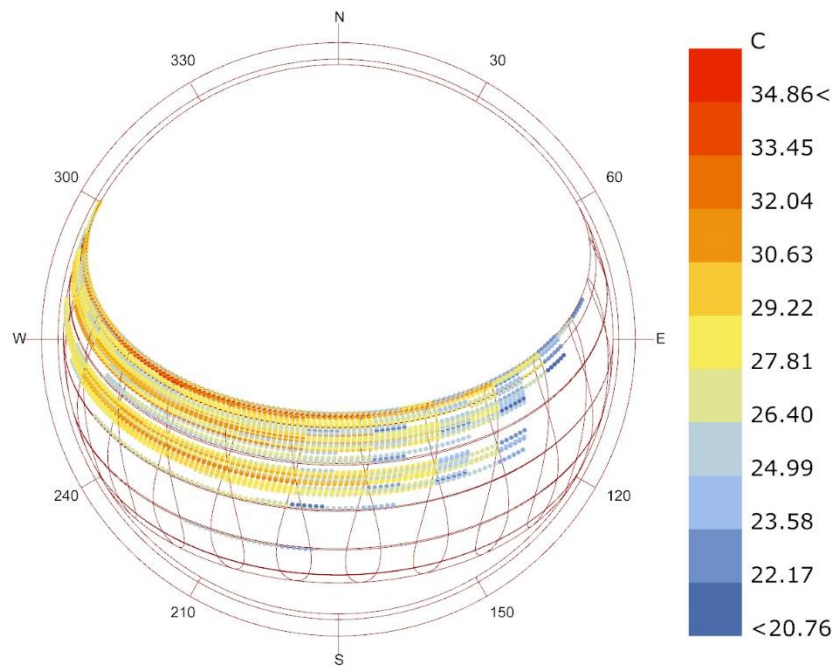


(b)

**Figure 34:** Shading zone from Dec 21 to June 21 (a) and June 21 to Dec 21 (b) based on UTI, Topeka, KS.



(a)



(b)

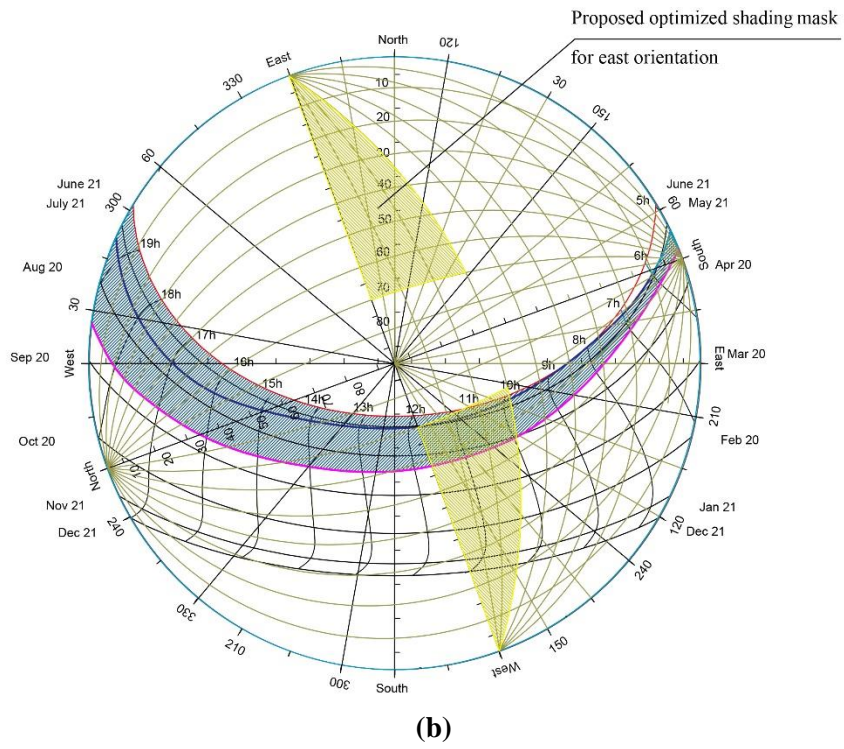
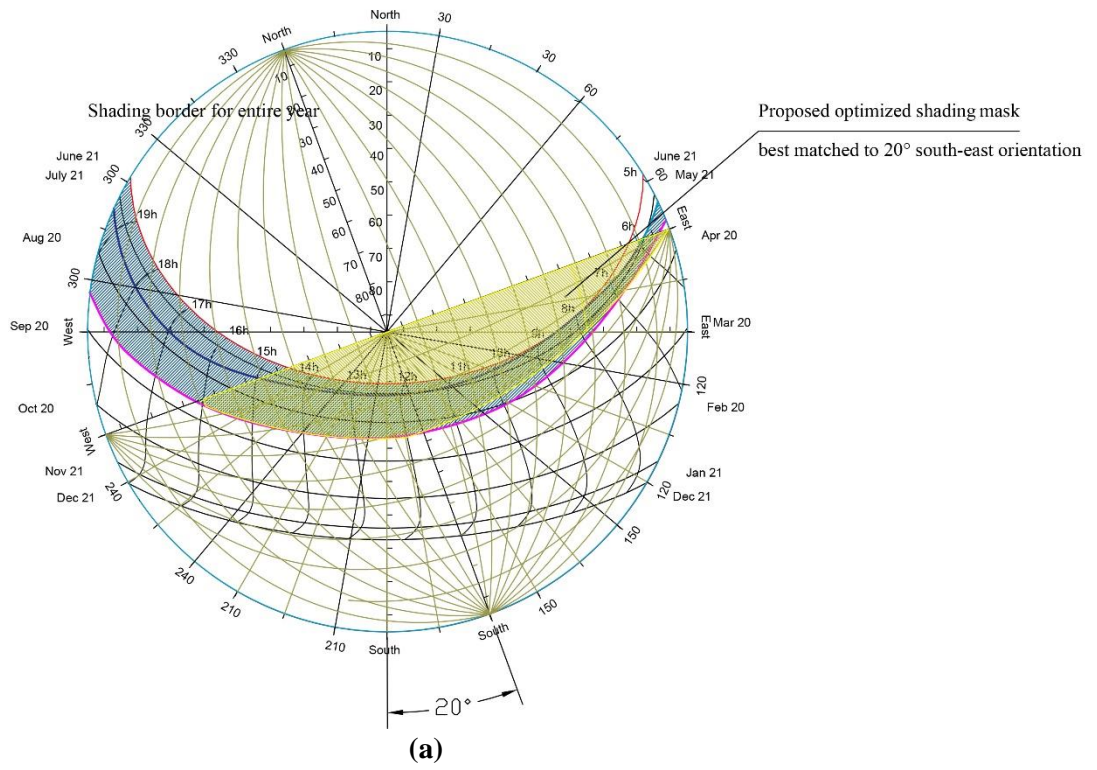
**Figure 35:** Shading zone from Dec 21 to June 21 (a) and Jun 21 to Dec 21 (b) based on TE, Topeka, KS.

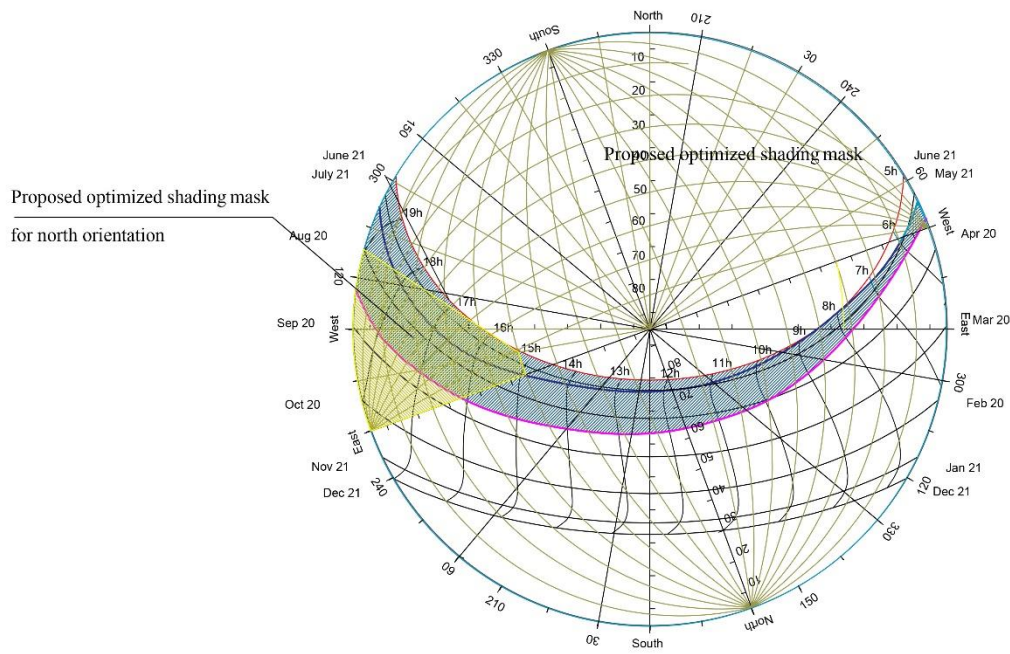


Despite the similarities between the shading zones derived from UTCI and TE, the results show slight differences in morning hours. Comparing the manually-drawn shading zone with the computer-based ones, it is recognizable that although the general shapes of shading zones are similar, the manually-drawn shading zone shows wider area in the afternoons. The general patterns of the shading zones for both manual and software simulations are similar. Since the proposed optimum shading zone is narrower than the outer border of both shading zones, it could be considered as the baseline for fixed shading design in this study. However, for automatic or dynamic shading design, the UTCI or TE-based shading zone would be more effective.

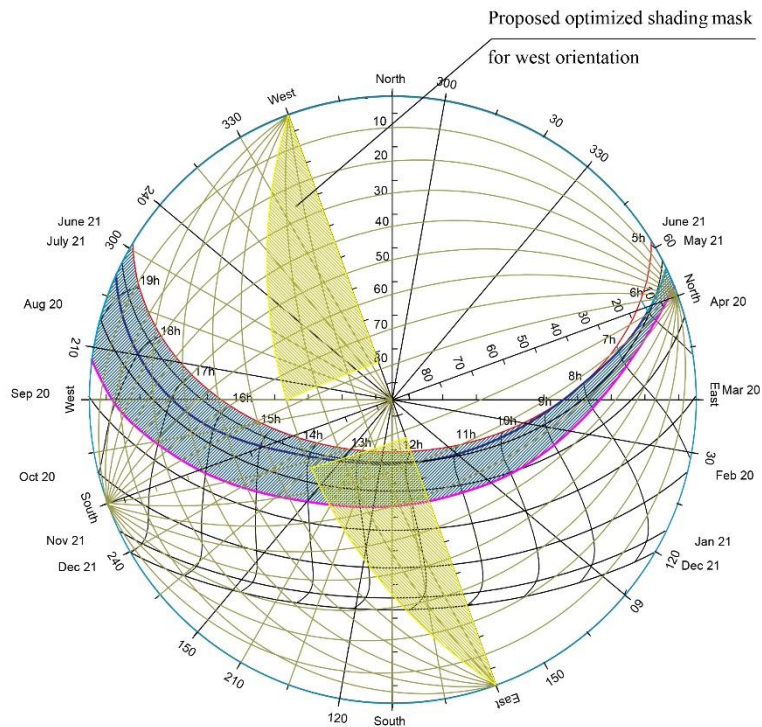
### **3.3.2.3 Optimized Shading Design**

Nonetheless, shading design is intended to satisfy thermal needs, lighting comfort, and aesthetical aspect of the building façade. In this study we have focused on thermal comfort through solar gain strategy. Accordingly, the results may not look normal. The shading design method used in this study is based on Olgyay shading design method [40]. Since the intention of this study has been an optimized shade, the building orientation was also taken in account.





(c)



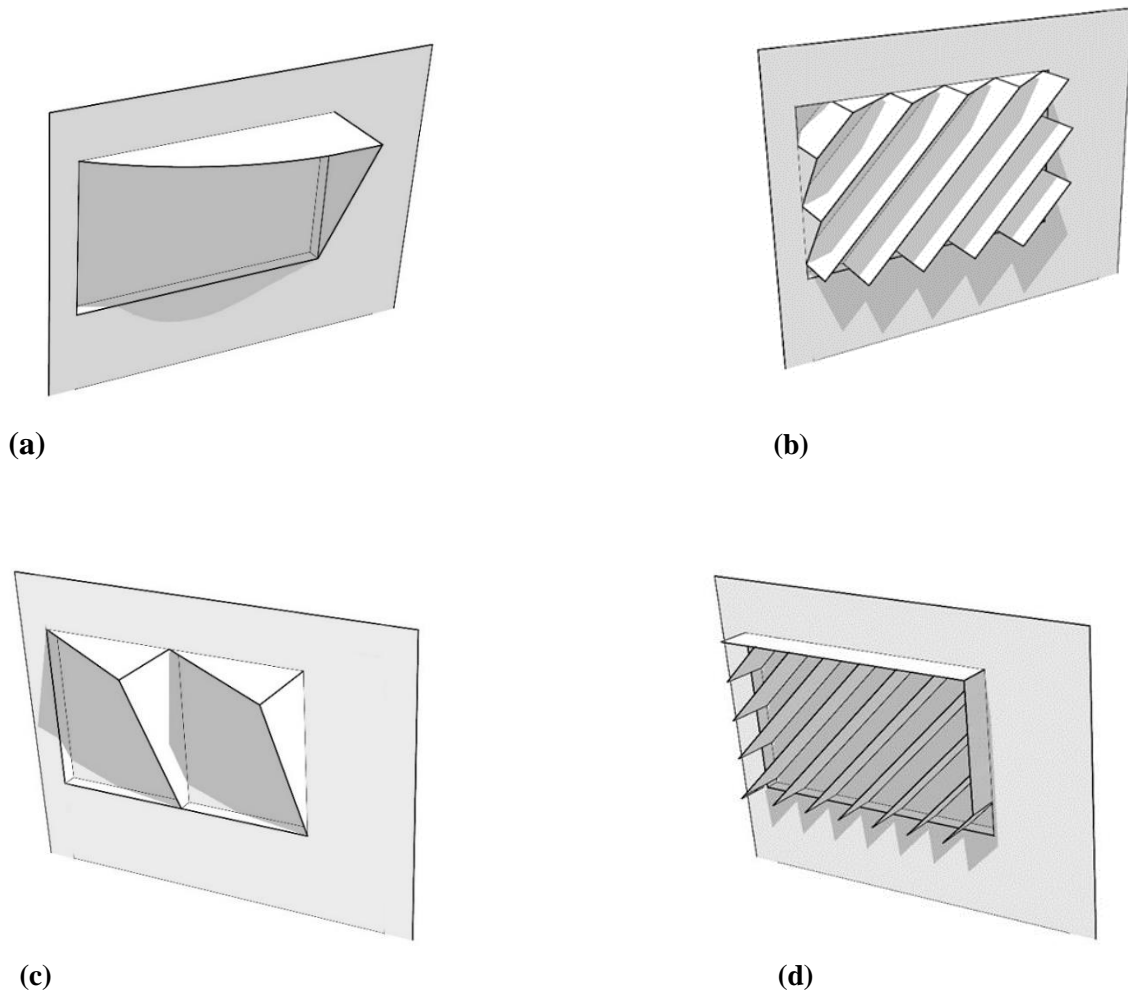
(d)

Figure 36: Shading masks for four orientations; (a) south, (b) east, (c) north, and (d) west.

Evaluating the outer line of shading area on the sun path chart, the ideal shading mask for south orientation best matched 20° south-east<sup>1</sup> (Figure 36(a)). This building orientation (20° south-east) provides the best result for the building direction. The shading masks of the four orientations were interpreted to architectural vertical and horizontal shading elements (Figures 37(a) and 37(d)). Notwithstanding, these fixed optimized shades are not supposed to work for the entire shading period, which was described previously (Figure 32).

---

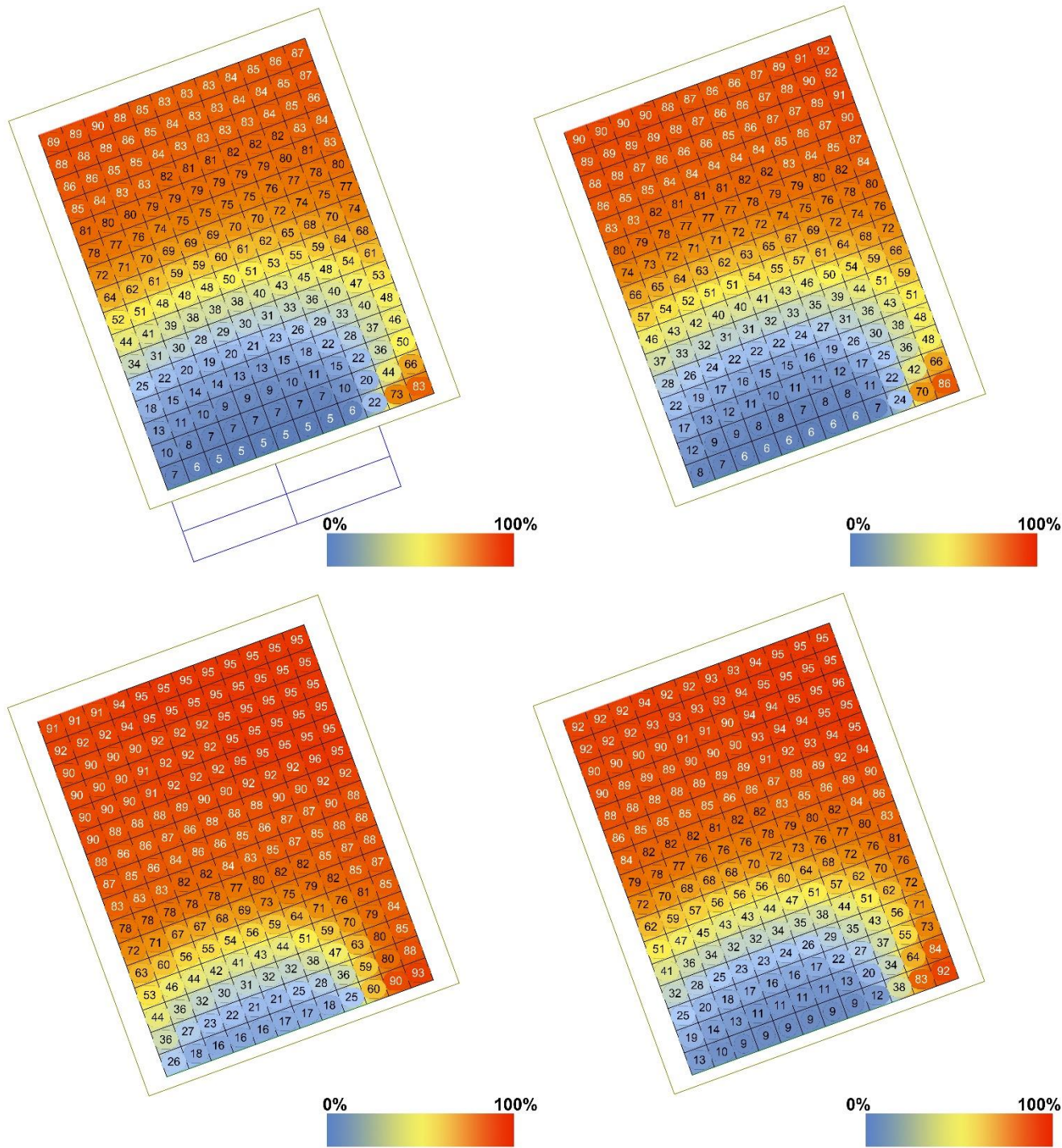
<sup>1</sup> In this study, the 20° south-east orientation south is called ‘south’, unless it is mentioned ‘true south’.



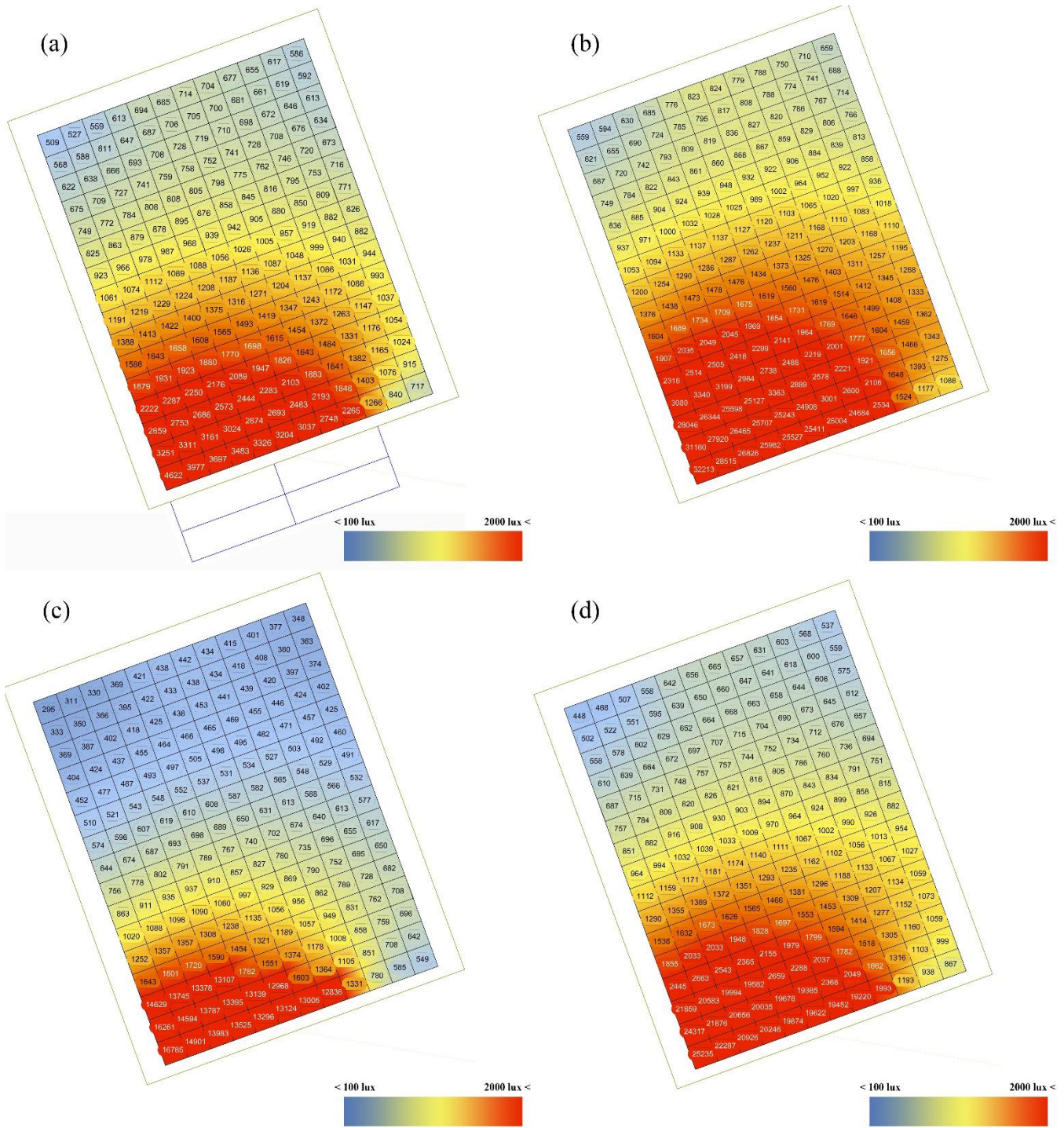
**Figure 37:** *Optimized shades for the four orientations; south (a), east (b), north (c), and west (d).*

### 3.3.2.3.1 Shading evaluation

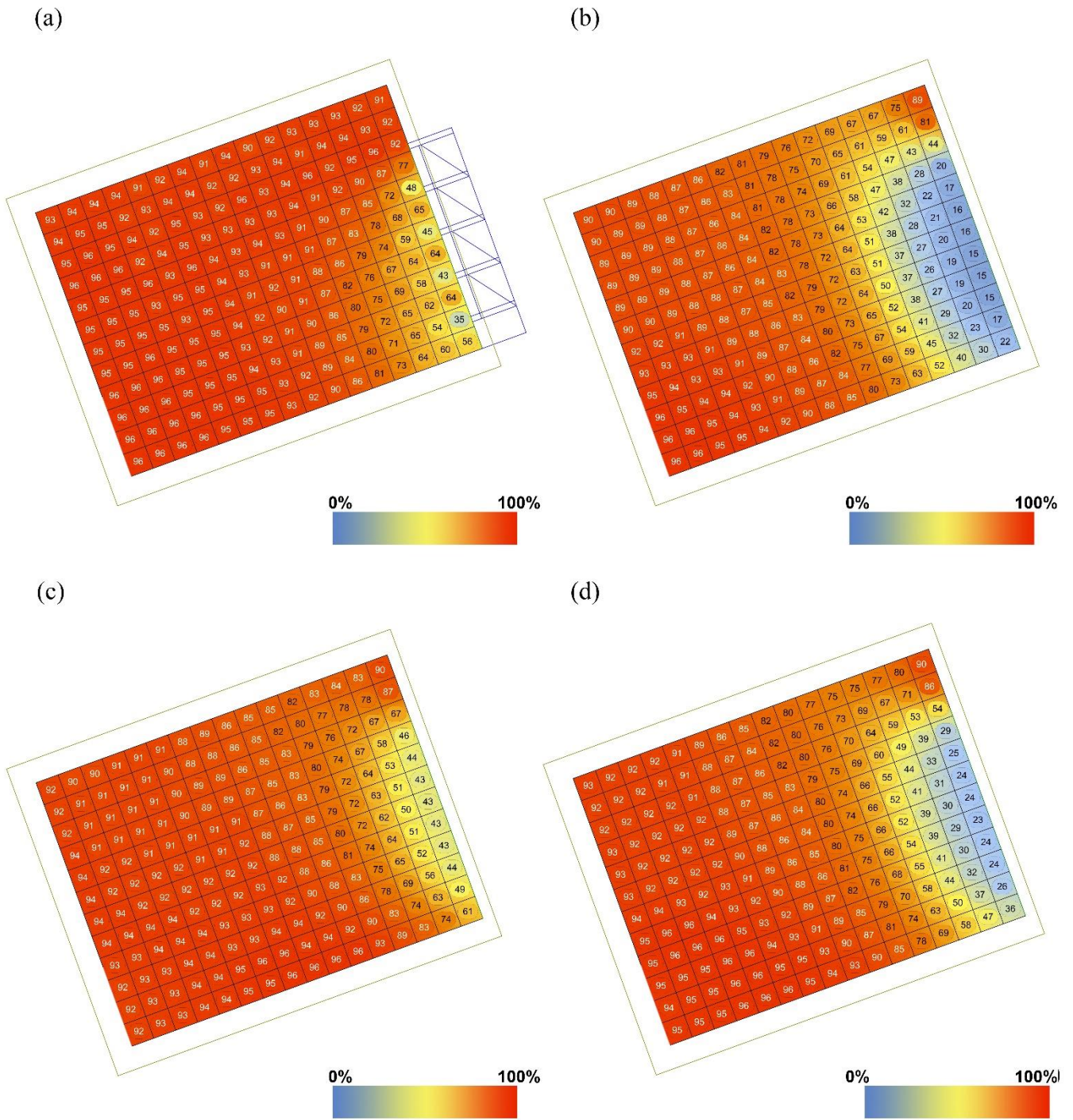
To evaluate the practicality of the shades, daylight simulations were conducted using the Diva® plugin on Grasshopper® for Rhino® [66] for the entire year as well as one shading demand date (August 1<sup>st</sup>) and the time for each orientation (south; 9:00 am, east; 8:30 am, north; 5:00 pm, west; 3:00 pm). The 100-2000 lux Useful Daylight Illuminance (UDI) and single-point-in-time were simulated for the baseline case and the test cases (figures 38 to 45). The results contrast the overall efficiency of optimized shading devices for the all four orientations.



**Figure 38:** South orientation illuminance (lux) evaluation; Useful Daylight Illuminance (UDI, 100-2000 lux) for optimized shade case (a), Low-E 65% (b), Low-E 39% (c), and Low-E 53% (d).

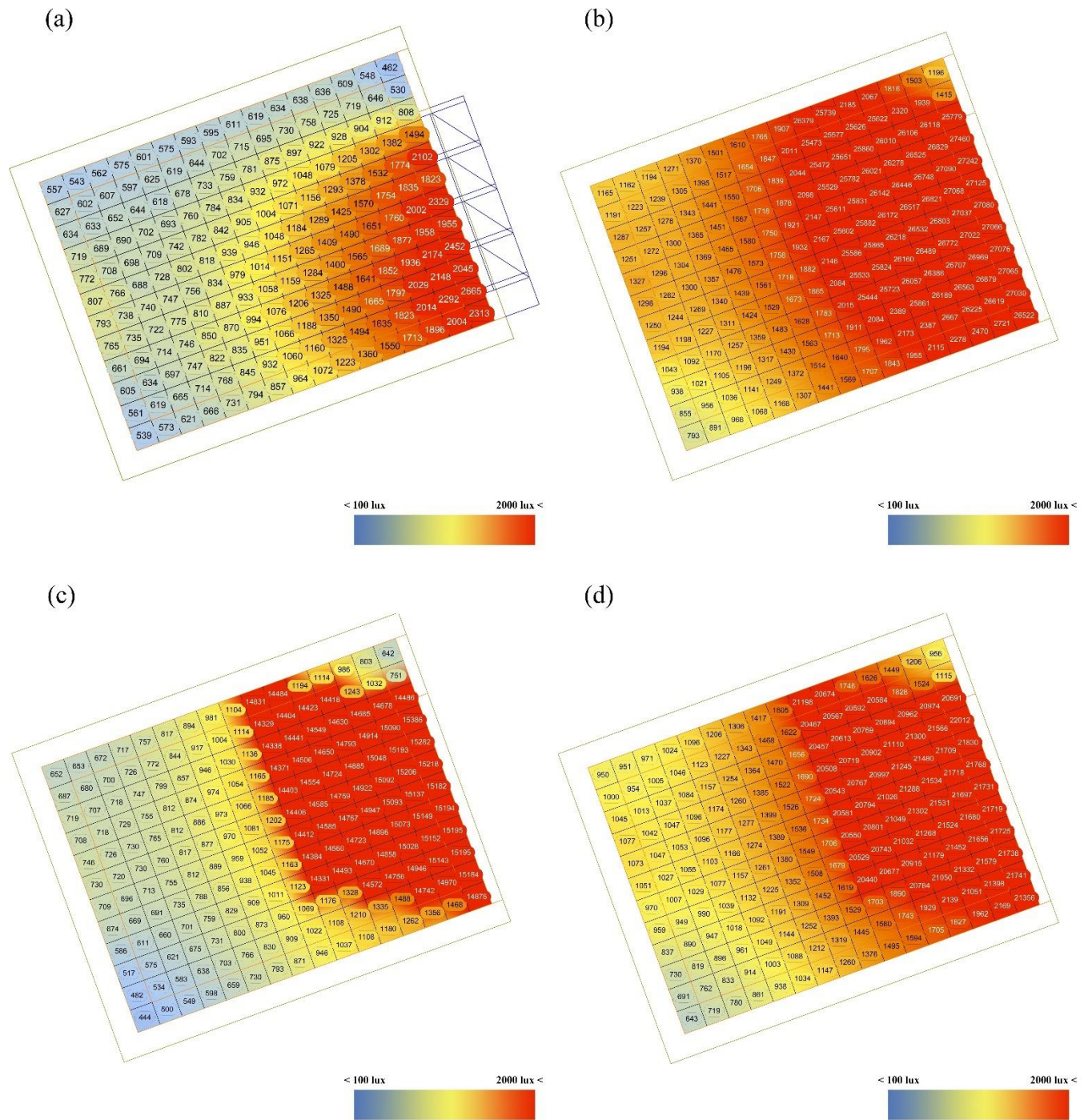


**Figure 39:** South orientation illuminance (lux) evaluation; Point-in-time (8/01 @ 9:00 am) illuminance for optimized shade case (a), Low-E 65% (b), Low-E 39% (c), and Low-E 53% (d).



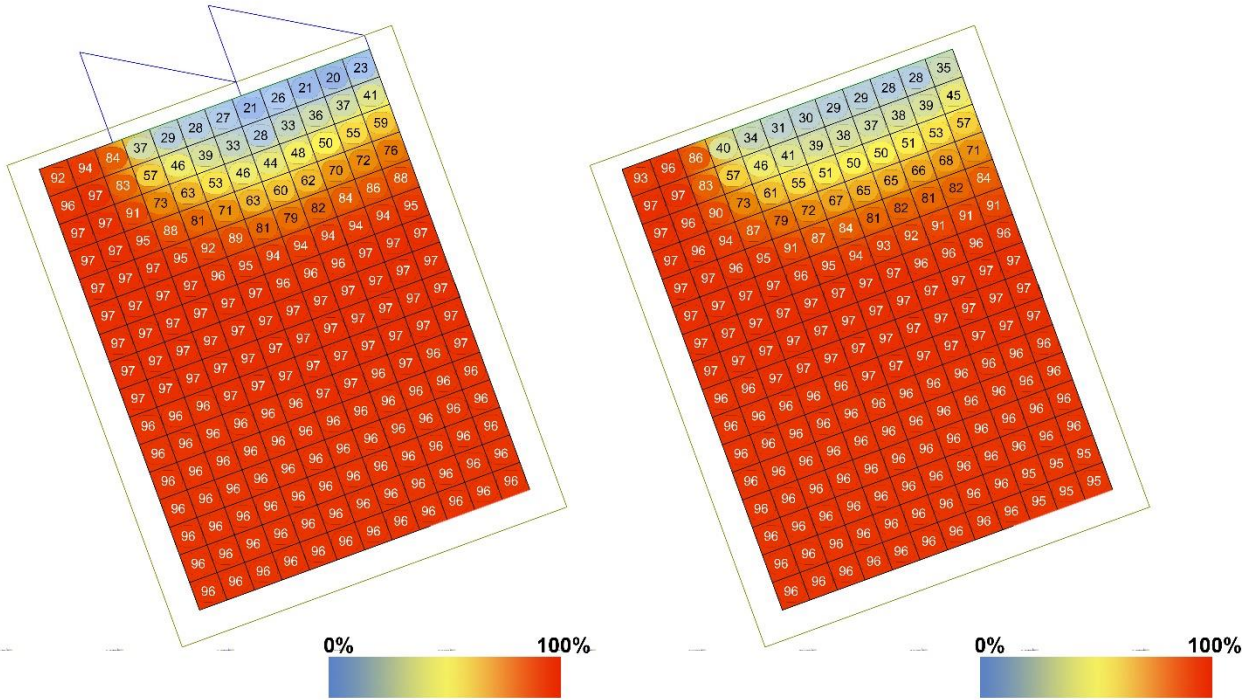
**Figure 40:** East orientation illuminance (lux) evaluation; Useful Daylight Illuminance (UDI, 100-2000 lux) for optimized shade case (a), Low-E 65% (b), Low-E 39% (c), and Low-E 53% (d).



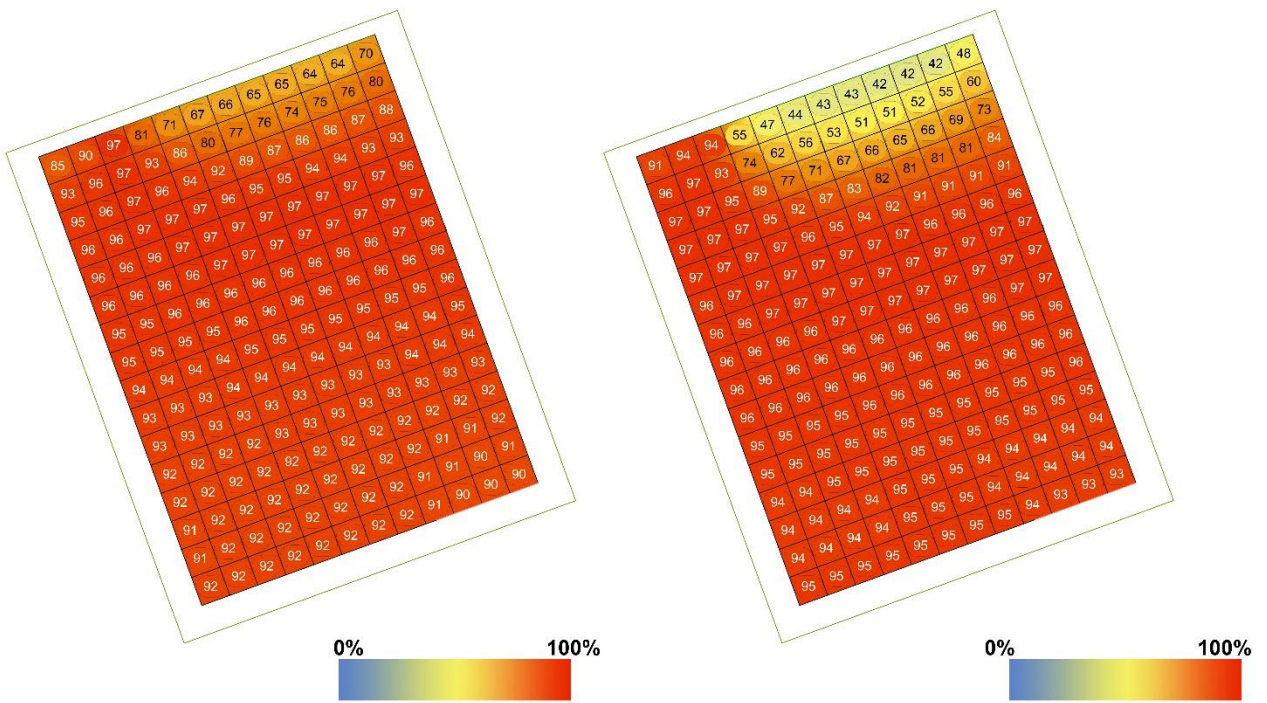


**Figure 41:** East orientation illuminance (lux) evaluation; Point-in-time (8/01 @ 8:30 am) illuminance for optimized shade case (a), Low-E 65% (b), Low-E 39% (c), and Low-E 53% (d).

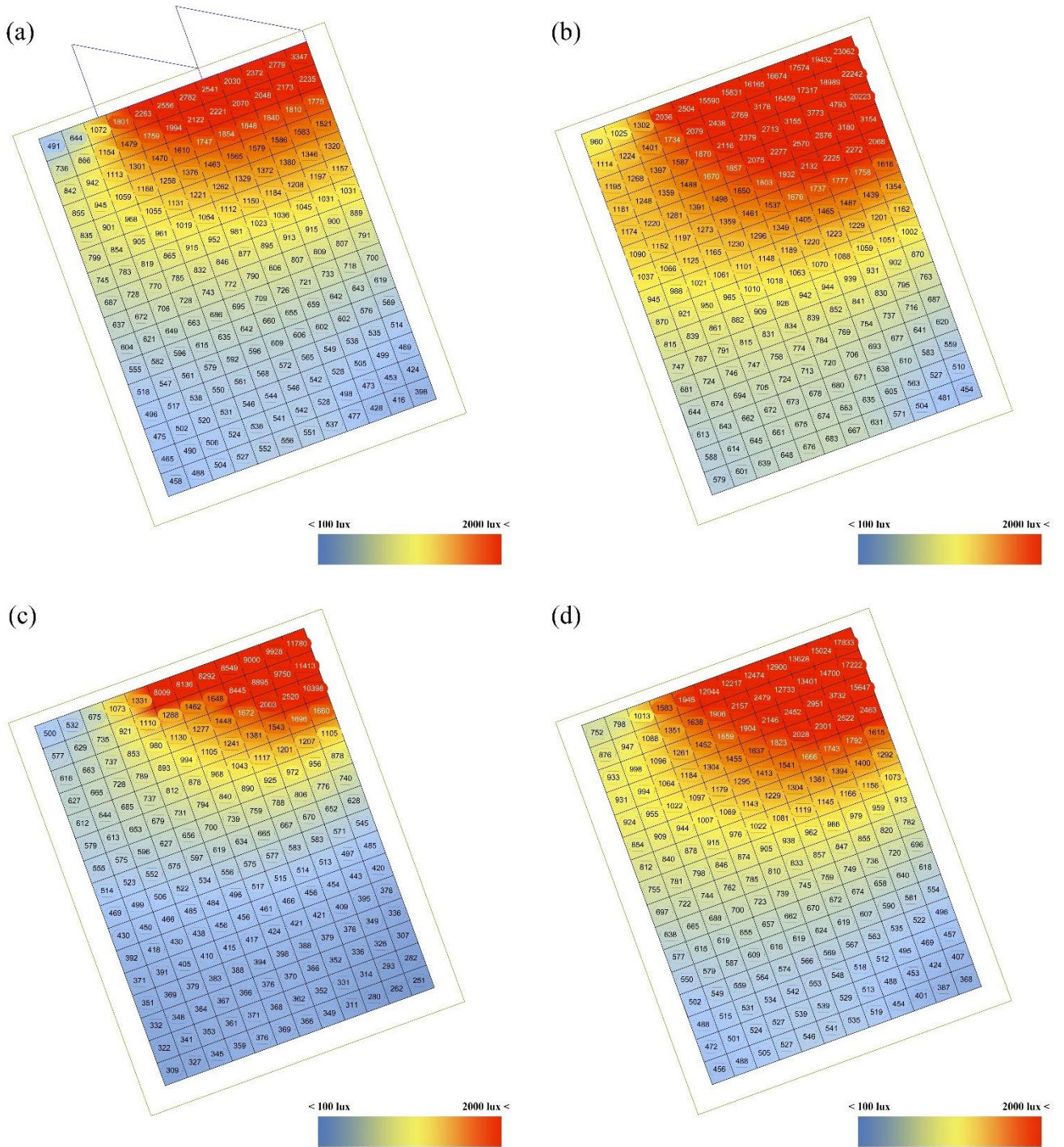
(a)



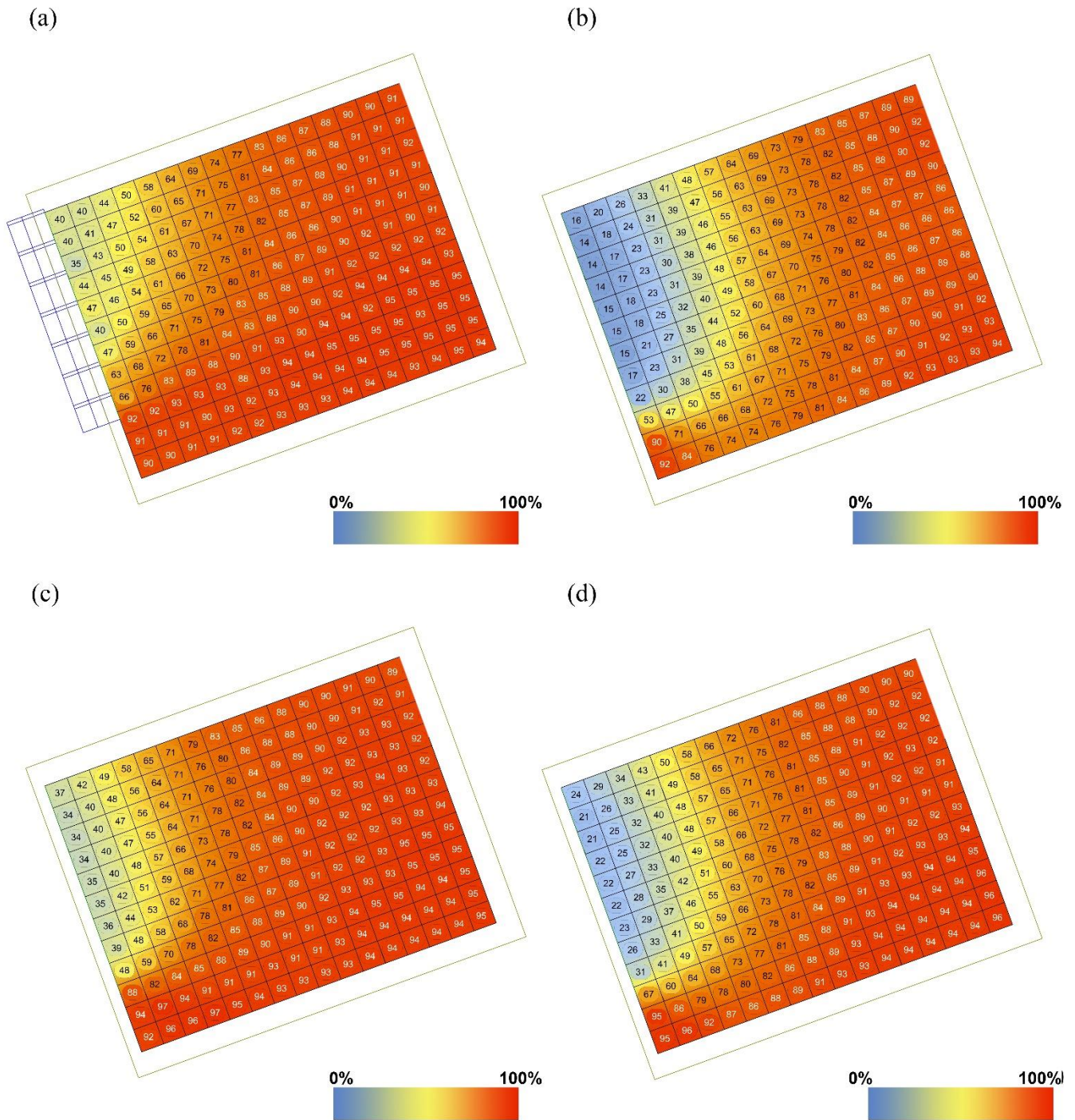
(c)



**Figure 42:** North orientation illuminance (lux) evaluation; Useful Daylight Illuminance (UDI, 100-2000 lux) for optimized shade case (a), Low-E 65% (b), Low-E 39% (c), and Low-E 53% (d).



**Figure 43:** North orientation illuminance (lux) evaluation; Point-in-time (8/01 @ 5:00 pm) illuminance for optimized shade case (a), Low-E 65% (b), Low-E 39% (c), and Low-E 53% (d).



**Figure 44:** West orientation illuminance (lux) evaluation; Useful Daylight Illuminance (UDI, 100-2000 lux) for optimized shade case (a), Low-E 65% (b), Low-E 39% (c), and Low-E 53% (d).

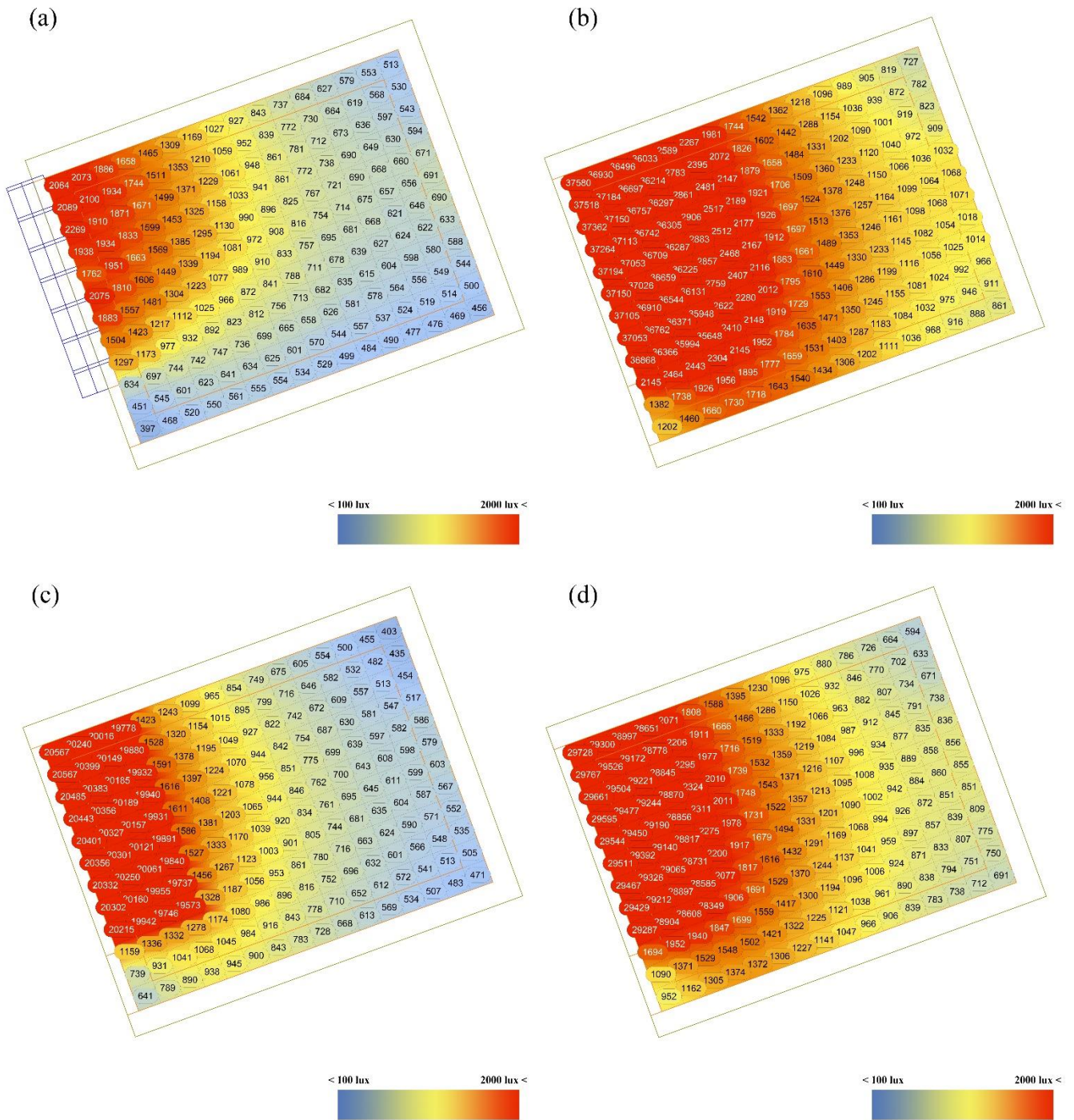
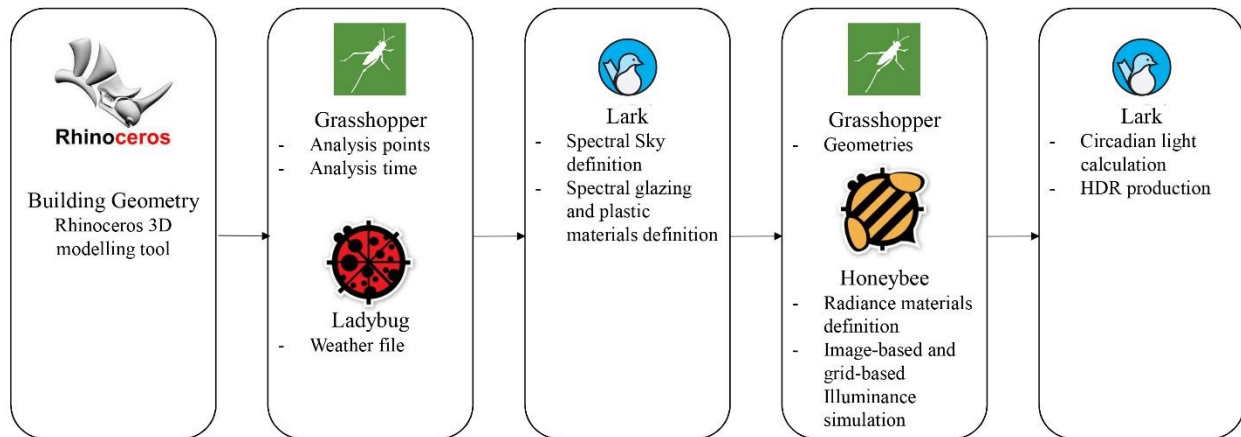


Figure 45: West orientation illuminance (lux) evaluation; Point-in-time (8/01 @ 3:00 pm) illuminance for optimized shade case (a), Low-E 65% (b), Low-E 39% (c), and Low-E 53% (d).

### 3.4 Circadian light computer simulation method

In this method, the Rhinoceros® software version 5 on the personal laptop (Dell Inspiron 15 Gaming 7567, Core i7-7<sup>th</sup> Gen 2.80 GHz with 16.0 GB RAM) was used to build the 3D geometry of the space, which was then connected to the Grasshopper®<sup>2</sup>. The three plugins on the Grasshopper® platform, Lark®, Honeybee®, and Ladybug® were used for the circadian illuminance simulation through the various scripts (Figure 46).



*Figure 46: Simulation process*

Up to the time of this study, there was no specific software for circadian light simulation except the open source Lark® tool on the Grasshopper® for Rhino®. However, another software called Alfa® [67] by Solemma LLC., was released by the mid-2018, when all the simulations for this study had already been finished. The Alfa® is a more user-friendly and seemingly more

---

<sup>2</sup> Grasshopper® is a graphical algorithm editor tightly integrated with Rhino’s 3-D modeling tools. Unlike RhinoScript, Grasshopper requires no knowledge of programming or scripting, but still allows designers to build form generators from the simple to the awe-inspiring [73].

accurate tool for the circadian light simulation. However, due to the time limitation, it was not possible to conduct another simulation study on Alfa® software.

### **3.4.1 Lark® characteristics**

The Lark® plugin, which has been used as a baseline for the simulations in this study, is an open-source tool consisted of three Grasshopper® components: spectral sky definition, spectral glazing and material definition, and photopic and circadian illuminance calculation. In fact, these components are some interfaces for the Radiance® and Daysim® tools previously introduced in the study background section. The Lark® tool introduces 3 and 9 spectral sky channels based on the input CIE sky CCT from the Daylight Series excel sheet developed by the Rochester Institute of Technology [68]. In the original Daysim® tool, the sky color is not considered in simulation (Figure 47). The sky component also was supposed to support three sky conditions: clear-sky, intermediate sky, and overcast sky of the CIE sky standards.

```

# start of sky definition for daylighting studies
# location name: COPENHAGEN_DNK LAT: 55.63
!gensky 3 21 6.0 -c -a 55.63 -o -12.67 -m -15.0 | xform -rz 0.0
skyfunc glow sky_mat
0
0
4
!1 1 1 0
sky_mat source sky
0
0
4
0 0 1 180
skyfunc glow ground_glow
0
0
4
1 .8 .5 0
ground_glow source ground
0
0
4
0 0 -1 180
# end of sky definition for daylighting studies
-----
!gensky 3 21 6.0 -c -B 11.8 -R -0.06 -a 55.63 -o -12.67 -m -15
skyfunc glow sky_mat
0
0
4
{0.581 0.829 0.837 0}
sky_mat source sky
0
0
4
0 0 1 180
skyfunc glow ground_glow
0
0
4
1 0.8 0.5 0
ground_glow source ground
0
0
4
0 0 -1 180

```

**Figure 47:** Sky file without (top) and with (bottom) color information. Image adapted from [48].

Although the 3 and 9 spectral sky channels seemed to be a unique idea in the plugin, according to several pre-simulations that was run here, the designed component showed some errors especially for the clear-sky condition<sup>3</sup>. Hence, the spectral sky information of the simulation was inserted manually.

---

<sup>3</sup> Despite contacts with the Lark® plugin developers, Inanici et al., they did not want to resolve the problem anymore.



### 3.4.2 Simulation input

#### 3.4.2.1 Weather file

The weather file for Topeka, Kansas was downloaded and employed from the National Renewable Energy Laboratory (NREL) [61].

#### 3.4.2.2 Analysis time

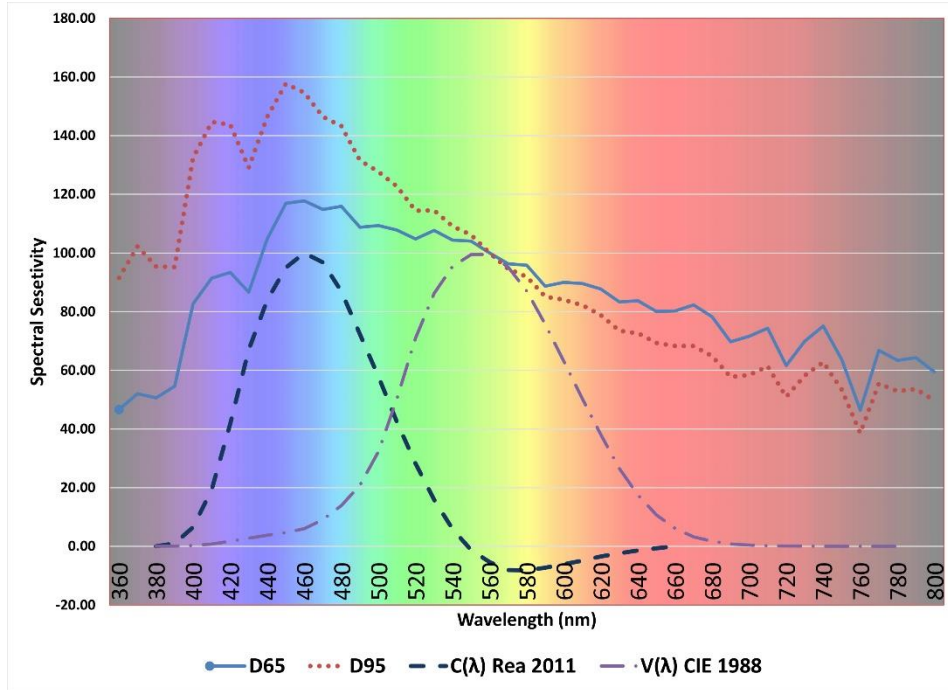
Due to the time limitation, the simulations were run only for four days in a year: spring equinox (21<sup>st</sup> March), summer solstice (21<sup>st</sup> of June), autumn equinox (21<sup>st</sup> September), and winter solstice (21<sup>st</sup> December). Three times per day: one in the morning (10 am), one at noon (1 pm), and one in the afternoon (5 pm); were chosen to fit in the usual 9am-to-5pm working schedule.

*Table 8: Simulation schedule*

<b>Month</b>	<b>Day</b>	<b>Time</b>		
<b>March</b>	20	10 am	1 pm	5 pm
<b>June</b>	21	10 am	1 pm	5 pm
<b>September</b>	20	10 am	1 pm	5 pm
<b>December</b>	21	10 am	1 pm	5 pm

#### 3.4.2.3 Sky conditions and the Correlated Color Temperature (CCT)

Among the three possible sky conditions, the overcast and clear-sky conditions were set for this study. Since the CIE sky CCTs are not available in the weather file and sky CCT is not a static standard, two CCTs - D65 (6500 CCT) and D95 (9500 CCT) - were preset for the overcast and clear sky conditions respectively (Figure 48). The estimations of the two sky CCTs are based on an experimental CCT measurement using Minolta Illuminance Spectrophotometer CL-500A in the week of February 2<sup>nd</sup>, 2018.



*Figure 48: CIE D65 and D95 skies SPD curves. (Produced by the author through Daylight Series excel sheet [69]).*

#### 3.4.2.4 Analysis points and directions

Nine analysis points (two are considered as the location of the two office workers), evenly distributed across the space (Figure 49) at the level of standing human eyes (4 feet), were chosen to be studied in the two directions: looking toward the window and looking to the front wall. Two more directions were then added to the locations of the two office workers (Points 1 and 3). Occupancy behavior and movement were not considered in this study. There were thus 22 view directions simulated in this space.

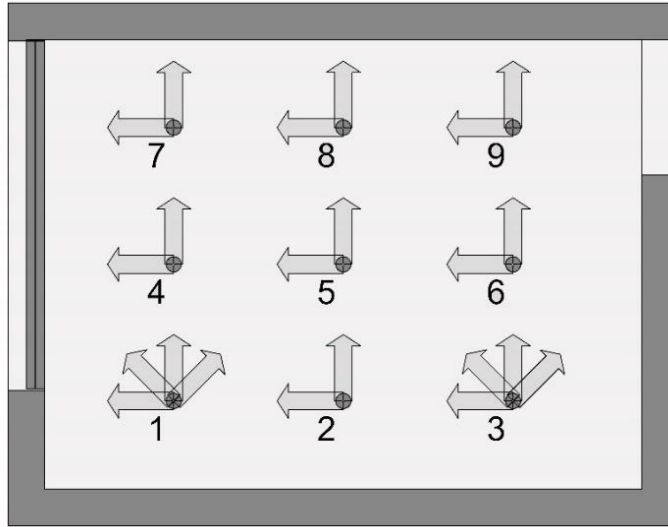


Figure 49: Study Points and direction of views.

### 3.4.2.5 Materials

The materials introduced in section 3.1.1 and 3.1.2 were associated with 5 nm interval spectral data. A material component in the Lark® tool converts the spectral \*.csv or \*.txt files to the 9-channel spectral Radiance® codes (Figure 50).

#### 3-channel RGB Radiance Material definition

void plastic White_painted_room_ceiling
0
0
5 0.8462 0.8206 0.7263 0.0044 0.0000



#### 9-channel Radiance Material definition

**White\_painted\_room\_ceiling**

```
void plastic White_painted_room_ceiling
0
0
5 0.488 0.734 0.767 0 0
```

**White\_painted\_room\_ceiling**

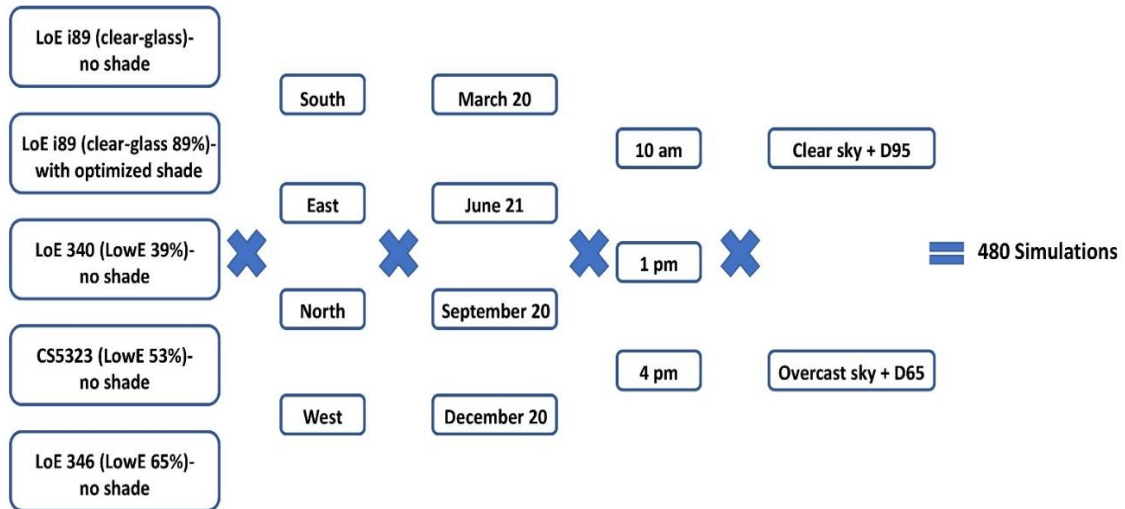
```
void plastic White_painted_room_ceiling
0
0
5 0.792 0.816 0.833 0 0
```

**White\_painted\_room\_ceiling**

```
void plastic White_painted_room_ceiling
0
0
5 0.840 0.847 0.850 0 0
```

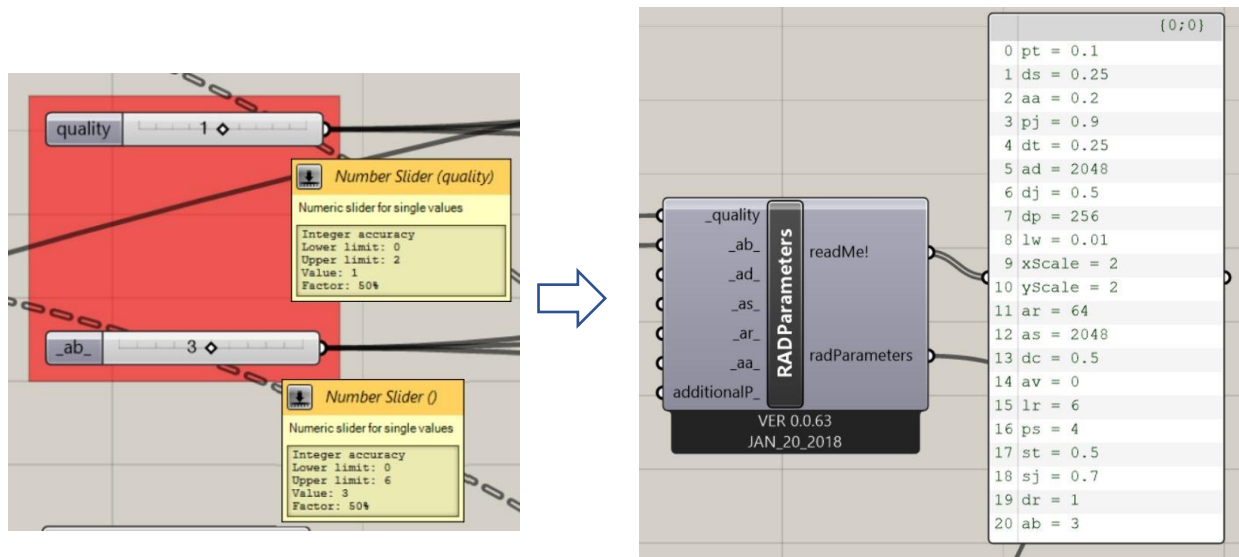
Figure 50: An example of extracted 9-channel RGB Radiance material. In contrast with the regular RGB channels, in LARK method, Inanici et al. have arranged the 9-channel from blue (B) channels to red (R) channels, B1, B2, B3, G1, G2, G3, R1, R2, R3.

### 3.4.3 Running the simulations



*Figure 51: Simulation scenarios*

The raytracing specifications were set on the medium quality (Figure 52). Each simulation with this quality took around 20 minutes, totally around 160 hours simulations excluding the pre-simulations and repeated simulations time. The simulations for the five glazing and shading scenarios based on the proposed schedule (Table 8) resulted in 480 simulations (Figure 51).



*Figure 52: Simulation quality set*

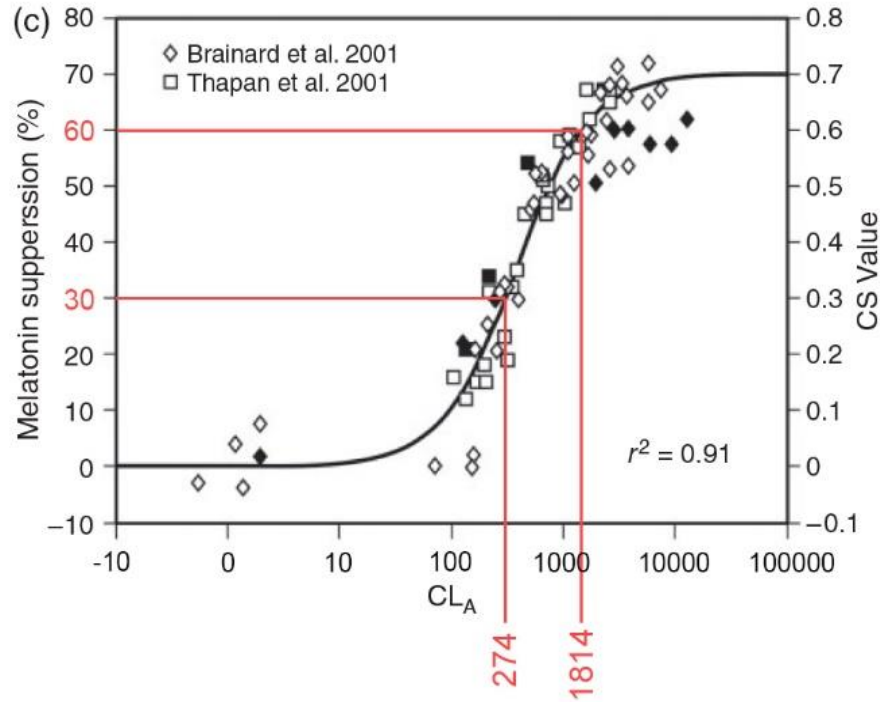
### 3.4.4 Simulation output

The outputs of the simulation were two excel (\*.csv) files for photopic and circadian light as well as the HDR images for one introduced point in the space. Since this study was intended to investigate the circadian light, the photopic lux and HDR images were not used in the data treatment.

### 3.5 Circadian light conversion

According to the developer [31], the number achieved from the simulation is sorted as the Rea et. al. [34] circadian light. However, it is not in the same scale as of the  $CL_A$ . Hence, using the Rea et al.'s excel sheet for calculating  $CL_A$  and CS [69] (Figure 53), the equivalent circadian lights (based on D65 and D95 daylight) for different steps of  $CL_A$  and CS were calculated (table 9). The values were then used to produce analyzable and scaled numbers. Circadian Stimuli (CS) ranged from 0 to 0.7 resulting in 0% to 70% melatonin suppression. Another study shows that at least 0.3

CS (30%) for a 1-hour duration is necessary to have an effective melatonin suppression [70]. Furthermore, the 30% threshold was considered as the minimum baseline in the data treatment.



**Figure 53:**  $CL_A$  curve based on CS values with highlighted 30% and 60% threshold [1].

### 3.6 Useful Circadian Light Frequency (UCLF)

Even though the higher CS values resulted from over-lit space affects circadian rhythm, it may also lead to discomfort or disable glare. The glare was not studied in this thesis, however, the ranges of circadian light that might produce discomfort visual conditions for the 9-point data arrangement were excluded. The categories in the Useful Daylight Illuminance (UDI) [24] were employed for this respect, which the illuminance number above 2000 lux is likely to produce visual

discomfort. The excluded numbers mainly represent the direct sunlight, where the interior blind should be activated. In this study, the interior blind schedule was not considered.

**Table 9:** The relationship between Inanici et al. CL [31] used in this study, Rea et al.  $CL_A$  and CS [1], and photopic lux based on D95 clear sky (a) and D65 overcast sky (b).

Inanici CL	Rea $CL_A$	Melatonin Suppression	CS value	Photopic lux	
17	35	5%	0.5	17	
35	70	10%	0.1	34	
55	108	15%	0.15	53	
80	154	20%	0.2	79	
103	209	25%	0.25	100	
135	274	30%	0.3	130	
174	360	35%	0.35	170	
226	460	40%	0.4	220	
293	603	45%	0.45	285	
393	815	50%	0.5	382	
460	966	52.5%	0.525	447	
550	1157	55%	0.55	535	
669	1418	57.5%	0.575	650	
844	1814	60%	0.6	820	
936	2025	61%	0.61	910	
1050	2284	62%	0.62	1020	
1194	2592	63%	0.63	1160	
1369	3054	64%	0.64	1330	
1626	3623	65%	0.65	1580	
1976	4503	66%	0.66	1920	
2573	6033	67%	0.67	2500	Visual discomfort
3600	8618	68%	0.68	3500	
6176	16817	69%	0.69	6000	

Inanici CL	Rea $CL_A$	Melatonin Suppression	CS value	Photopic lux	
18	35	5%	0.5	23	
37	70	10%	0.1	47	
57	108	15%	0.15	72	
80	154	20%	0.2	102	
110	209	25%	0.25	138	
140	274	30%	0.3	180	
185	360	35%	0.35	235	
240	460	40%	0.4	300	
310	603	45%	0.45	390	
415	815	50%	0.5	520	
490	966	52.5%	0.525	615	
580	1157	55%	0.55	730	
705	1418	57.5%	0.575	885	
880	1814	60%	0.6	1100	
980	2025	61%	0.61	1235	
1100	2284	62%	0.62	1380	
1235	2592	63%	0.63	1550	
1430	3054	64%	0.64	1800	
1670	3623	65%	0.65	2100	
2030	4503	66%	0.66	2550	Visual discomfort
2625	6033	67%	0.67	3300	
3580	8618	68%	0.68	4500	
6360	16817	69%	0.69	8000	

The frequent points and directions categorized in the circadian light ranges were scaled to the Rea et al.  $CL_A$  and CS [1] values for CIE D95 and D65 sky lights (Table 9). The values were then weighted based on the average melatonin suppression for each range. The ranges for melatonin suppression shown in the Table 9 are not the same because as higher CS (melatonin suppression) is targeted, wider circadian light range is needed.

**Table 10:** Circadian light frequency scales based on Rea et al.  $CL_A$  and CS [1], and photopic lux in this study, (a) D65 overcast sky and (b) D95 clear sky.

Range	Melatonin suppression scale	Frequent points in both direction	Circadian light range	Photopic lux range	Range	Melatonin suppression scale	Frequent points in both direction	Circadian light range	Photopic lux range
1	0%-5%	0 - 18	0 - 18	0 - 23	1	0%-5%	0 - 18	0 - 17	0 - 17
2	5%-10%	0 - 18	18 - 37	23 - 47	2	5%-10%	0 - 18	17 - 35	17 - 34
3	10%-15%	0 - 18	37 - 57	47 - 72	3	10%-15%	0 - 18	35 - 55	34 - 53
4	15%-20%	0 - 18	57 - 80	72 - 102	4	15%-20%	0 - 18	55 - 80	53 - 79
5	20%-25%	0 - 18	80 - 110	102 - 138	5	20%-25%	0 - 18	80 - 103	79 - 100
6	25%-30%	0 - 18	110 - 140	138 - 180	6	25%-30%	0 - 18	103 - 135	100 - 130
7	30%-35%	0 - 18	140 - 185	180 - 235	7	30%-35%	0 - 18	135 - 174	130 - 170
8	35%-40%	0 - 18	185 - 240	235 - 300	8	35%-40%	0 - 18	174 - 226	170 - 220
9	40%-45%	0 - 18	240 - 310	300 - 390	9	40%-45%	0 - 18	226 - 263	220 - 285
10	45%-50%	0 - 18	310 - 415	390 - 520	10	45%-50%	0 - 18	293 - 393	285 - 382
11	50%-52.5%	0 - 18	415 - 490	520 - 615	11	50%-52.5%	0 - 18	393 - 460	382 - 447
12	52.5%-55%	0 - 18	490 - 580	615 - 730	12	52.5%-55%	0 - 18	460 - 550	447 - 535
13	55%-57.5%	0 - 18	580 - 705	730 - 885	13	55%-57.5%	0 - 18	550 - 669	535 - 650
14	57.5%-60%	0 - 18	705 - 880	885 - 1100	14	57.5%-60%	0 - 18	669 - 844	650 - 820
15	60%-61%	0 - 18	880 - 980	1100 - 1235	15	60%-61%	0 - 18	844 - 936	820 - 910
16	61%-62%	0 - 18	980 - 1100	1235 - 1380	16	61%-62%	0 - 18	936 - 1050	910 - 1020
17	62%-63%	0 - 18	1100 - 1235	1380 - 1550	17	62%-63%	0 - 18	1050 - 1194	1020 - 1160
18	63%-64%	0 - 18	1235 - 1430	1550 - 1800	18	63%-64%	0 - 18	1194 - 1369	1160 - 1330
19	64%-65%	0 - 18	1430 - 1670	1800 - 2100	19	64%-65%	0 - 18	1369 - 1626	1330 - 1580
(a)					20	65%-66.2%	0 - 18	1626 - 2058	1580 - 2000

(b)

### 3.6.1 UCLF equation development

From the Table 10, the number of points in all view directions that fall within each circadian light range (19 ranges for D65 sky and 20 ranges for D95) are counted and multiplied by the average melatonin suppression for each range. The sum stands for Useful Circadian Light Frequency (UCLF) for each circadian light simulation for the current method and software. The maximum possible melatonin suppression for each study time in this method is 65.75% for the clear sky and 64.5% for the overcast sky.

Useful Circadian Light Frequency (UCLF) =

$$\sum \left( \frac{\text{Number of points in each range}}{\text{Total points}} \right) *$$

$$\text{Average melatonin suppression of each range} = \left( \frac{\text{Range 1 points}}{\text{Total points}} \right) * 2.5\% +$$

$$\left( \frac{\text{Range 2 points}}{\text{Total points}} \right) * 7.5\% + \dots \left( \frac{\text{Range 11 points}}{\text{Total points}} \right) * 51.25\% +$$



$$\left(\frac{\text{Range 12 points}}{\text{Total points}}\right) * 53.75\% + \dots \left(\frac{\text{Range 15 points}}{\text{Total points}}\right) * 60.5\% +$$

$$\left(\frac{\text{Range 16 points}}{\text{Total points}}\right) * 61.5\% + \dots$$

From the above multiplication the following equation is derived:

$$UCLF = \left(\sum_{n=0}^{n=9} \frac{F_{n+1}}{\text{Total}_p} * (2n + 1) * 2.5\right) + \left(\sum_{n=0}^{n=4} \frac{F_{n+10}}{\text{Total}_p} * (n + 41) * 1.25\right) +$$

$$\left(\sum_{n=0}^{n=4} \frac{F_{n+15}}{\text{Total}_p} * (n + 60.5)\right) \quad (25)$$

Where:

$F_n$  : Number of points (in both directions) in each circadian light range.

$\text{Total}_p$  : Total number of points in both directions, here 18.

Up to this point, the optimized shades for the four orientations were designed based on interior thermal needs. The shades were then evaluated and compared to the three test cases (Low-E windows) according to the annual and single-point-in-time illuminance. Two conversion tables (Tables 9(a) and 9(b)) were set to convert the circadian light simulation outputs to the  $CL_A$  and CS. In this chapter a new analysis method, UCLF, was also introduced to exclude the effect of probable glare-associated light from circadian light analysis. In the next chapter, the data will be treated in four different categories. The results of the circadian light for the Points 1 and 3, the average circadian light in three distances from the windows, the total circadian light, and the UCLF will be further discussed in the next chapter.

## **CHAPTER 4**

### **RESULTS AND DISCUSSIONS**

#### **4.1 Results**

The main objectives in this study are: the circadian light reached to the locations of the two office workers, total circadian light changes based on the distances from the window, and Useful Circadian Light Frequency (UCLF) functionality in comparison with total circadian stimulation in the space. Hence, the data were treated in four main categories: (i) circadian light values at Point 1 and Point 3 (locations of two office workers), (ii) the average circadian light values based on the three distances from the window at two directions (window and wall), (iii) UCLF, and (iv) total circadian stimulation.

##### **4.1.1 Circadian illuminance for points 1 & 3**

The average values of the three view directions (Figure 49) resulted from the simulations are plotted on the temporal graphs for points 1 and 3 (locations of two office workers). The values represent the Inanici et al. [31] circadian illuminance. The 30% and 60% threshold of the maximum 70% melatonin suppression are highlighted on each graph. The 30% threshold in these data stands for the minimum effective circadian light [70]. The graphs also categorized under the clear sky (CIE D95) and the overcast sky (CIE D65) conditions. Due to differences in the D95 and D65 circadian light intensity (Figure 48), the 30% and 60% threshold line levels are slightly different in the two sky conditions. The values under 50 circadian illuminance, which are negligible in terms of melatonin suppression, and over 5000 circadian illuminance that are close to 70% melatonin suppression are not plotted on the graphs.

South orientation  
Clear sky

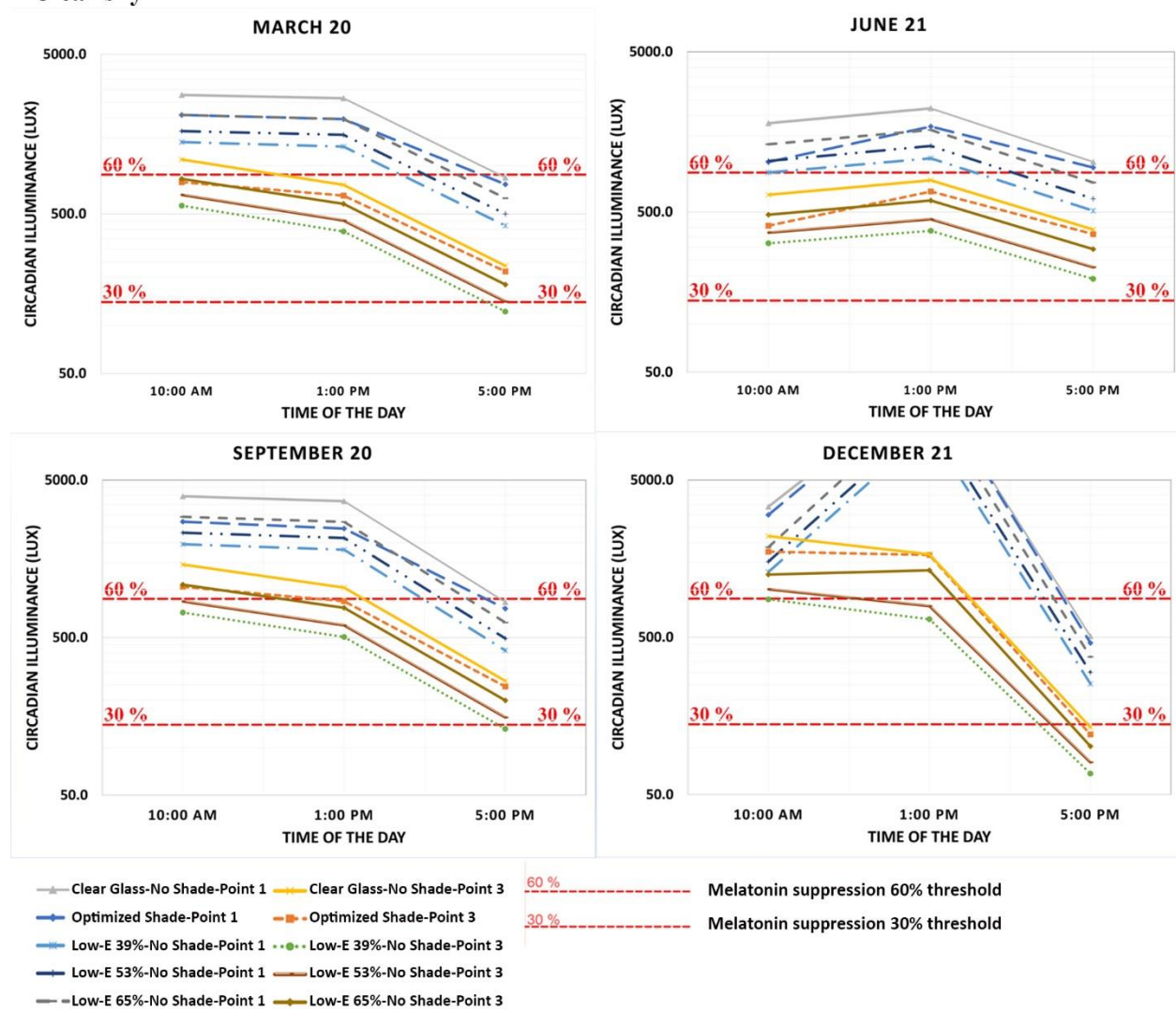
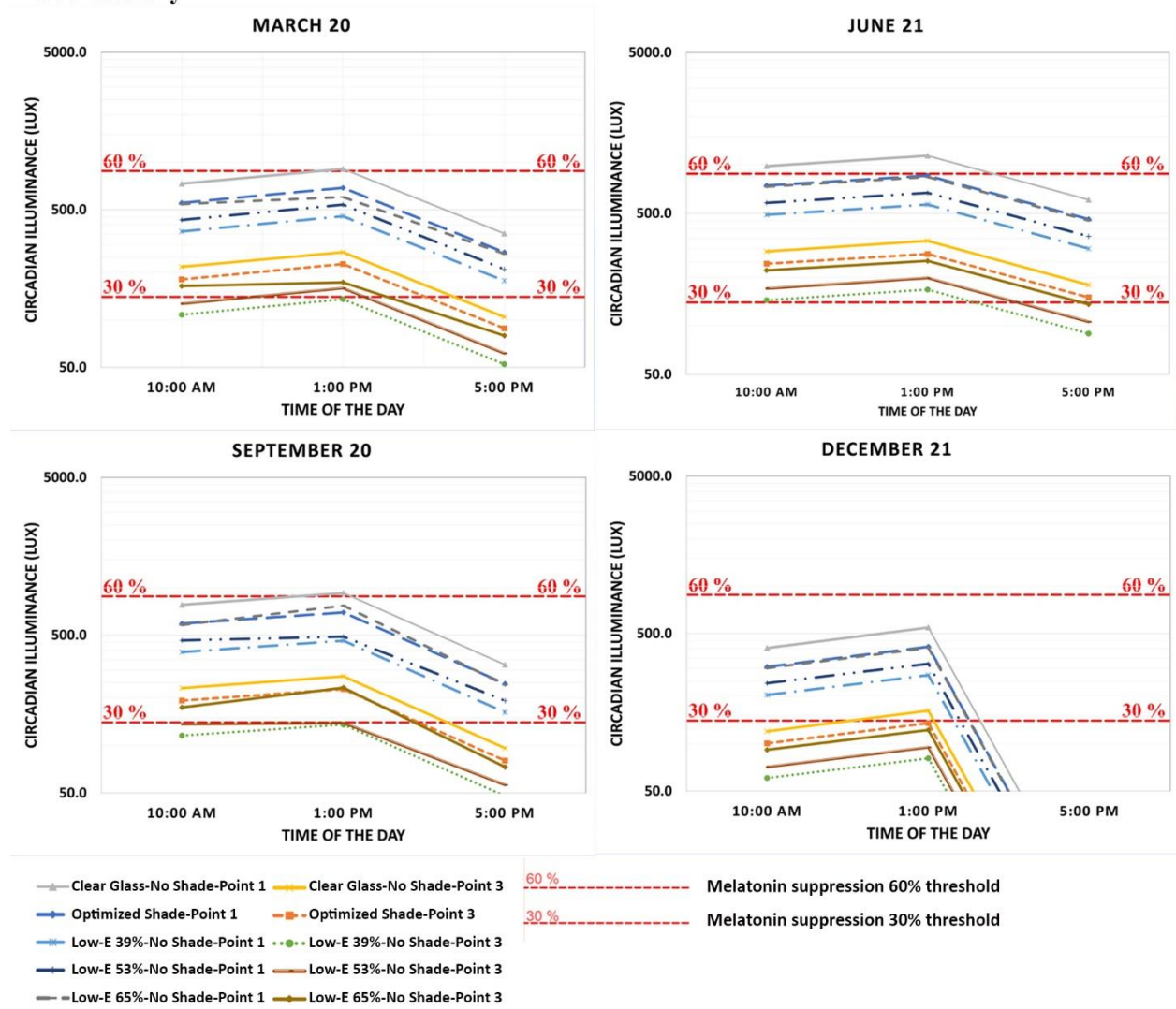


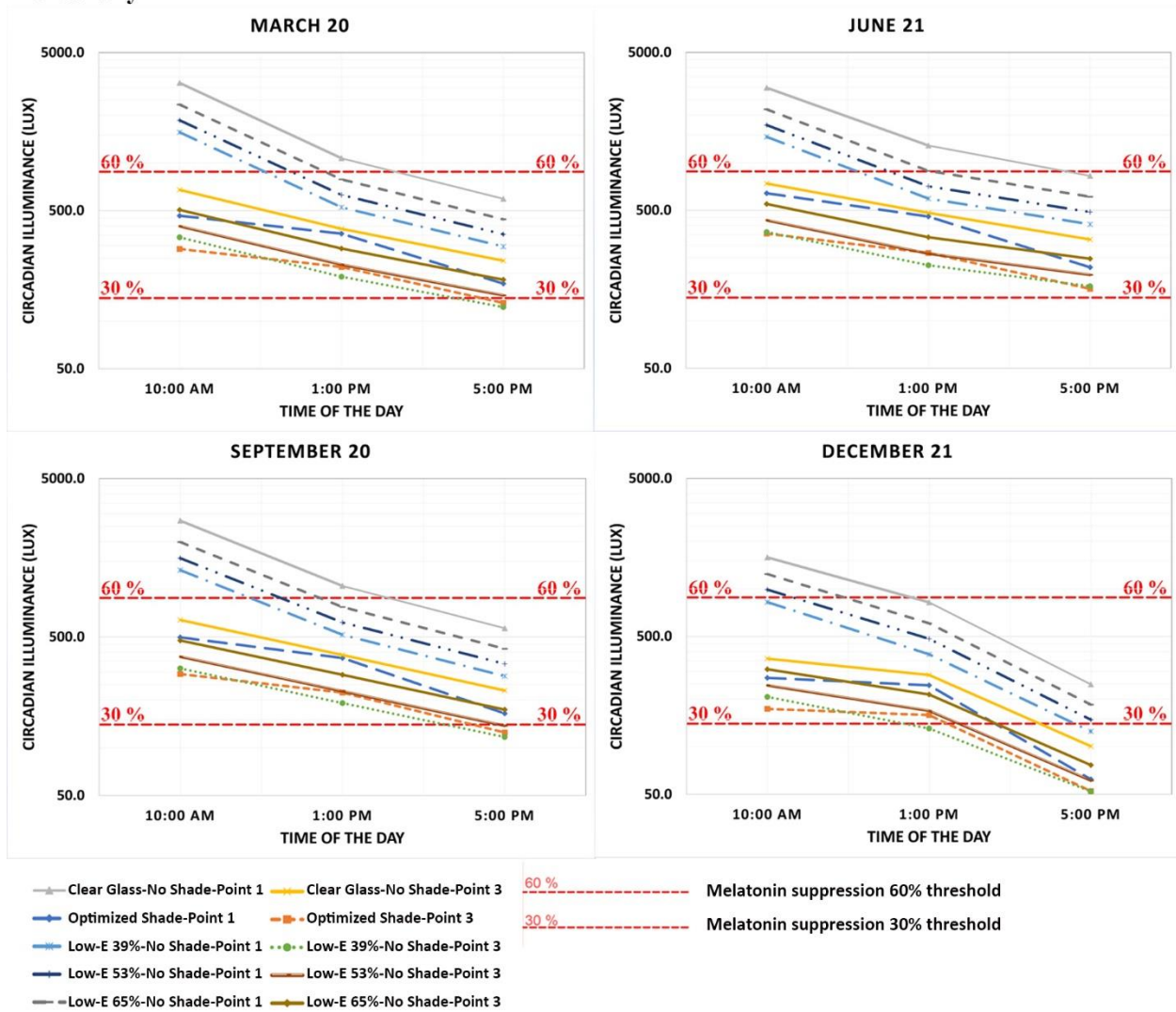
Figure 54: Circadian illuminance reached to the two office workers locations (points 1 & 3) for 4 study dates from south under clear sky condition.

**South orientation  
Overcast sky**



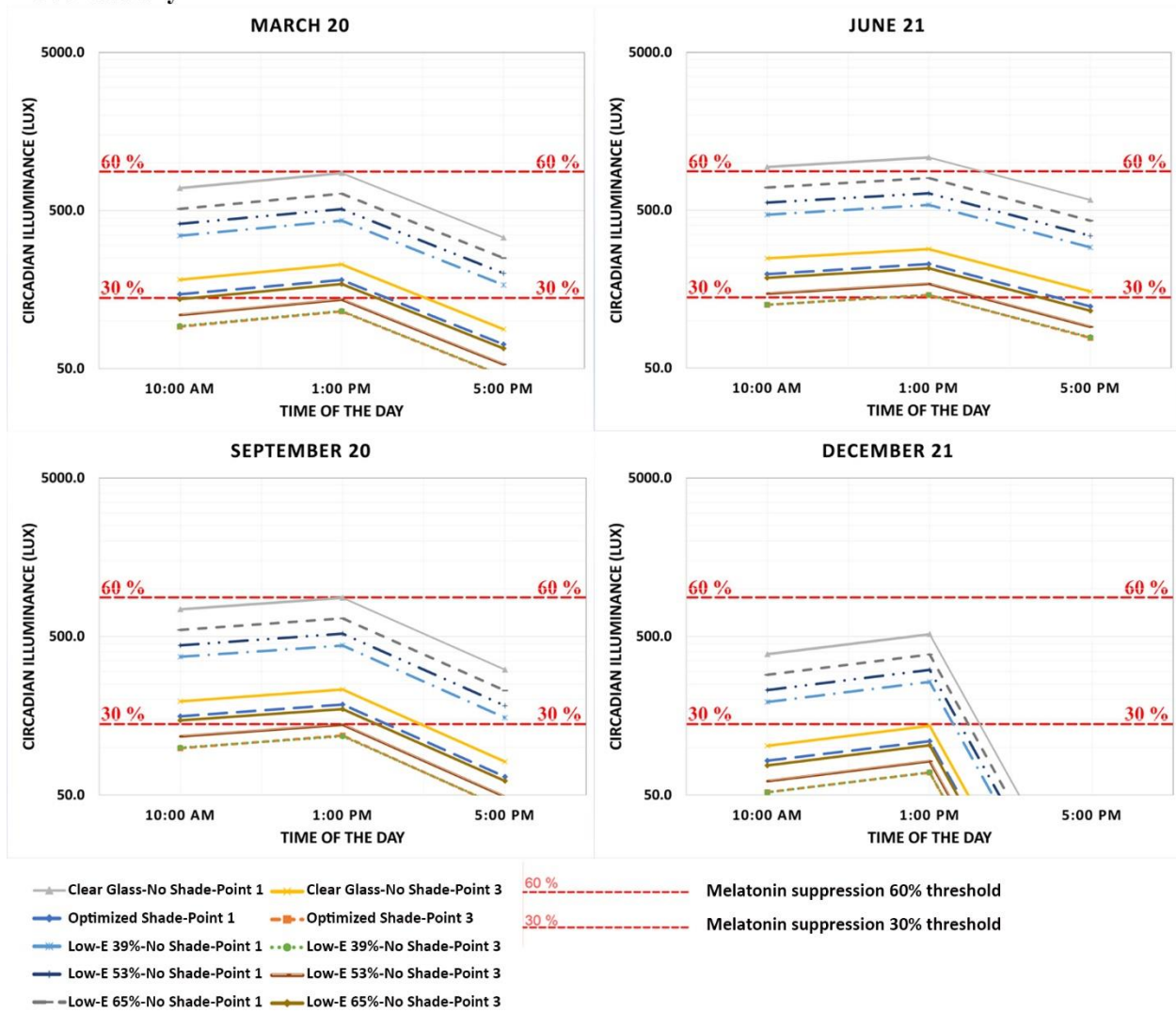
*Figure 55: Circadian illuminance reached to the two office workers locations (points 1 & 3) for 4 study dates from south under overcast sky condition.*

**East orientation**  
**Clear sky**



*Figure 56: Circadian illuminance reached to the two office workers locations (points 1 & 3) for 4 study dates from east under clear sky condition.*

**East orientation**  
**Overcast sky**



*Figure 57: Circadian illuminance reached to the two office workers locations (points 1 & 3) for 4 study dates from east under overcast sky condition.*

North orientation  
Clear sky

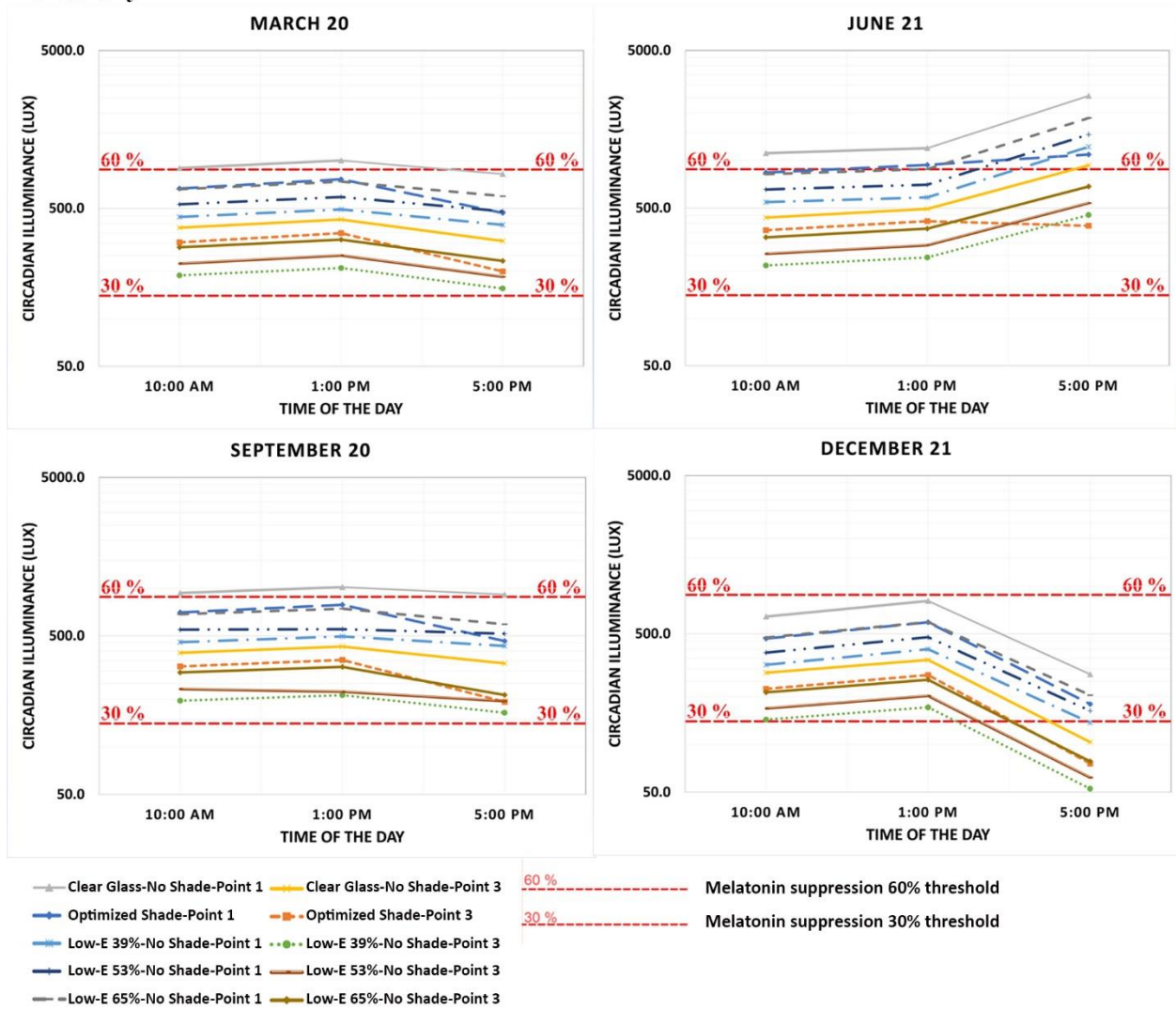


Figure 58: Circadian illuminance reached to the two office workers locations (points 1 & 3) for 4 study dates from North under clear sky condition.

North orientation  
Overcast sky

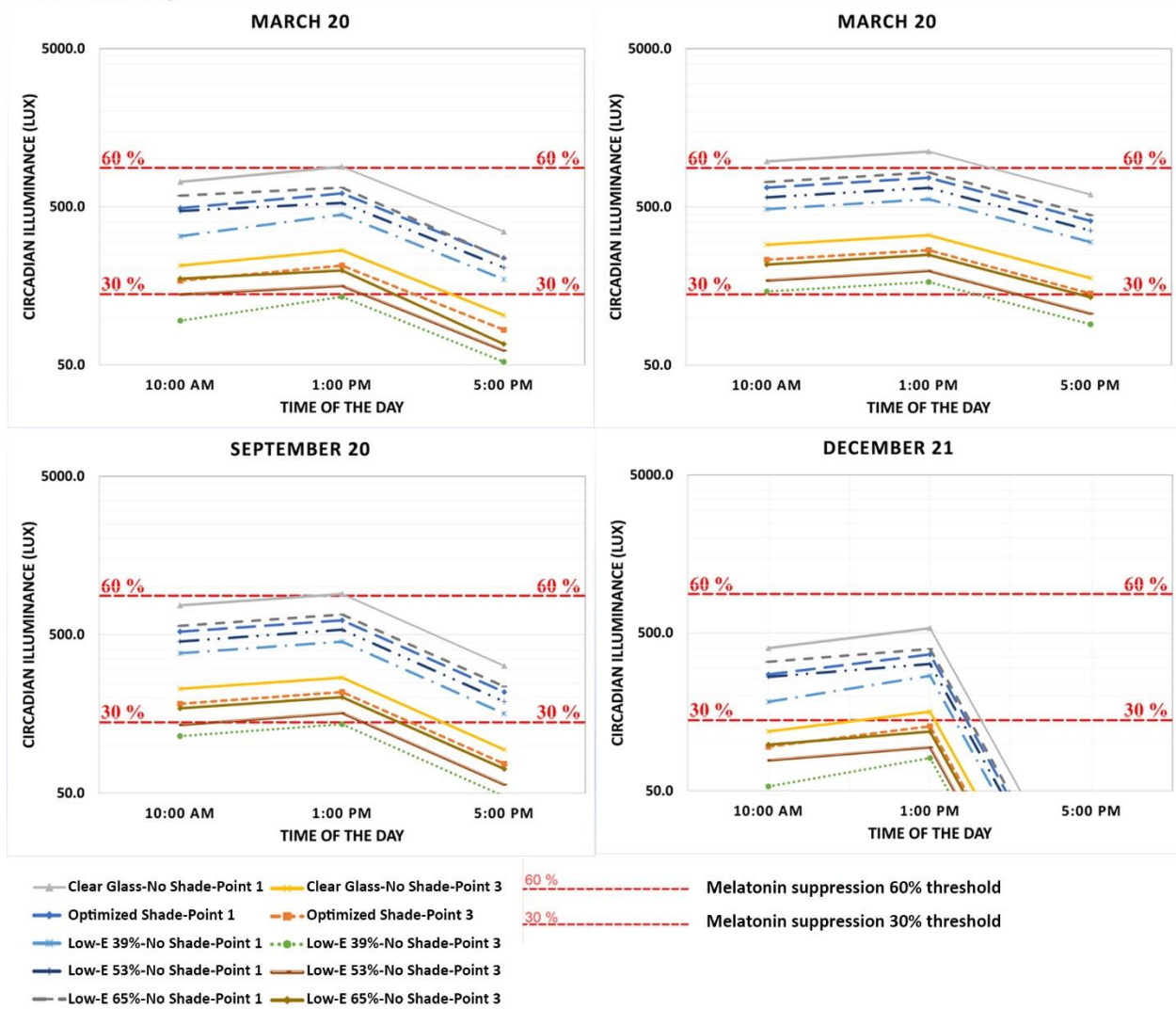


Figure 59: Circadian illuminance reached to the two office workers locations (points 1 & 3) for 4 study dates from North under overcast sky condition.



West orientation  
Clear sky

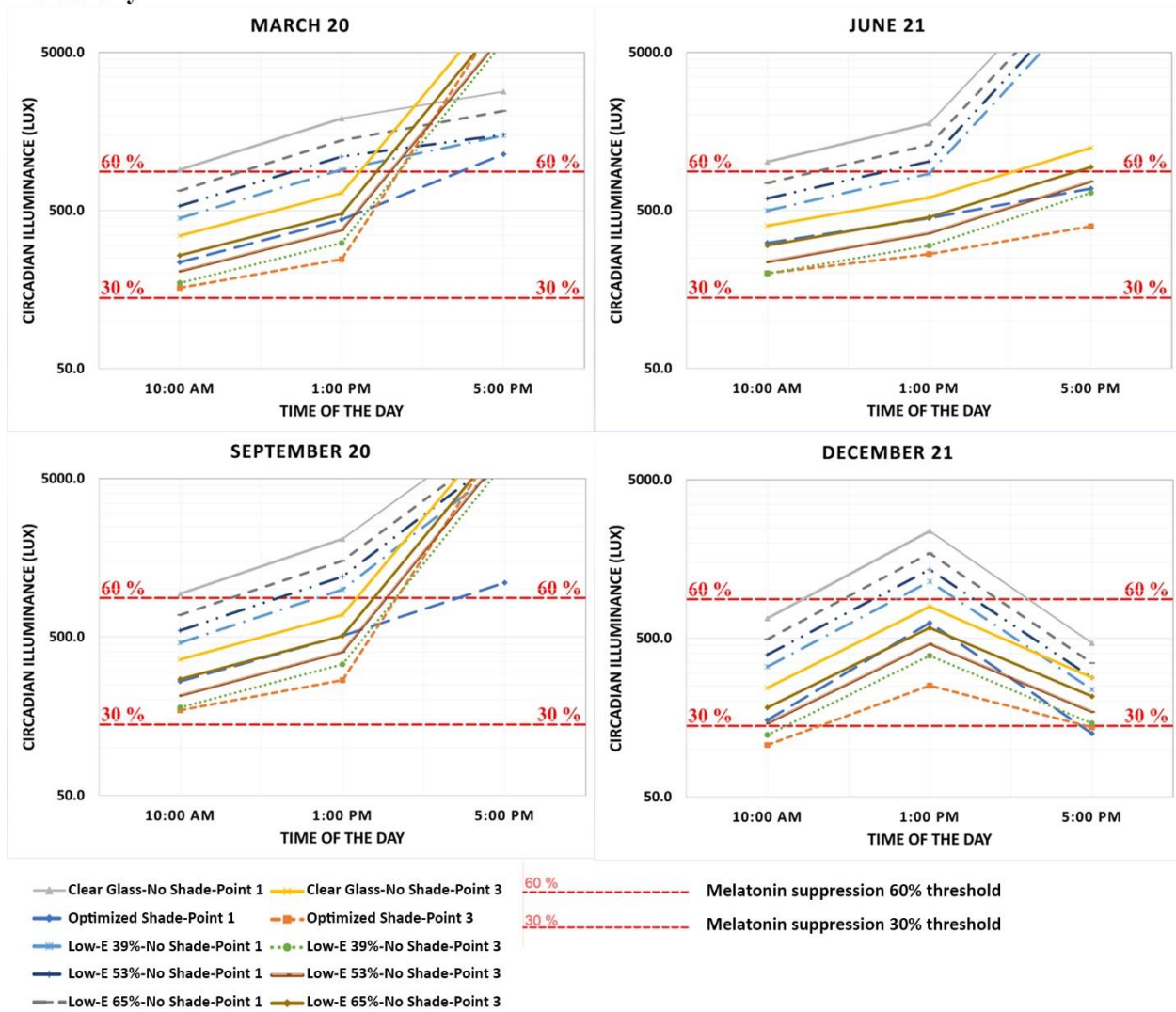


Figure 60: Circadian illuminance reached to the two office workers locations (points 1 & 3) for 4 study dates from west under clear sky condition.

West orientation  
Overcast sky

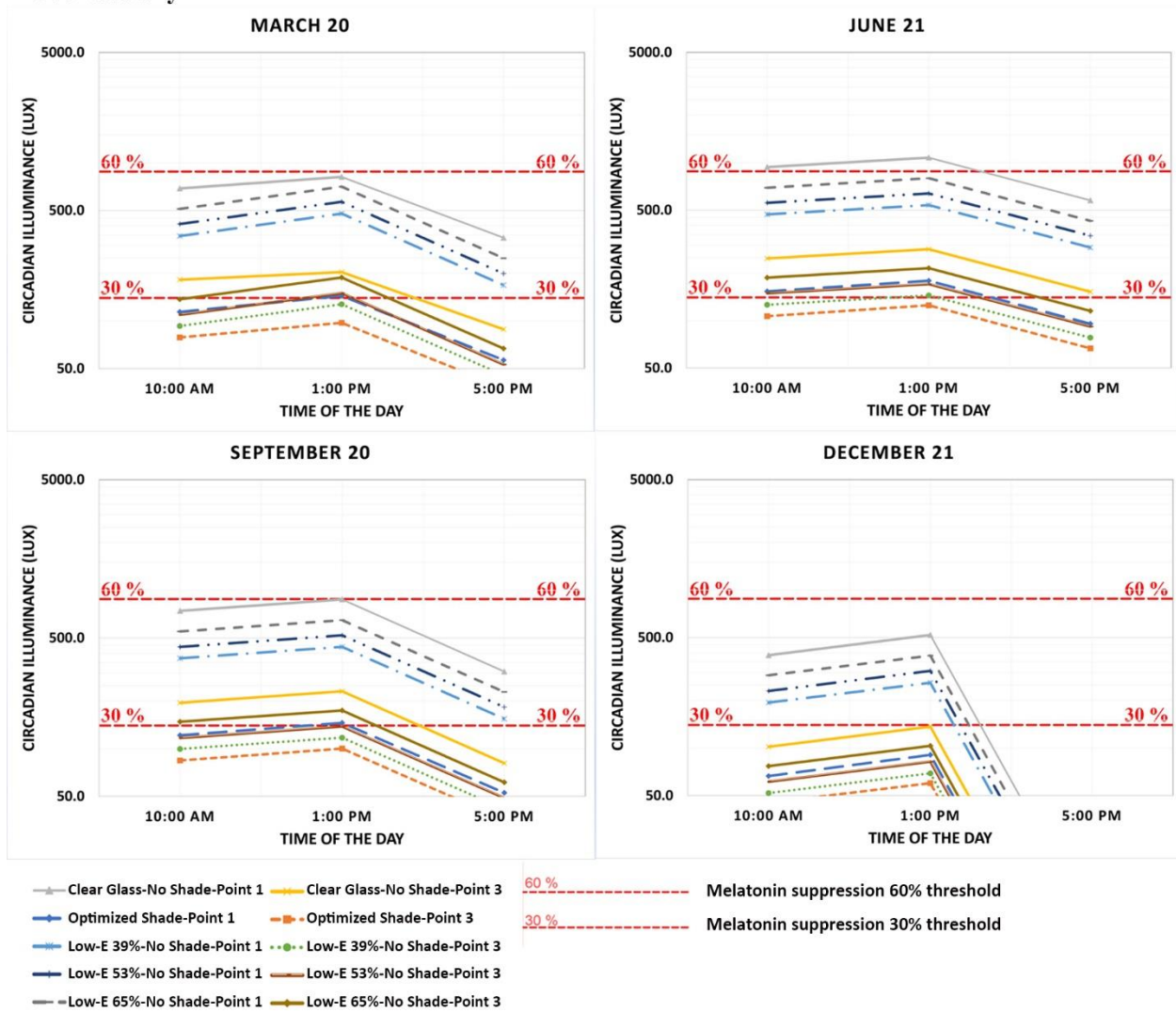
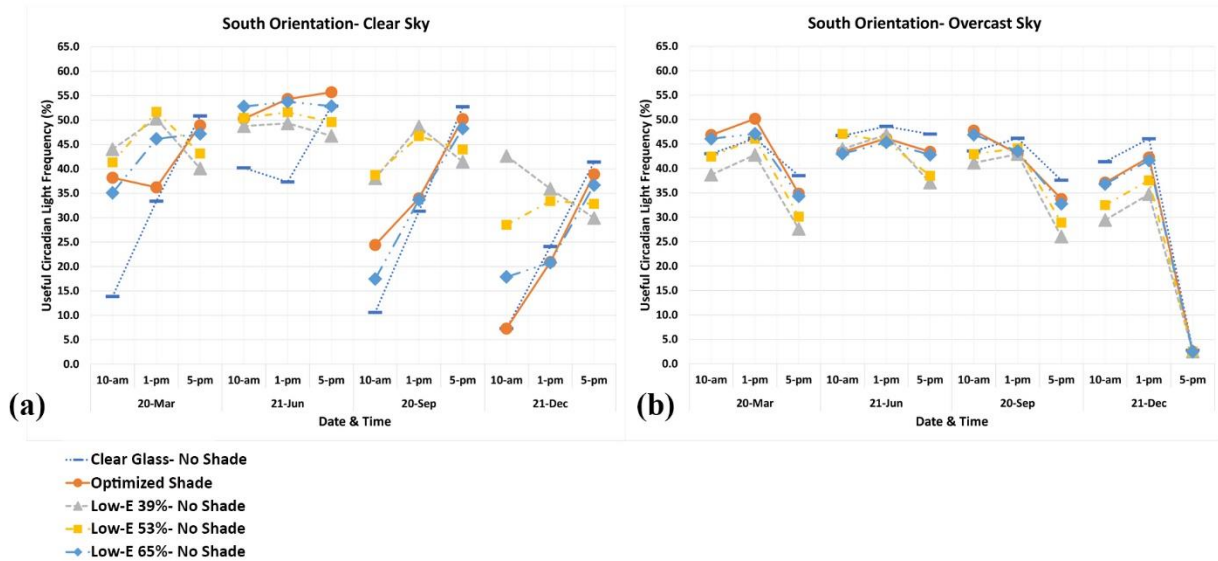


Figure 61: Circadian illuminance reached to the two office workers locations (points 1 & 3) for 4 study dates from west under overcast sky condition.

### 4.1.2 Useful Circadian Light Frequency (UCLF)

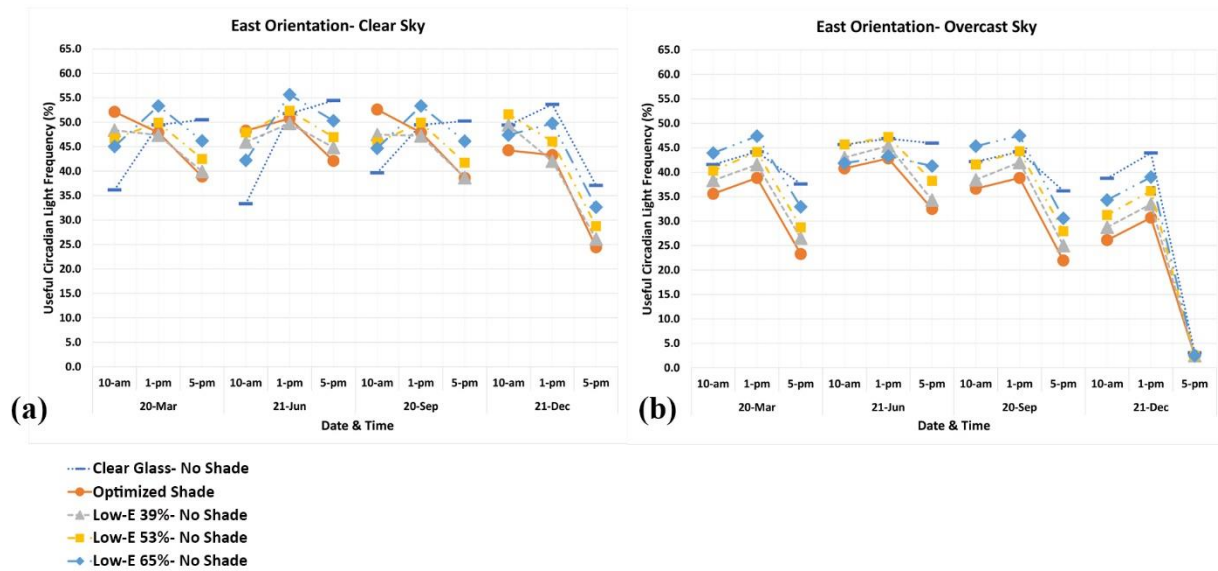
The following graphs represent the temporal UCLF values for the five case studies: the baseline case (clear glass with optimized shade), the reference case (clear glass without shade), and the three test cases. The UCLF data are calculated based on the 9 evenly distributed points in two directions (Figure 49) under clear and overcast sky conditions, and at south, east, north, and west orientations. The values fall within 0% to 66% for the clear sky (D95) and 0% to 65% for the overcast sky (D65) due to differences in circadian light intensities (Table 10).

#### South orientation



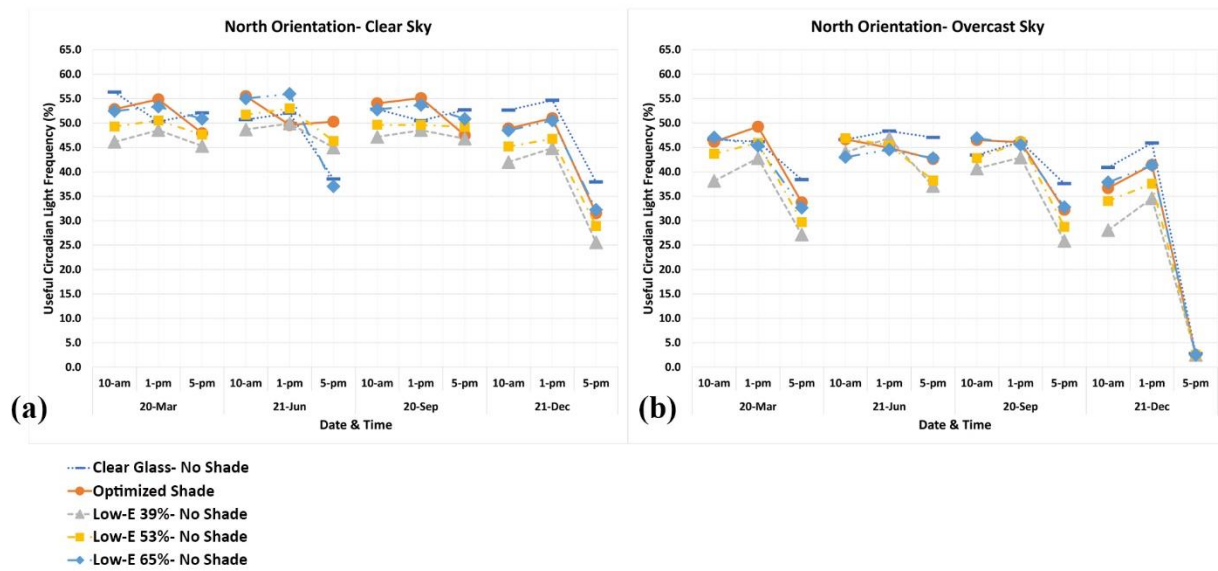
**Figure 62:** Useful Circadian Light Frequency (UCLF) for south orientation and two sky conditions, clear sky (a) and overcast sky (b)

## East orientation



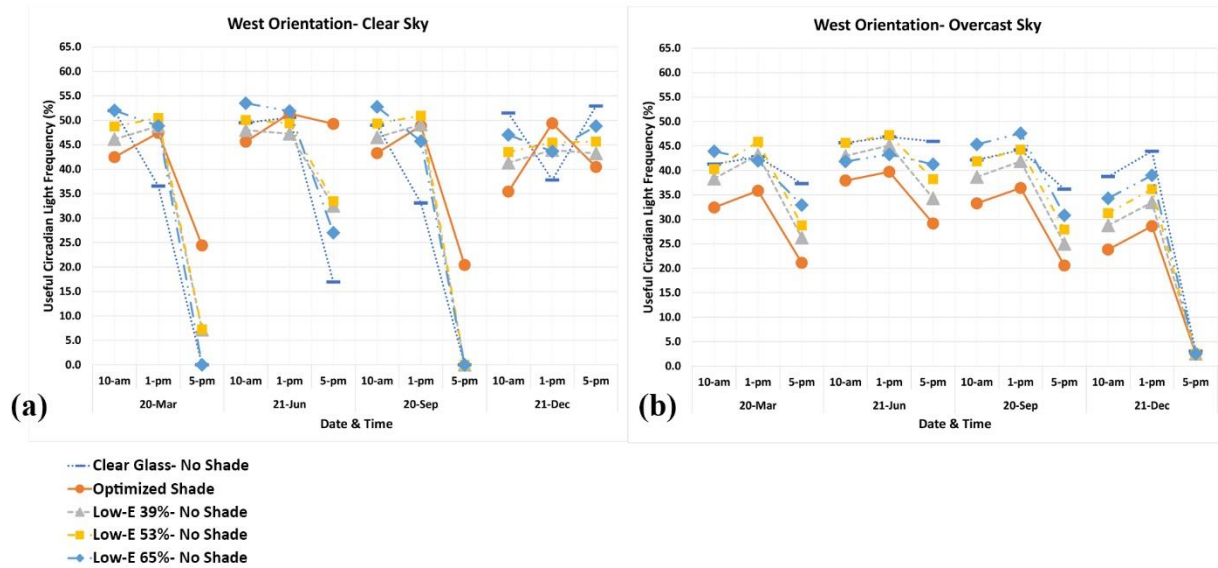
**Figure 63:** Useful Circadian Light Frequency (UCLF) for south orientation and two sky conditions, clear sky (a) and overcast sky (b)

## North orientation



**Figure 64:** Useful Circadian Light Frequency (UCLF) for North orientation and two sky conditions, clear sky (a) and overcast sky (b)

## West orientation

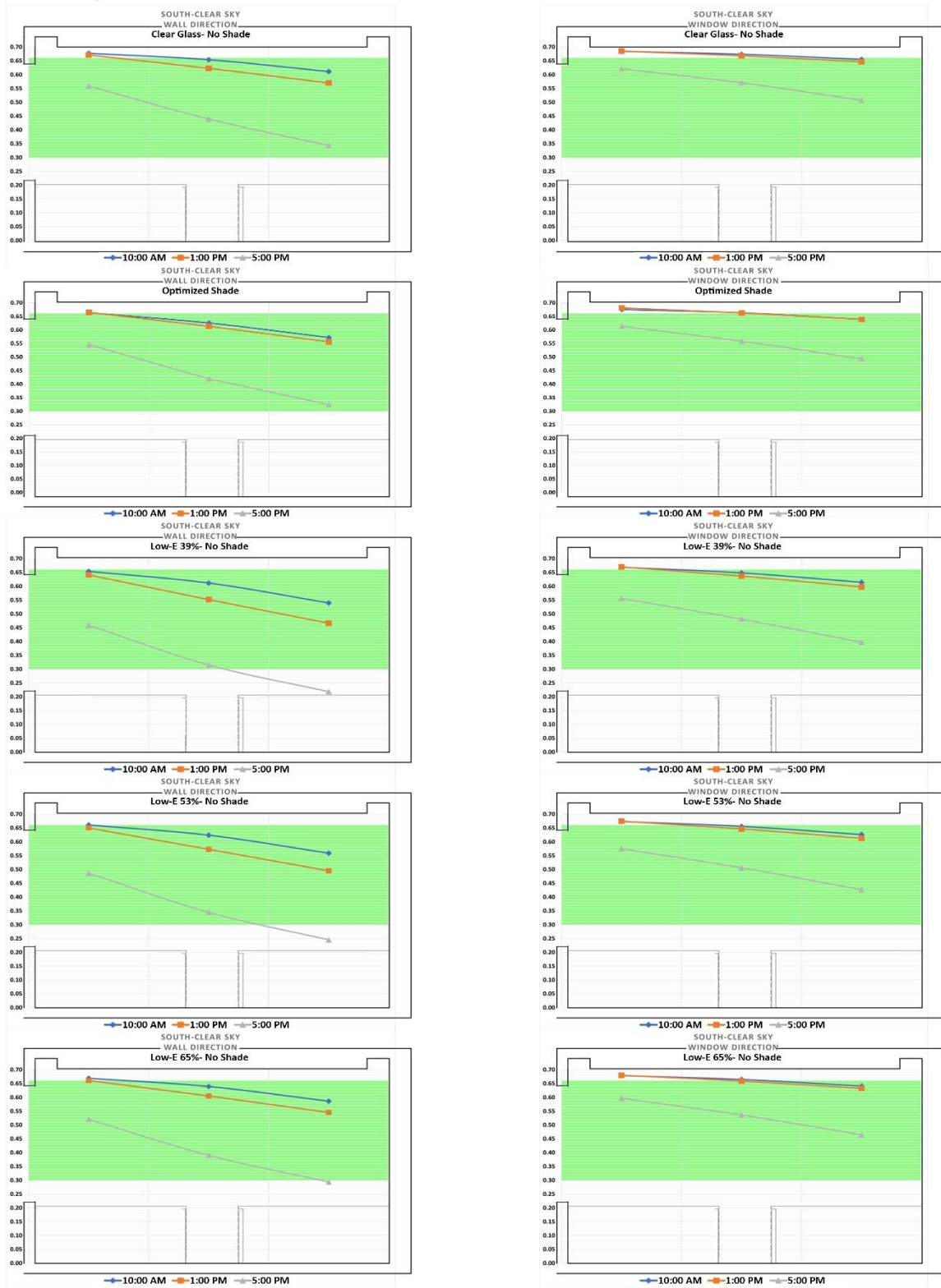


**Figure 65:** Useful Circadian Light Frequency (UCLF) for west orientation and two sky conditions, clear sky (a) and overcast sky (b)

### 4.3 Circadian light availability based on the distance from window

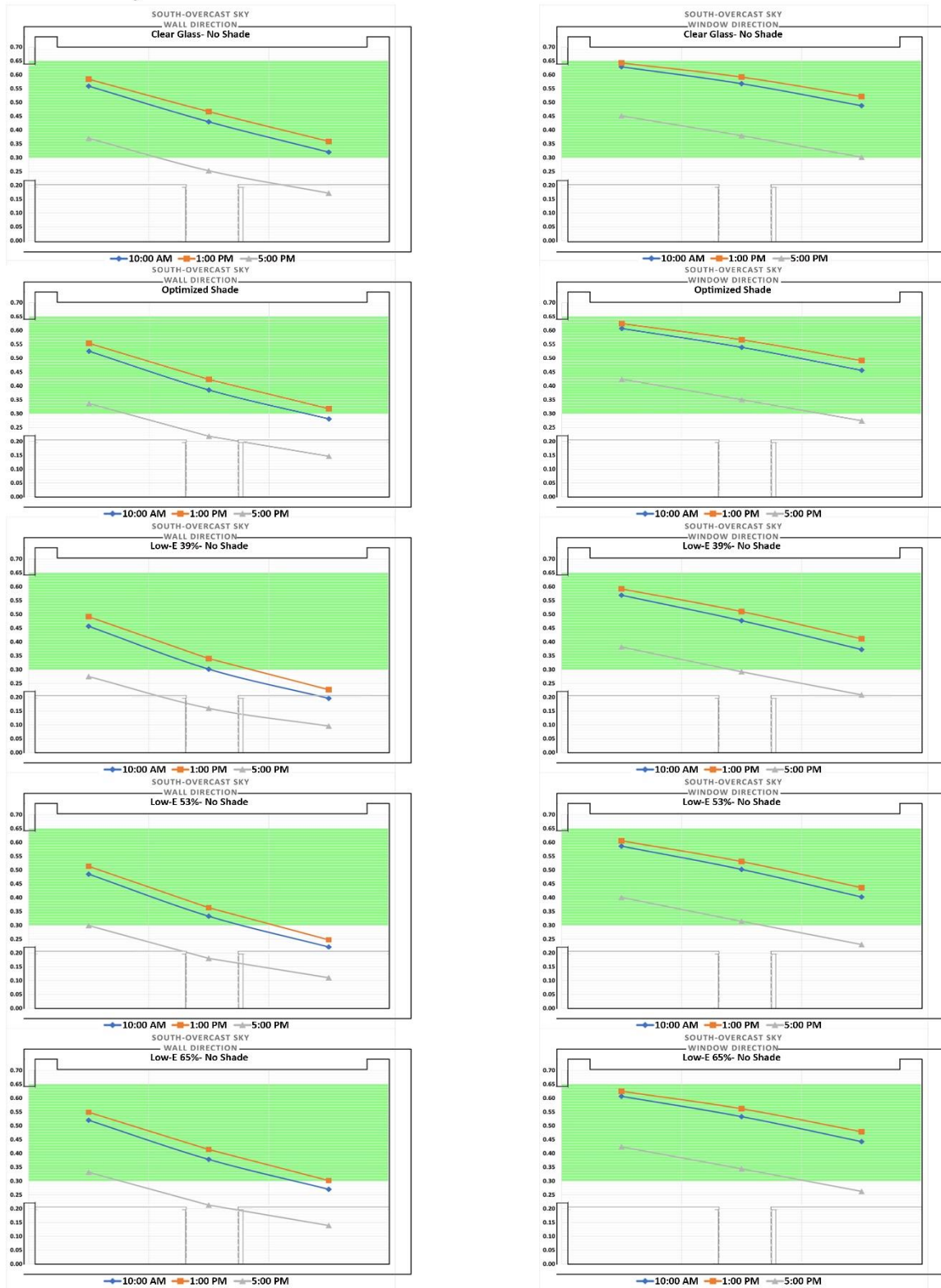
The average of circadian stimuli (CS) for three rows, points 1,4,7, points 2,5,8, and points 3,6,9, in three distances of 2'-8", 8', and 5'-4" from the window (Figure 22) are graphed on sections for each case study and for two view directions (window and wall). Each graph shows the average circadian stimuli (melatonin suppression) of four study days based on three times per day; 10 a.m., 1 p.m., and 5 p.m. The circadian stimuli values are from 0% to 70%, and the shaded area represents the useful melatonin suppression range.

## South- Clear sky



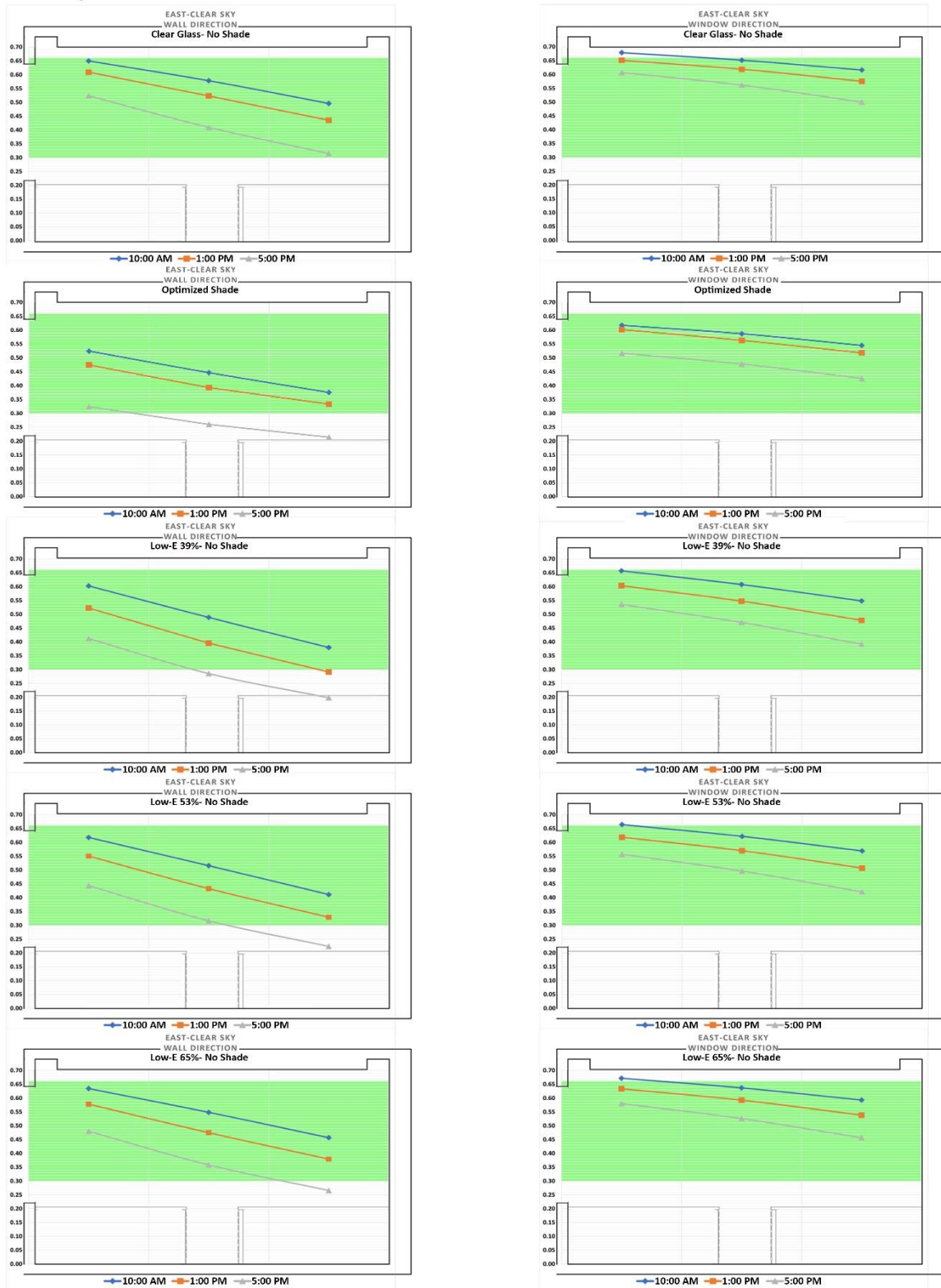
**Figure 66:** Total circadian light availability for south orientation-clear sky condition in three distances from window and two directions of view, window direction (right) and front wall direction (left). The shaded area represents the useful circadian light, 30% to 66%.

## South- Overcast sky



**Figure 67:** Total circadian light availability for south orientation-overcast sky condition in three distances from window and two directions of view, window direction (right) and front wall direction (left). The shaded area represents the useful circadian light, 30% to 65%.

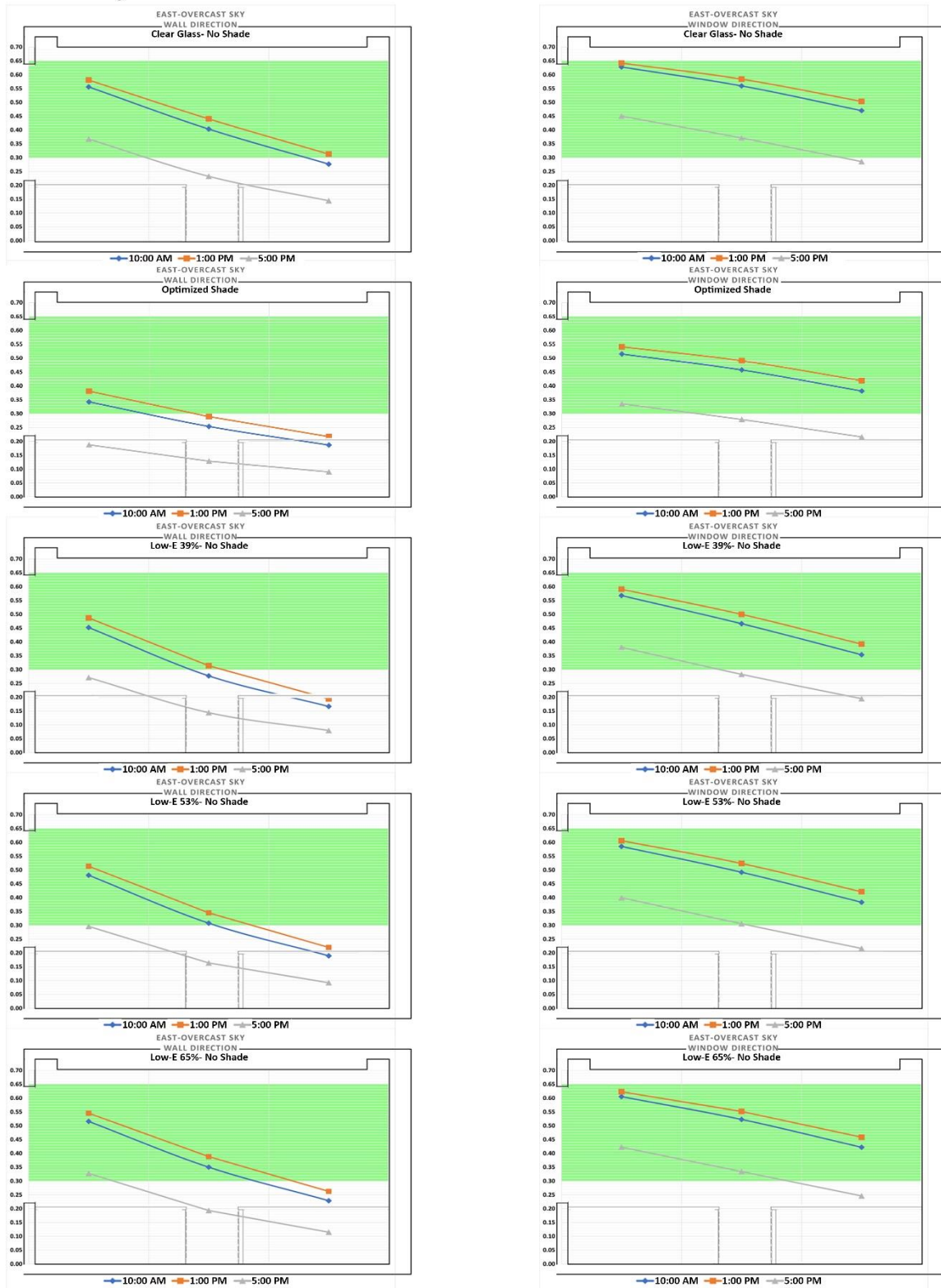
## East- Clear sky



**Figure 68:** Total circadian light availability for east orientation-clear sky condition in three distances from window and two directions of view, window direction (right) and front wall direction (left). The shaded area represents the useful circadian light, 30% to 66%.

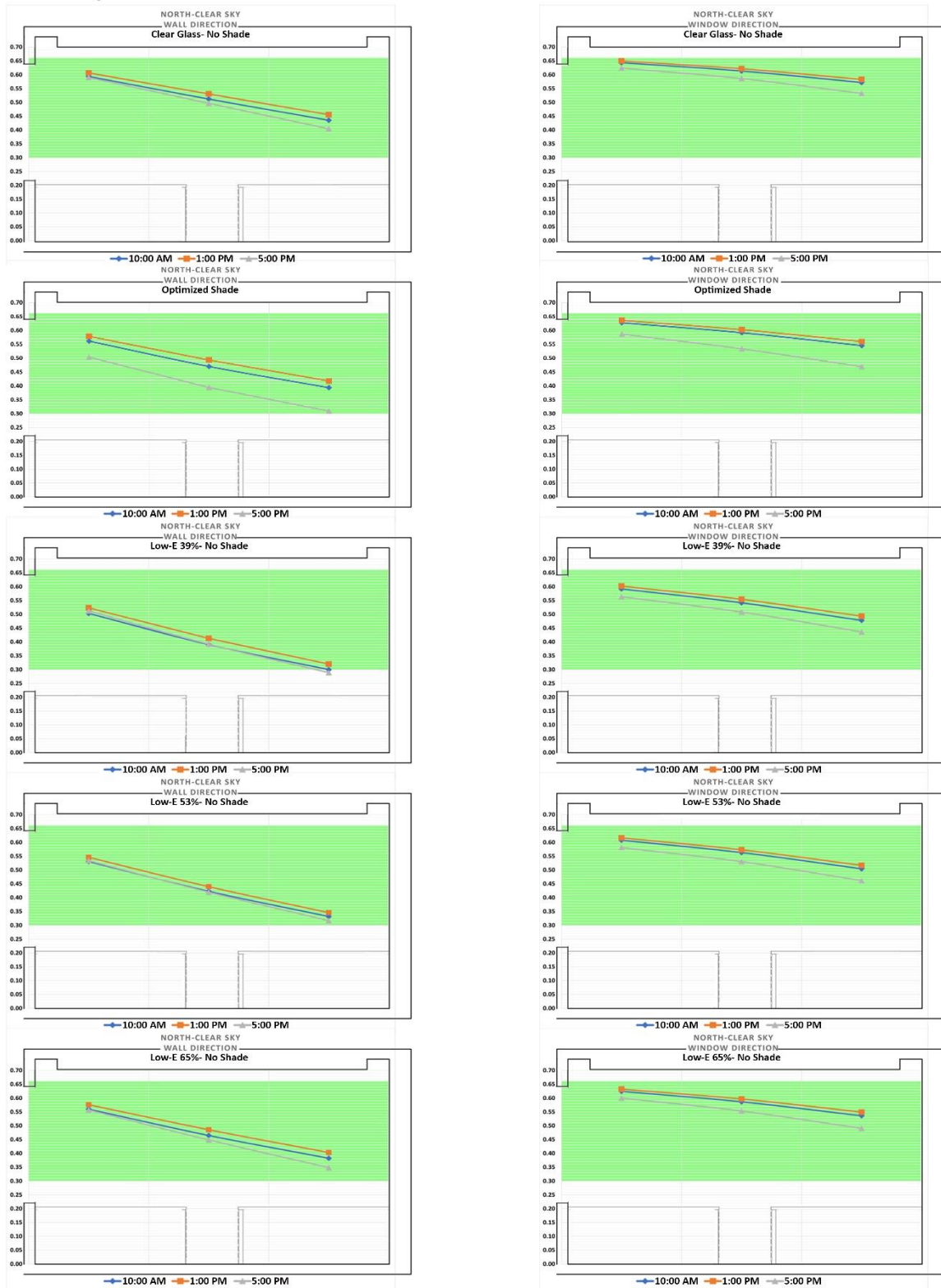


## East- Overcast sky



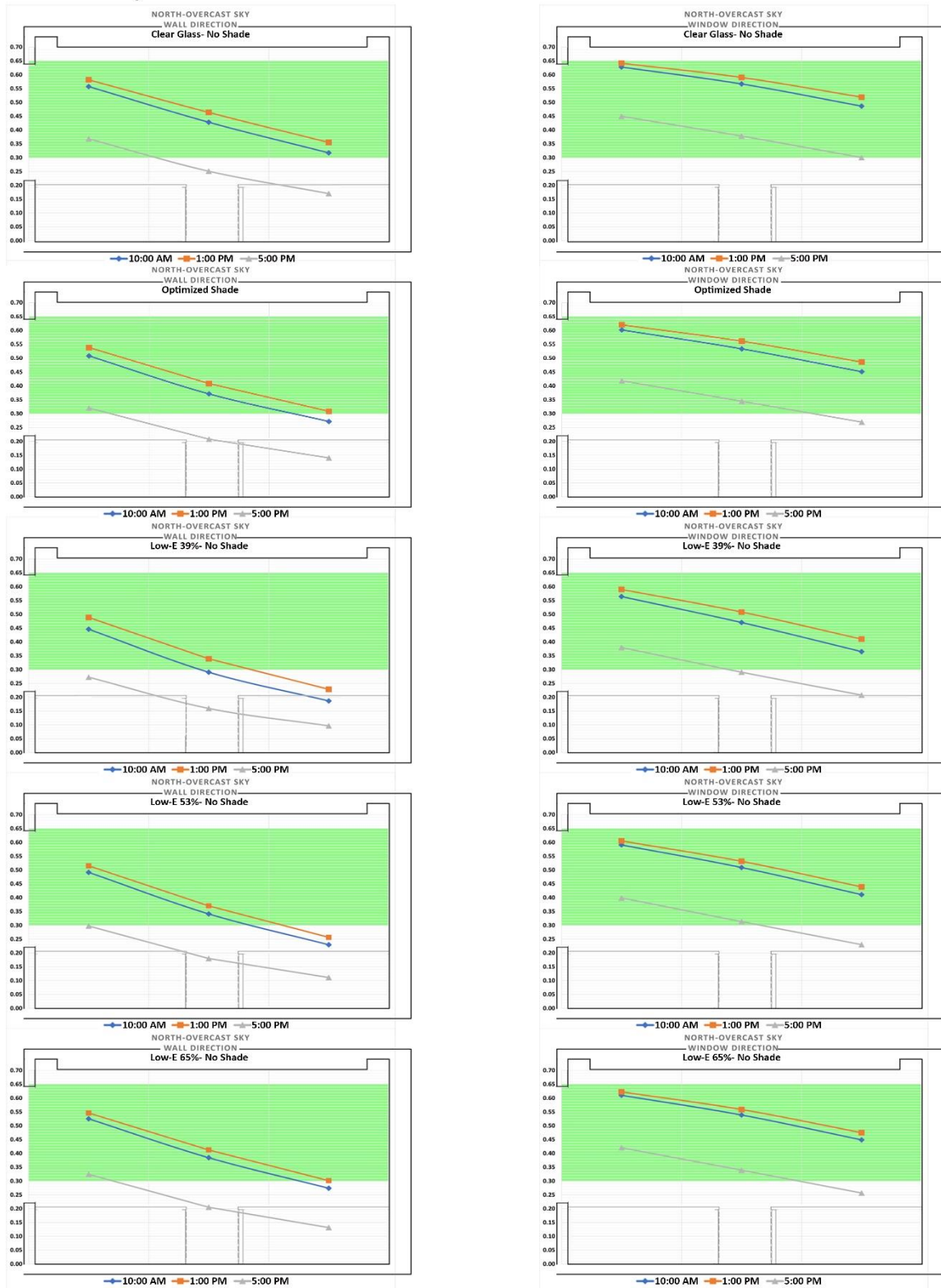
**Figure 69:** Total circadian light availability for east orientation-overcast sky condition in three distances from window and two directions of view, window direction (right) and front wall direction (left). The shaded area represents the useful circadian light, 30% to 65%.

## North- Clear sky



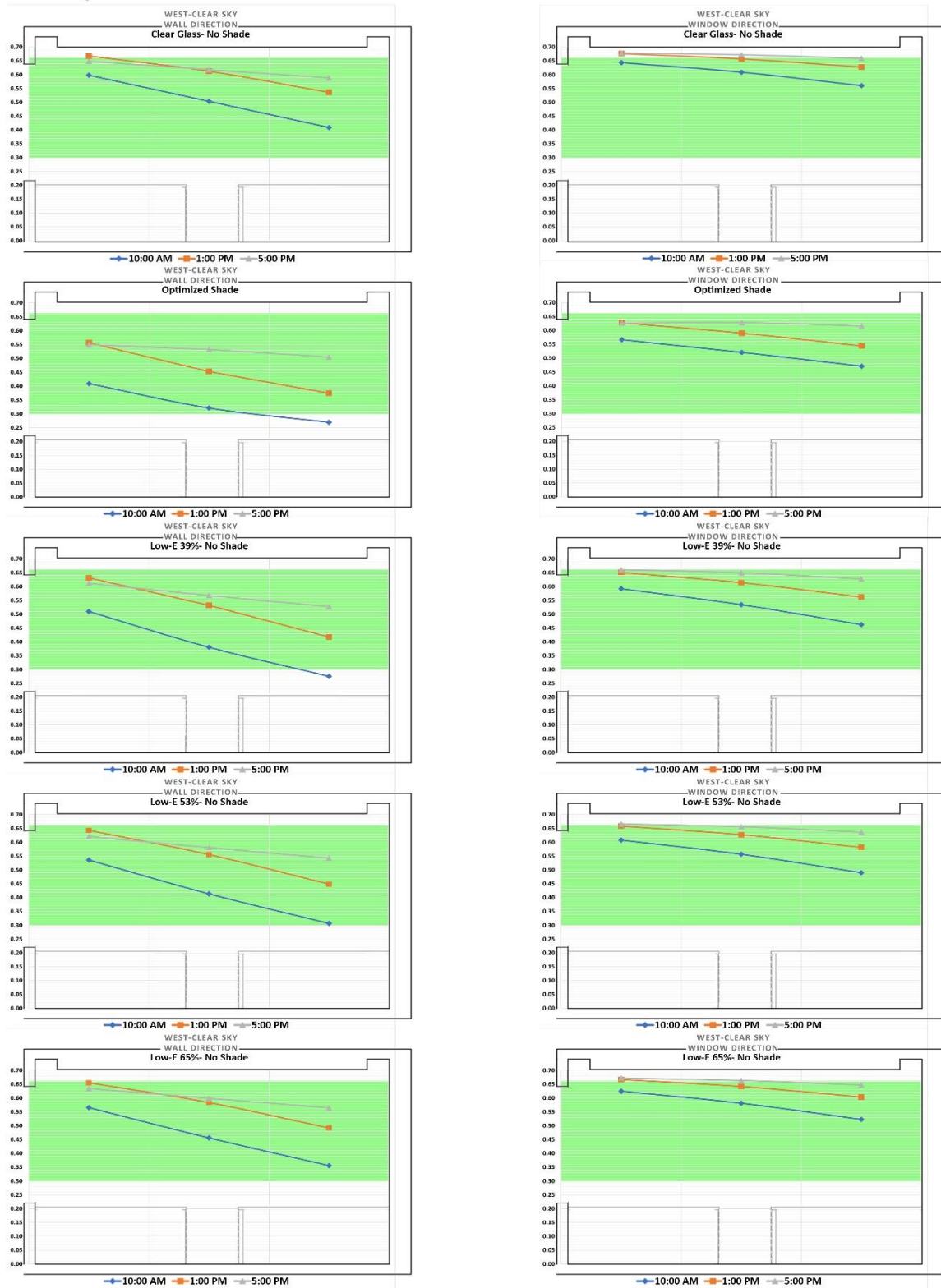
**Figure 70:** Total circadian light availability for north orientation-clear sky condition in three distances from window and two directions of view, window direction (right) and front wall direction (left). The shaded area represents the useful circadian light, 30% to 66%.

## North- Overcast sky



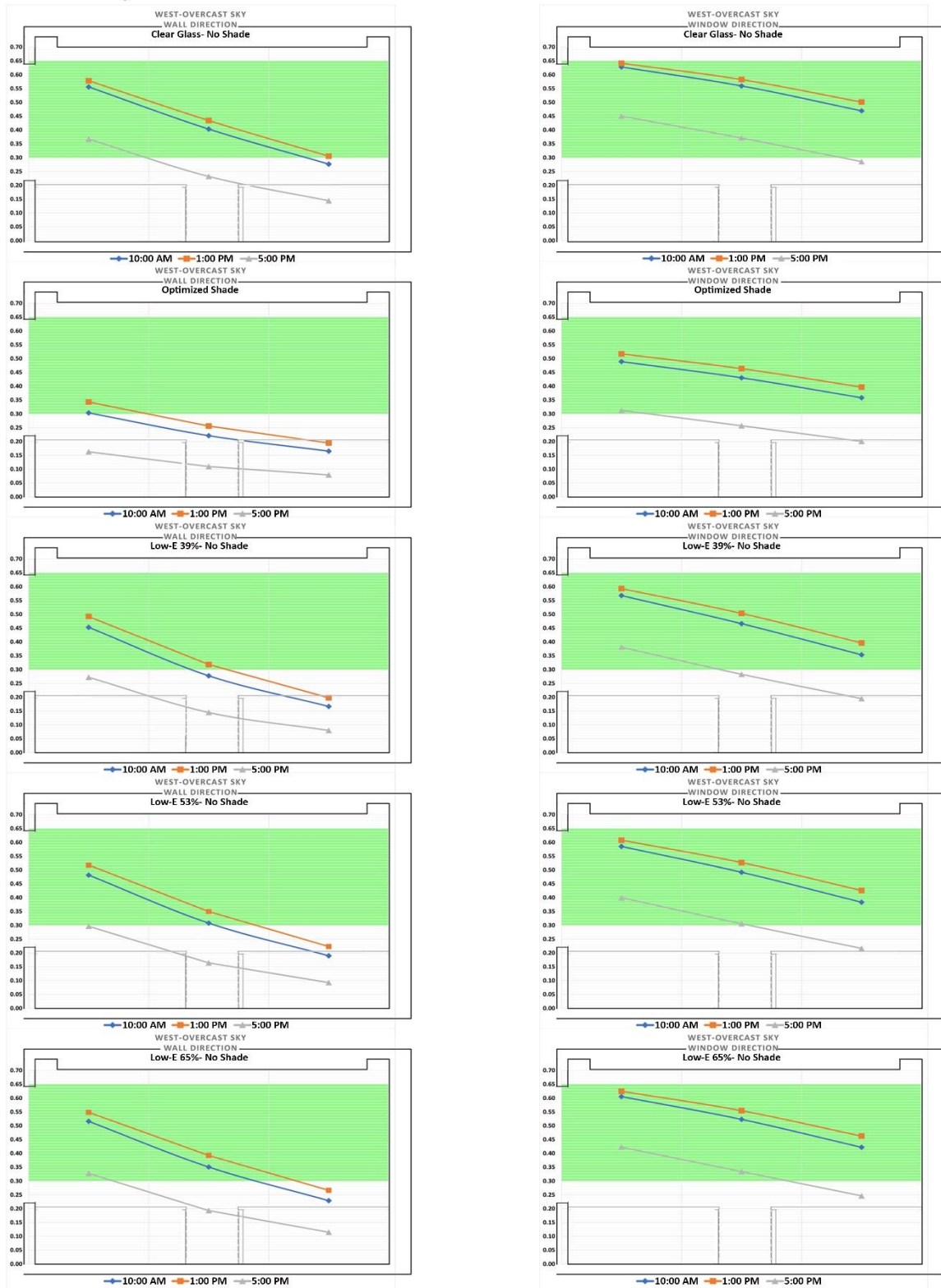
**Figure 71:** Total circadian light availability for north orientation-overcast sky condition in three distances from window and two directions of view, window direction (right) and front wall direction (left). The shaded area represents the useful circadian light, 30% to 65%.

## West- Clear sky



**Figure 72:** Total circadian light availability for west orientation-clear sky condition in three distances from window and two directions of view, window direction (right) and front wall direction (left). The shaded area represents the useful circadian light, 30% to 66%.

## West- Overcast sky



**Figure 73:** Total circadian light availability for west orientation-overcast sky condition in three distances from window and two directions of view, window direction (right) and front wall direction (left). The shaded area represents the useful circadian light, 30% to 65%.

## 4.2 Discussions

The results presented here give an idea of how glazing materials with different VTs, in comparison with optimized shade for each orientation, can affect circadian light distribution across the interior space. The data were scaled to the CS metric to give a better sense of melatonin suppression as the main factor in human alertness. The results in different categories prove this fact that under the clear sky condition, the circadian light has a close relationship with the orientation; while, the circadian light is nearly independent of orientation under the overcast sky condition. The results also emphasize on the effect of distance from the window on the circadian light (Figures 62 to 69). The impact of glazing materials is proportional to the VT of the medium. The relationship between the  $C_e$  (circadian efficiency) of the glazing materials (introduced in the section 2.4.3) were not recognized. More detailed results and discussions are disclosed below.

### 4.2.1 Total circadian light received at Point 1 and 3

The data for the points 1 and 3 show that, except for December 21 at 5 pm, both office workers receive above 30 % threshold circadian light for all four study days and all five scenarios under the clear sky condition. In the case of south orientation, the Point 1 reaches even above 60% threshold for 10 am and 1 pm. The north orientation provides the most stable circadian light between 30% to 60% for both Points 1 and 3 under the clear sky condition. Due to the solar position and direct sunlight, 10 am for the east and 5 pm for the west orientation show higher circadian light.

In terms of the overcast sky, on December 21 at 5 pm, none of the cases can provide above 30% threshold circadian light. Except for the baseline case, all other windows follow nearly the same trend of circadian light availability in the four orientations, which is between 30% to 60%

for point 1. The Low-E 65% at 1 pm supply the point 3 with above but close to 30% threshold circadian light.

Among the four study cases, total circadian light reached to the point 1 in optimized shading with clear glass (i89) is the highest for the south orientation (under both sky conditions) and the north orientation (under the clear sky). However, the optimized shades provide the most total circadian light for point 3 for both south and north orientations under both sky conditions. In the east and west orientations under both sky conditions, the total circadian lights received by Points 1 and 3 are the least for optimized shade cases (Figure 70). The circadian light differences between point 1 and point 3 in most cases are the lowest for optimized shades showing that the two office workers receive closer circadian light amount during the four study days in this scenario (Table 11).

**Table 11:** Circadian light differences between point 1 and point 3, the locations of two office workers. The greater negative numbers show the greater differences.

Scenario	Point 3 to Point 1 circadian light difference							
	Clear sky				Overcast sky			
	South	East	North	West	South	East	North	West
<b>Clear Glass- No Shade</b>	-15.6	-22.4	-19.5	-11.1	-33.7	-39.6	-34.5	-40.4
<b>Optimized Shade</b>	-16.7	-13.8	-21.8	-10.9	-36.5	-23.9	-34.0	-21.9
<b>Low-E 39%</b>	-23.5	-31.0	-29.0	-20.4	-46.4	-50.1	-45.7	-49.5
<b>Low-E 53%</b>	-21.9	-29.7	-28.4	-19.5	-43.9	-48.3	-43.2	-48.7
<b>Low-E 65%</b>	-18.6	-26.2	-23.6	-16.4	-38.4	-44.5	-40.1	-45.2

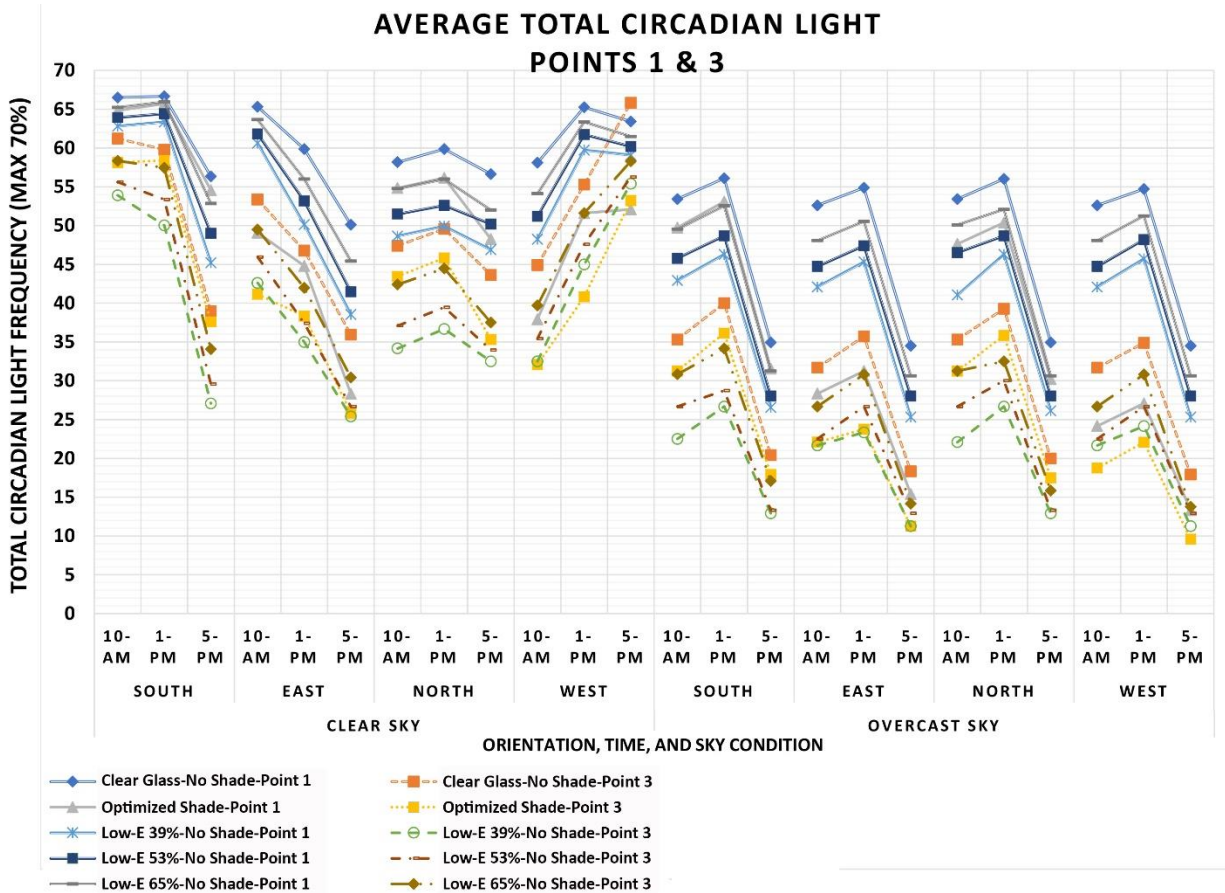


Figure 74: Average total circadian light for point 1 and 3, the locations of two office workers.

#### 4.2.2 Circadian light distribution across the space

The UCLF analysis results under clear sky condition showed different patterns from the total circadian light results. Based on this proposal, there is no single scenario that works well for all or even the most conditions. In contrast to our hypothesis, Low-E 39%, which was supposed to be the worst case, has better UCLF on average in the south orientation under the clear sky condition (Figure 54(a)). While, the optimized shade cases have higher UCLF than other test cases in the south orientation under the overcast sky condition, and the north orientation under both sky conditions (Figure 54(a)). Although, the optimized shades lead to the lowest UCLF in east and west orientations under overcast sky conditions, in case of clear sky it is not the worst scenario



especially in the west orientation. The Low-E 65% case, which has the highest VT among the case studies, contributes to higher UCLFs for the east (both sky conditions) and the west (overcast sky condition). The complete numerical data for the UCFL can be found in Appendix B.

In the total circadian light method (Figure 75), the glare-associated light is also included. However, people normally avoid such a light, and the circadian light incorporated to the glare-associated light does not affect the circadian rhythm at that specific time as expected. The threshold line does not also help in the discussed case. This conflict supports the use of UCLF method in this study for blind-less spaces.

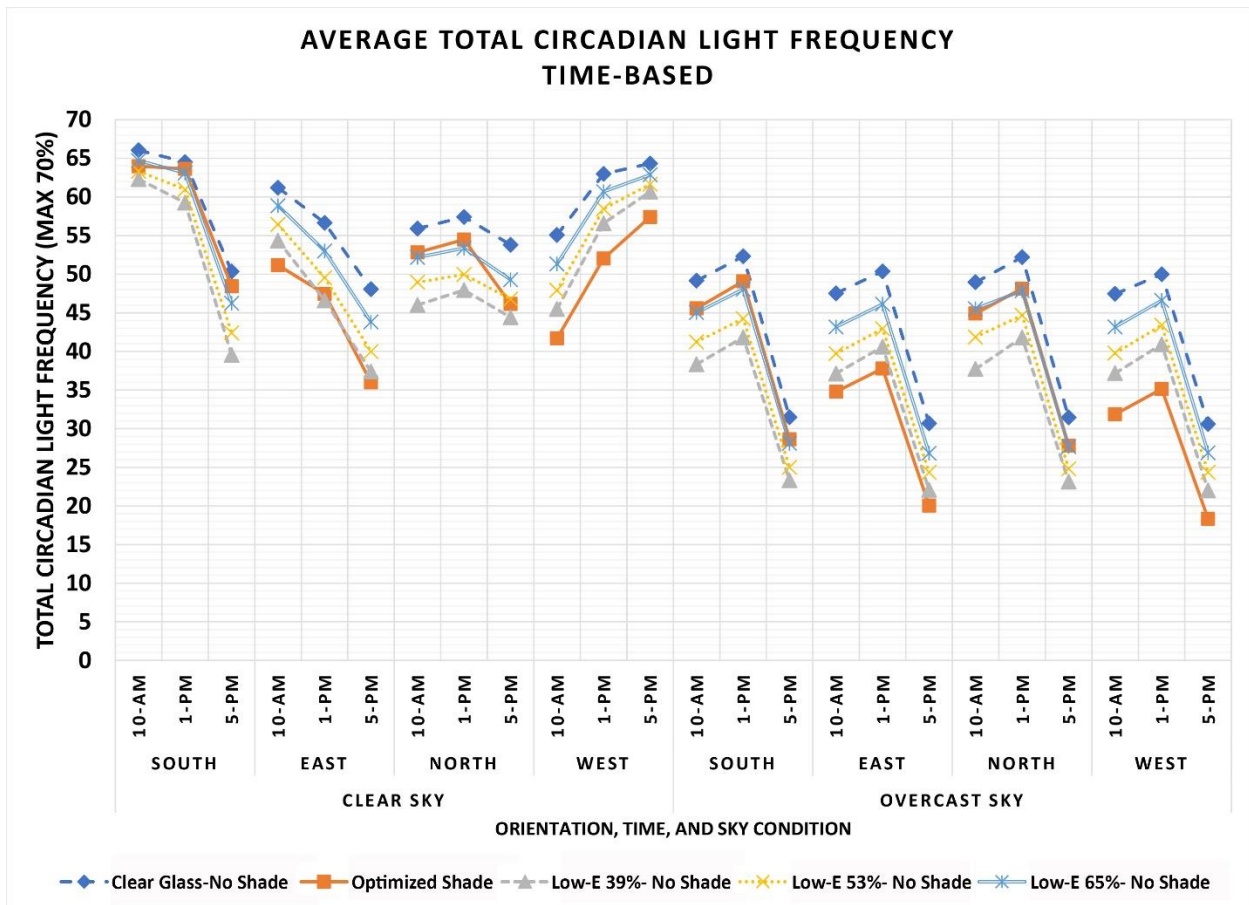


Figure 75: Average of total circadian light available in the space in different times and conditions.

### 4.2.3 The effect of distance from window

The average circadian light data plotted on graphic sections for both window and wall directions emphasize on a direct relationship between circadian light and distance from the window for all scenarios. In terms of direction of view, the decrease in circadian light for wall direction is more descending than the window direction for all cases. Under the overcast sky condition, the circadian light availability suffers more when the target point take distance from the window in comparison with the clear sky condition (Figures 58 to 65).

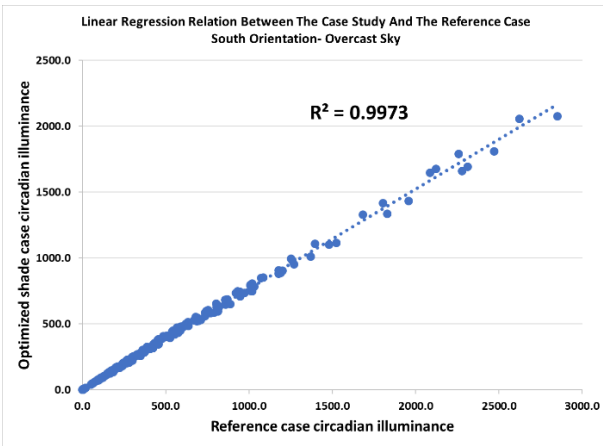
### 4.2.4 Linear regression analysis and uniformity

As a proportion of the photopic light, the circadian light uniformity results from this study (Table 12) approve the results from another study [39]. The regression analyses for all scenarios (considering the clear i89-No shade as the reference case) indicate that the circadian light has a linear relationship to the glazing VT. The  $r^2$  numbers for the circadian light distributed through optimized shade system state slightly less connection to the reference case than the other cases (Figures 76-79).

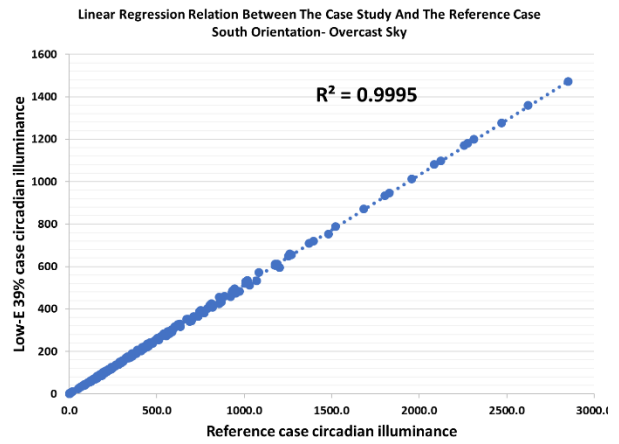
**Table 12:** Circadian light uniformity (avg/min) for all scenarios in two sky conditions and different orientations.

Scenario	Direction of view	South		East		North		West	
		Clear sky	Overcasty sky	Clear sky	Overcasty sky	Clear sky	Overcasty sky	Clear sky	Overcasty sky
Clear Glass- No Shade	Win. dir	3.83	2.40	2.08	2.58	1.91	2.39	3.33	2.58
	Wall dir	3.86	3.13	3.16	3.90	2.87	3.11	3.95	3.92
Optimized Shade	Win. dir	3.08	2.22	2.04	2.68	1.86	2.23	4.78	2.72
	Wall dir	3.73	3.15	1.97	2.01	2.51	2.99	2.47	1.93
Low-E 39%	Win. dir	3.83	2.42	2.07	2.58	1.92	2.40	3.36	2.58
	Wall dir	4.03	3.34	3.27	4.00	2.96	3.27	4.07	4.01
Low-E 53%	Win. dir	3.83	2.42	2.07	2.58	1.93	2.39	3.42	2.58
	Wall dir	3.95	3.38	3.25	4.02	3.00	3.24	4.09	4.04
Low-E 65%	Win. dir	3.67	2.39	2.07	2.57	1.92	2.40	3.33	2.57
	Wall dir	3.51	3.12	3.10	3.82	2.86	3.12	3.91	3.84

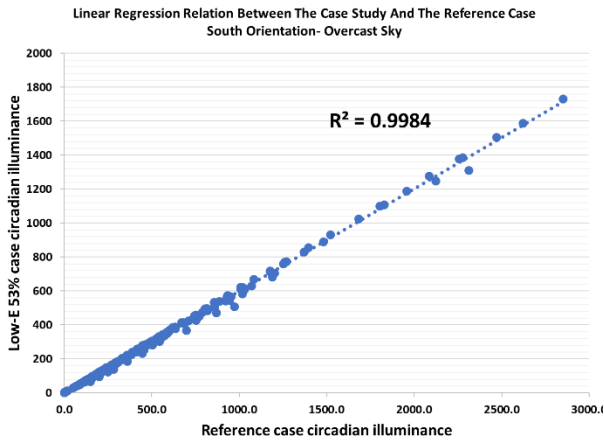
## South Orientation



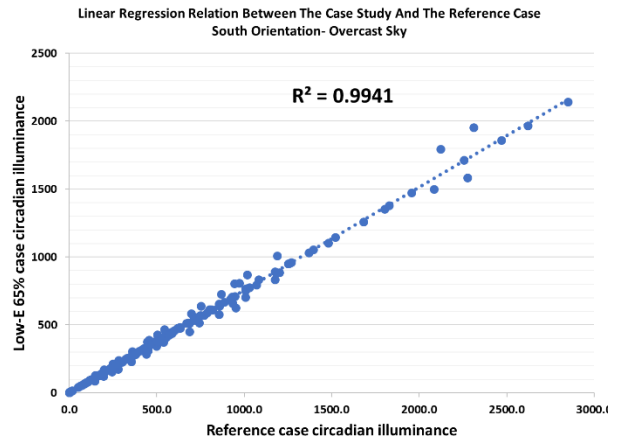
(a)



(b)



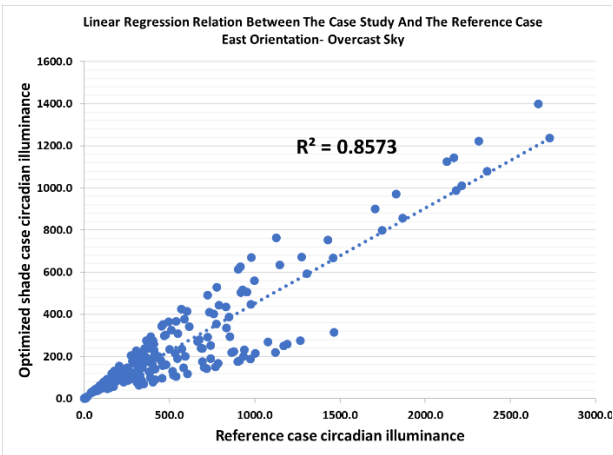
(c)



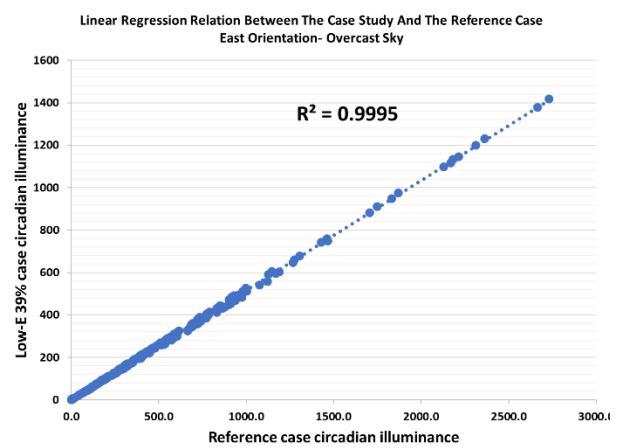
(d)

**Figure 76:** Linear regression relation between the case study; (a) optimized shade, (b) Low-E 39%, (c) Low-E 53%, (d) Low-E 65%; and the reference case (clear glass with no shade) at south orientation and under overcast sky condition.

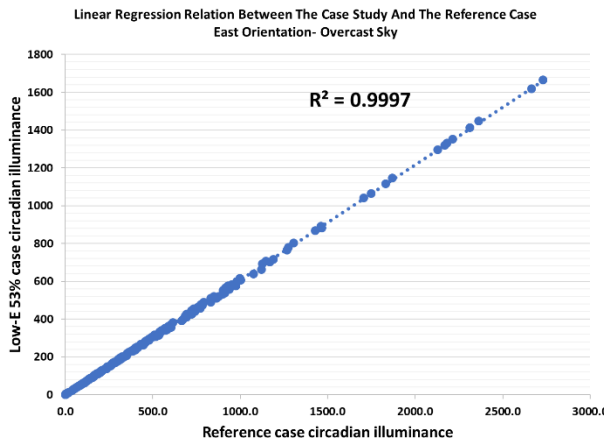
## East Orientation



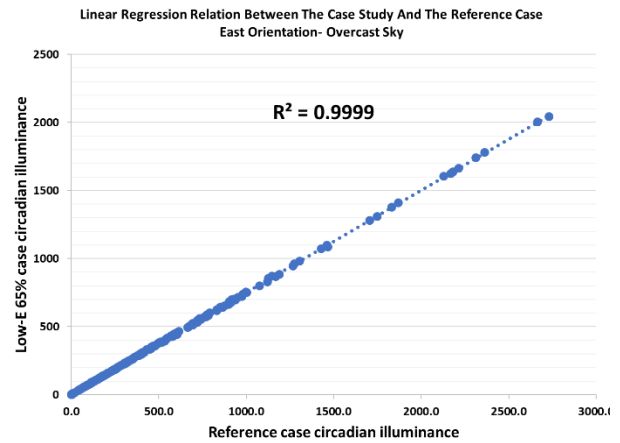
(a)



(b)



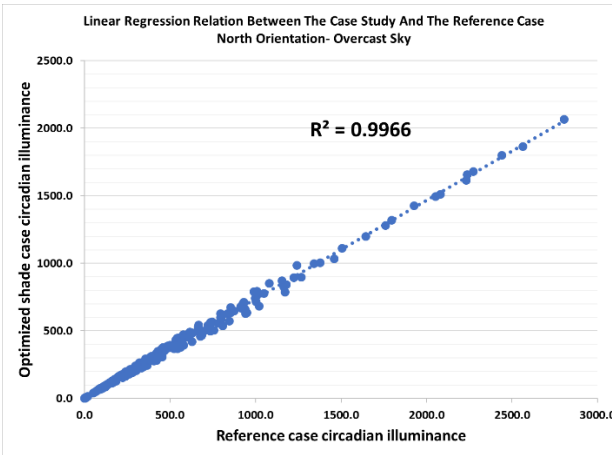
(c)



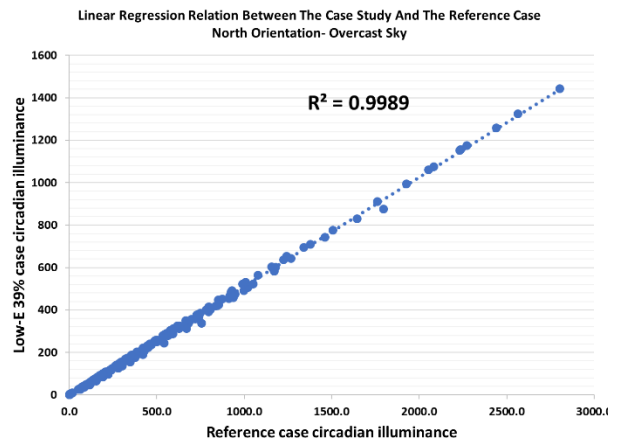
(d)

**Figure 77:** Linear regression relation between the case study; (a) optimized shade, (b) (b) Low-E 39%, (c) Low-E 53%, (d) Low-E 65%; and the reference case (clear glass with no shade) at east orientation and under overcast sky condition.

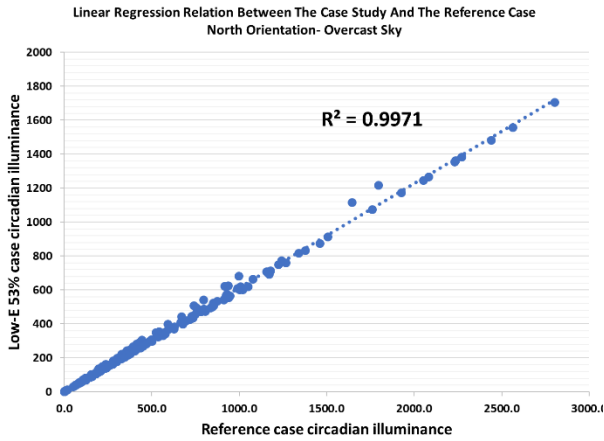
## North Orientation



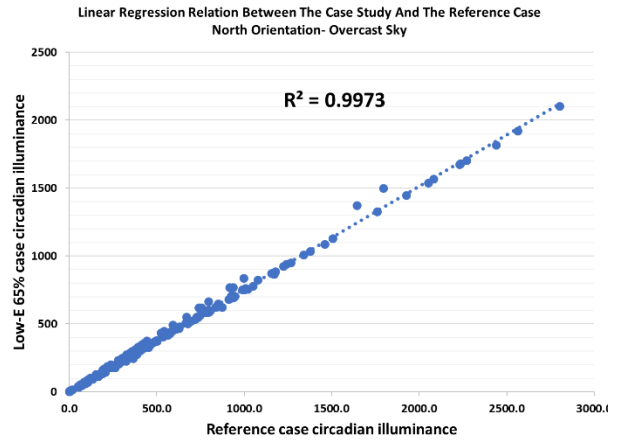
(a)



(b)



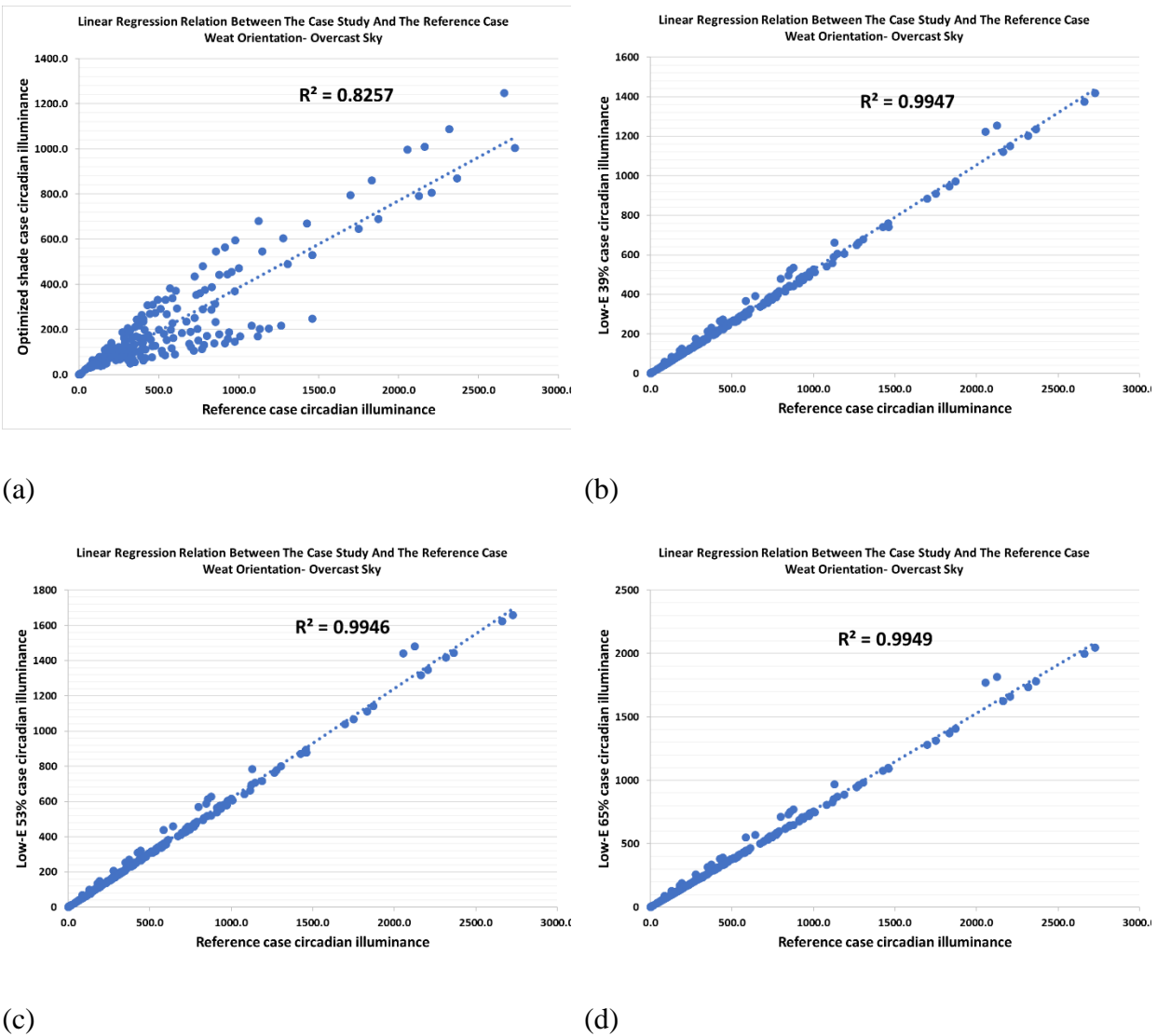
(c)



(d)

**Figure 78:** Linear regression relation between the case study; (a) optimized shade, (b) (b) Low-E 39%, (c) Low-E 53%, (d) Low-E 65%; and the reference case (clear glass with no shade) at north orientation and under overcast sky condition.

## West Orientation



**Figure 79:** Linear regression relation between the case study; (a) optimized shade, (b) (b) Low-E 39%, (c) Low-E 53%, (d) Low-E 65%; and the reference case (clear glass with no shade) at west orientation and under overcast sky condition.

Having disclosed the results, the effect of glazing VT and optimized shade on the circadian light distribution across the space was discussed for four orientations and two sky conditions. The conclusions of this study followed by the recommendations and study limitations are presented in the final chapter.

## CHAPTER 5

### CONCLUSIONS AND RECOMMENDATIONS

#### 5.1 Conclusions

The results from this study support the favorable design of optimized shades at both south-east (south) and north-west (north) orientations for interior circadian light compared to Low-E glazing windows with VT below 65%. The circadian light distribution of the optimized shades is very close to that of the Low-E 65% in the south-east (south) and the north-west (north) orientations. However, the annual and hot seasons illuminance performances of the baseline case are better than the Low-E 65% results (Figures 38-39, 42-43). By contrast, in the east and west orientations, the optimized shade cases do not have well-distributed circadian light in the interior space. However, optimized shades in all orientations deliver more uniform circadian light in the interior space, which would provide more similar circadian light environment for the occupants in comparison with the Low-E case studies.

Since the circadian light is measured and evaluated based on the observer's viewing direction, the UCLF analysis method, introduced in this study, gives more reasonable evaluation of circadian light distribution than the total circadian light. In the absence of interior blinds, the window with lower VT (39%) tends to provide higher UCLF than other cases (53% and 65% VT) at the south orientation under clear sky condition.

## 5.2 Recommendations

While lighting simulation employed in this study gives a good estimation of light and circadian light distribution, the Rea et al circadian light metrics such as  $CL_A$  and CS were not directly resulted here. Therefore, the analyzed CS in this study was just a scaled value of circadian light result that may differ in the physical space measurement. Accordingly, a model or real space measurement using spectrophotometer would give an ultimate result and conclusion.

Although the study dates and times were chosen to represent all seasons, four days and three times per day would not track the changes over a full year well enough. It turned out that a pre-study on the glazing scenarios could help to reduce the number of scenarios and increase the study times and view directions.

To evaluate the overall benefit of clear class windows equipped with shading devices compared to the Low-E glass windows, it is encouraging to continue researching on a new generation of optimized shades using different opacity and solar control materials.



## REFERENCES

- [1] M. S. Rea and M. G. Figueiro, "Light as a circadian stimulus for architectural lighting," *Lighting Res. Technol.*, vol. 0, pp. 1-14, 2016.
- [2] N. E. Klepeis, W. C. Nelson, W. R. Ott, J. P. Robinson, A. M. Tsang and P. Switzer, "The National Human Activity Pattern Survey (NHAPS); A Resource for Assessing Exposure to Environmental Pollutants," Lawrence Berkeley National Laboratory, Berkeley, 2001.
- [3] I. Sarbu and C. Sebarchievici, "Aspects of indoor environmental quality assessment in buildings," *Energy and Buildings*, vol. 60, p. 410–419, 2013.
- [4] J. a. Enezi, V. Revell, T. Brown, J. Wynne, L. Schlangen and R. Lucas, "A "Melanopic" Spectral Efficiency Function Predicts the Sensitivity of Melanopsin Photoreceptors to Polychromatic Lights," *Journal of Biological Rhythms*, vol. 26, no. 4, pp. 314-323, 2011.
- [5] D. Gall and K. Bieske, "Definition and measurement of circadian radiometric quantities," in *CIE symposium '04*, Vienna, 2004.
- [6] M. S. Rea, M. G. Figueiro and B. Andrew, "Circadian Light," *Journal of Circadian Light*, vol. 8, no. 2, 2010.
- [7] M. Inanici, "Lark Spectral Lighting," University of Washington and ZGF LLP, 2015. [Online]. Available: [http://faculty.washington.edu/inanici/Lark/Lark\\_home\\_page.html](http://faculty.washington.edu/inanici/Lark/Lark_home_page.html). [Accessed 10 November 2017].
- [8] D. W. G. Clausen, "The combined effects of many different indoor environmental factors on acceptability and office work performance," *HVAC&R Research 14 (1)*, pp. 103-113, 2008.
- [9] L. T. Wong, K. W. Mui and P. S. Hui, "A multivariate-logistic model of acceptance for indoor environment quality (IEQ) in offices," *Building and Environment*, vol. 43, pp. 1-6, 2008.
- [10] J. A. Veitch, K. E. Charles, K. M. J. Farley and G. R. Newsham, "A model of satisfaction with open-plan office conditions: COPE field findings," *Journal of Environment Psychology*, vol. 27, pp. 177-189, 2007.
- [11] P. C. Hughes, "An examination of the beneficial action of natural light on the psychobiological system of man," CIE 20th Session, Paris, 1983.
- [12] J. A. Veitch, G. R. Newsham and S. Mancini, "NRC-IRC Research Report RR-306:Lighting and Office Renovation Effects on Employee and Organizational Well-Being," National Research Council Canada Institute for Research in Construction, 2010.
- [13] D. H. Kin and K. P. Mansfield, "A cross-cultural study on perceived lighting quality and occupants' well-being between UK and South Korea," *Energy and Building*, vol. 119, pp. 211-217, 2019.

- [14] O. A. Abdou, "Effects of Luminous Environment on Worker Productivity in Building Spaces," *Journal of Architectural Engineering*, vol. 3, pp. 0124-0132, 1997.
- [15] NEMA, "Lighting and human performance: a review," National Electrical Manufacturers Association, New York, 1989.
- [16] P. M. Bluysen, M. Aries and P. V. Mommelen, "Comfort of workers in office buildings: The European HOPE project," *Building and Environment*, vol. 46, pp. 280-288, 2010.
- [17] A. C. K. Lai, K. W. Mui, W. L. T. and L. Y. Law, "An evaluation model for indoor environmental quality (IEQ) acceptance in residential buildings," *Energy and Building*, vol. 41, pp. 930-936, 2009.
- [18] M. B. C. Aries, M. P. J. Aarts and J. V. Hoof, "Daylight and health: A review of the evidence and consequences for the built environment," *Lighting Research Technology*, vol. 47, pp. 6-27, 2015.
- [19] M. S. Rea, "Reference and Application," in *IESNA Lighting Handbook*, New York, Illuminating Engineering Society of North America, 2000.
- [20] J. Mardaljevic, L. Heschong and E. Lee, "Daylight metrics and energy savings," *Lighting Research Technology*, vol. 41, pp. 261-283, 2009.
- [21] www.energydesignresources.com, "Design Brief: Understanding Daylight Metrics," 12 June 2009. [Online]. Available: <https://energydesignresources.com/resources/publications/design-briefs/design-brief-understanding-daylight-metrics.aspx>. [Accessed 23 August 2018].
- [22] NASI/IES, "Nomenclature and Definitions for Illuminating Engineering; IES LM-83-12," 2012. [Online]. Available: <https://www.ies.org/definitions/spatial-daylight-autonomy-sda/>. [Accessed 23 August 2018].
- [23] ARCHSIM, "Spatial Daylight Autonomy," [Online]. Available: <http://archsim.com/documentation/dla/>. [Accessed 23 August 2018].
- [24] A. Nabil and J. Mardaljevic, "Useful Daylight Illuminance: A New Paradigm for Assessing Daylight in Buildings," *Lighting Research and Technology*, vol. 37, no. 1, pp. 41-59, 2005.
- [25] J. F. Duffy and C. A. Czeisler, "Effect of Light on Human Circadian Physiology," *Sleep Med Clin.*, vol. 4, no. 2, pp. 165-177, 2009.
- [26] J. F. Duffy and K. P. Wright, "Entrainment of the Human Circadian System by Light," *JOURNAL OF BIOLOGICAL RHYTHMS*, vol. 20, no. 2, pp. 326-338, 2005.
- [27] P. R. Boyce, "Fundamentals; Non-Image-Forming System," in *Human Factors in Lighting*, Boca Raton, FL, Taylor & Francis Group, LLC, 2014, pp. 91-111.
- [28] H. J. Bailes and R. J. Lucas, "Human melanopsin forms a pigment maximally sensitive to blue light (479 nm) supporting activation of Gq/11 and Gi/o signalling cascades," *Proceeding of the Royal Society B*, vol. 280, 2013.

- [29] M. S. Rea, M. G. Figueiro, J. D. Bullough and A. Bierman, "A model of phototransduction by the human circadian system," *Brain Research Reviews*, vol. 50, p. 213 – 228, 2005.
- [30] R. J. Lucas, S. N. Peirson, D. M. Berson, T. M. Brown, H. M. Cooper and C. A. Czeisler, "Measuring and using light in the melanopsin age," *Trends in Neurosciences*, vol. 37, no. 1, 2014.
- [31] M. Inanici, M. Brennan and E. Clark, "Spectral daylighting simulations: computing circadian light," 2015.
- [32] G. Brainard, J. Hanifin, J. Greeson, B. Byrne and G. Glickman, "Action spectrum for melatonin regulation in," *J. Neurosci.*, no. 21, p. 6405– 6412, 2001.
- [33] K. Thapan, J. Arendt and D. Skene, "An action spectrum for melatonin suppression: evidence for a novel non-rod, non-cone photoreceptor," *J. Physiol.*, no. 535, p. 261–267, 2001.
- [34] M. Rea, M. Figueiro, A. Bierman and R. Hamner, "Modelling the spectral sensitivity of the human circadian system," *Lighting Res. Technol.*, no. 44, p. 386–396, 2012.
- [35] G. Ward Larson, "Radiance," [Online]. Available: <http://radsite.lbl.gov/radiance/refer/filefmts.pdf>. [Accessed 31 August 2018].
- [36] "WELL," International WELL Building Institute, 2017. [Online]. Available: <https://www.wellcertified.com/en>. [Accessed 7 September 2018].
- [37] A. Tzempelikos and A. K. Athienitis, "The impact of shading design and control on building cooling and lighting demand," *Solar Energy*, vol. 81, p. 369–382, 2007.
- [38] A. Tzempelikos and H. Shen, "Comparative control strategies for roller shades with respect to daylighting and energy performance," *Building and Environment*, vol. 67, p. 179e192, 2013.
- [39] M.-C. Ho, C.-M. Chiang, P.-C. Chou, K.-F. Chang and C.-Y. Lee, "Optimal sun-shading design for enhanced daylight illumination of subtropical classrooms," *Energy and Buildings*, vol. 40, p. 844–1855, 2008.
- [40] A. Olgyay, *Solar Control and Shading Devices*, Princeton: Princeton University Press, 1957.
- [41] K. Kensek, Noble, M. Schiler and M. Setiadarma, "SHADING MASK: A teaching tool for sun shading devices," *Automation in Construction*, vol. 5, no. 3, pp. 219-231, 1996.
- [42] M. S. Roudsari and C. Mackey, "Ladybug Tools," Ladybug Tools LLC, 2017-2018. [Online]. Available: <https://www.ladybug.tools/index.html>. [Accessed 10 November 2017].
- [43] R. Leslie, A. Smith, L. Radetsky, M. Figueiro and L. Yue, "Patterns to Daylight Schools for People and Sustainability," Lighting Research Center, Troy, 2010.
- [44] J. Michaels, "COMMERCIAL BUILDINGS ENERGY CONSUMPTION SURVEY (CBECS)," 18 March 2016. [Online]. Available: <https://www.eia.gov/consumption/commercial/reports/2012/energyusage/index.php>. [Accessed 6 September 2018].


- [45] C. Berry, "RESIDENTIAL ENERGY CONSUMPTION SURVEY (RECS)," 31 May 2017 & 2018. [Online]. Available: <https://www.eia.gov/consumption/residential/reports/2015/methodology/index.php>. [Accessed 6 September 2018].
- [46] Y. N. J.-I. Huang and T.-m. Chung, "Comprehensive analysis on thermal and daylighting performance of glazing and shading designs on office building envelope in cooling-dominant climates," *Applied Energy*, vol. 134, p. 215–228, 2014.
- [47] ANSI/ASHRAE/IES Standard 90.1-2016 -- Energy Standard for Buildings Except Low-Rise Residential Buildings, Atlanta: ASHRAE, 2016.
- [48] D. L. DiLaura, G. R. Steffy, K. W. Houser and R. G. Mistrick, *The Lighting Handbook*, IESNA, 2011.
- [49] P. Hartman, P. Sujanova and J. Hraska, "Circadian Characteristics of Special Glazing," *Athens Journal of Sciences*, vol. 1, no. 4, pp. 241-254, 2014.
- [50] P. Tregenza and I. Waters, "Daylight coefficients," *Lighting Research and Technology*, vol. 2, no. 15, pp. 65-71, 1983.
- [51] R. Perez, P. Ineichen and R. Seals, "Modelling daylight availability and irradiance components from direct and global irradiance," *Solar energy*, vol. 44, no. 5, pp. 271-289, 1990.
- [52] C. F. Reinhart and O. Walkenhorst, "Validation of dynamic RADIANCE-based daylight simulations for a test office with external blinds," *Energy and Buildings*, vol. 33, no. 7, pp. 683-697, 2001.
- [53] R. Compagnon, "RADIANCE: a simulation tool for daylighting systems," 1997. [Online]. Available: [radsite.lbl.gov/radiance/refer/rc97tut.pdf](http://radsite.lbl.gov/radiance/refer/rc97tut.pdf). [Accessed 2018].
- [54] M. M. Shalaby, Master Thesis: The Effect of Architectural Configurations on the Biological Light Response in Residential Buildings, Lund University, 2016.
- [55] J. Krochmann, P. Polato, F. Geotti-Bianchini, D. Gundlach, J. J. Hsia, L. Morren, H. Terstiege and J. Verrill, "Practical methods for the measurement of reflectance and transmittance, CIE 130," CIE General Bureau, Vienna, 1998.
- [56] Lawrence Berkeley National Laboratory, "Windows & Daylighting, Optics version 6," University of California, 2018. [Online]. Available: <https://windows.lbl.gov/software/optics>. [Accessed 1 August 2018].
- [57] Design for Climate and Comfort Lab, "Lighting Materials for Simulation," Singapore University of Technology and Science, 2015. [Online]. Available: <http://lighting-materials.com/>. [Accessed 15 April 2018].
- [58] P. Kaiser, "CIE 1988 2° SPECTRAL LUMINOUS EFFICIENCY FUNCTION FOR PHOTOPIC VISION," CIE, 1988. [Online]. Available: <http://www.cie.co.at/publications/cie-1988-2-spectral-luminous-efficiency-function-photopic-vision-0>. [Accessed 2018].

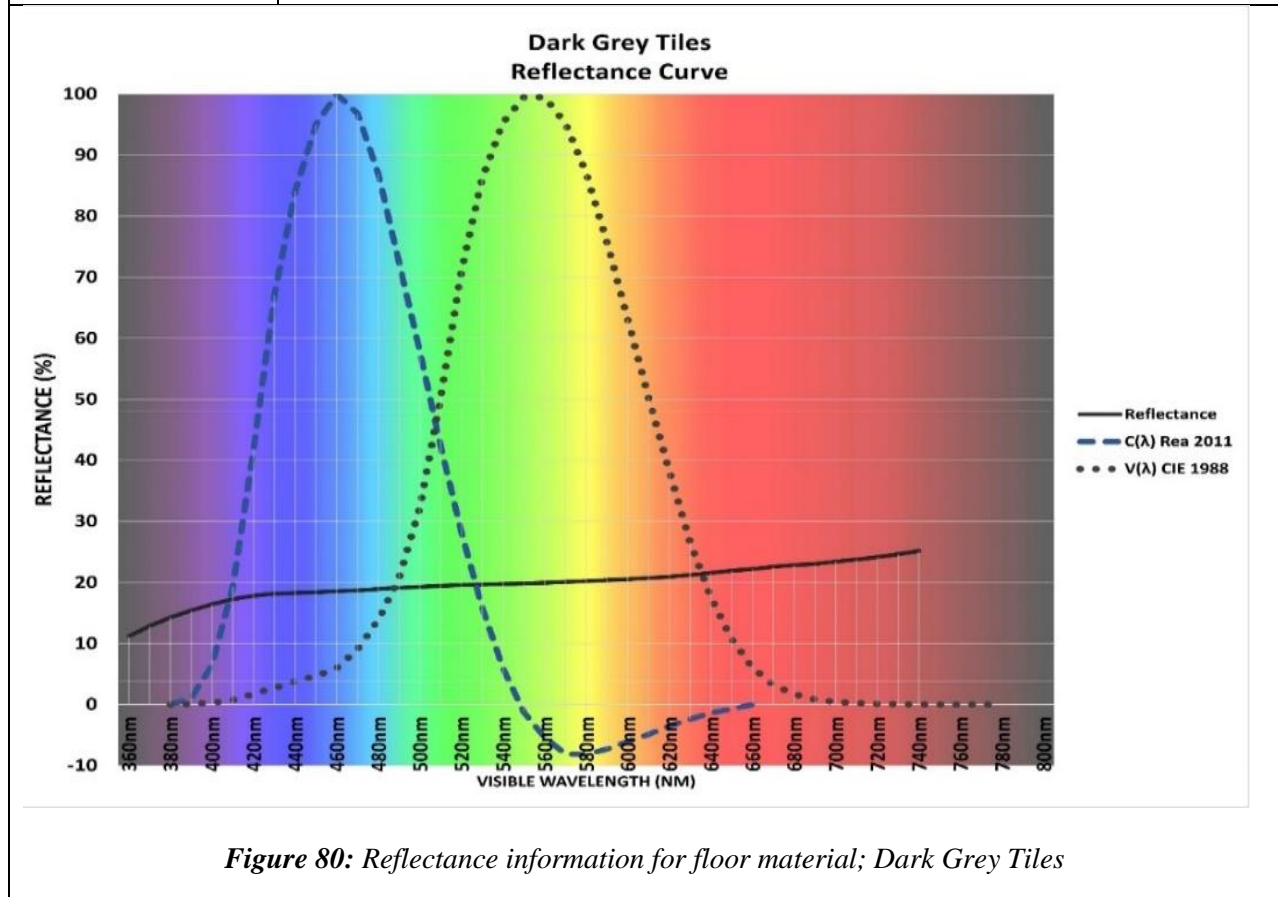
- [59] P. Maa, L.-S. Wang and N. Guo, "Maximum window-to-wall ratio of a thermally autonomous building as a function of envelope U-value and ambient temperature amplitude," *Applied Energy*, vol. 146, pp. 84-91, 2015.
- [60] National Weather Forecast Office, "NOAA Online Weather Data," National Weather Service, 2017. [Online]. Available: <http://w2.weather.gov/climate/xmacis.php?wfo=top>. [Accessed 15 December 2017].
- [61] National Renewable Energy Laboratory (NREL), "EnergyPlus, Weather Data for Topeka, KS," National Renewable Energy Laboratory (NREL), 1996-2017. [Online]. Available: [https://energyplus.net/weather-region/north\\_and\\_central\\_america\\_wmo\\_region\\_4/USA/KS](https://energyplus.net/weather-region/north_and_central_america_wmo_region_4/USA/KS). [Accessed 15 December 2017].
- [62] H. Tyler, S. Stefano, P. Alberto, C. Toby, M. Dustin and S. Kyle, "CBE Thermal Comfort Tool, Center for the Built Environment," University of California Berkeley, 2017. [Online]. Available: <http://cbe.berkeley.edu/comforttool/>. [Accessed 2018 January 2018].
- [63] Weather Spark, "Average Weather in Topeka," Cedar Lake Ventures, Inc., 2017. [Online]. Available: <https://weatherspark.com/y/9454/Average-Weather-in-Topeka-Kansas-United-States-Year-Round#Sections-Humidity>. [Accessed 2017 December 2017].
- [64] Solar Radiation Monitoring Laboratory, "Sun path chart program," University of Oregon, 2007. [Online]. Available: <http://solardat.uoregon.edu/SunChartProgram.html>. [Accessed 20 December 2017].
- [65] K. Błażejczyk, G. Jendritzky, P. Bröde, D. Fiala, G. Havenith, Y. Epstein, A. Psikuta and B. Kampmann, "An introduction to the Universal Thermal Climate Index (UTCI)," *Geographia Polonica*, vol. 86, no. 1, pp. 5-10, 2013.
- [66] C. Reinhart, "Design Iterate Validate Adapt (DIVA) version 4," Solemma LLC, 2017. [Online]. Available: <https://www.solemma.com/Diva.html>. [Accessed 17 September 2017].
- [67] Solemma LLC, "ALFA," Collaboration between Solemma and sleep experts at the Alertness CRC in Australia, 2018. [Online]. Available: <https://www.solemma.com/Alfa.html>. [Accessed 1 June 2018].
- [68] Rochester Institute of Technology, "Rochester Institute of Technology," Rochester Institute of Technology, [Online]. Available: [www.rit-mcsl.org/UsefulData/DaylightSeries.xls](http://www.rit-mcsl.org/UsefulData/DaylightSeries.xls). [Accessed 1 February 2018].
- [69] Lighting Research Center, "CS Calculator," 5 May 2017. [Online]. Available: [www.lrc.rpi.edu/resources/CSCalculator\\_2017\\_05\\_05.xlsm](http://www.lrc.rpi.edu/resources/CSCalculator_2017_05_05.xlsm). [Accessed 11 November 2017].
- [70] M. G. Figueiro, K. Gonzales and D. Pedler, "Designing with circadian stimulus," *LD+A*, pp. 30-34, October 2016.
- [71] D. W. G. Clausen, "The combined effects of many different indoor environmental factors on acceptability and office work performance," *HVAC&R Research*, vol. 14, no. 1, pp. 103-113, 2008.


- [72] G. Ward, "Radiance," Lawrence Berkeley National Lab, 2016. [Online]. Available: <https://www.radiance-online.org/>. [Accessed 3 August 2018].
- [73] D. Rutton, "Grasshopper," Robert McNeel and associates, 2018. [Online]. Available: <https://www.grasshopper3d.com/>. [Accessed 3 August 2018].
- [74] R. Perez, P. Ineichen and R. Seals, "Modelling daylight availability and irradiance components from direct and global irradiance," *Solar energy*, vol. 44, no. 5, pp. 271-289, 1990.
- [75] M. Freedman, R. Lucas, B. Soni, M. v. Schantz, M. Munoz, Z. David-Gray and R. Foster, "Regulation of mammalian circadian behavior by non-rod, non-cone, ocular photoreceptors," *Science*, no. 284, pp. 502-504, 1999.

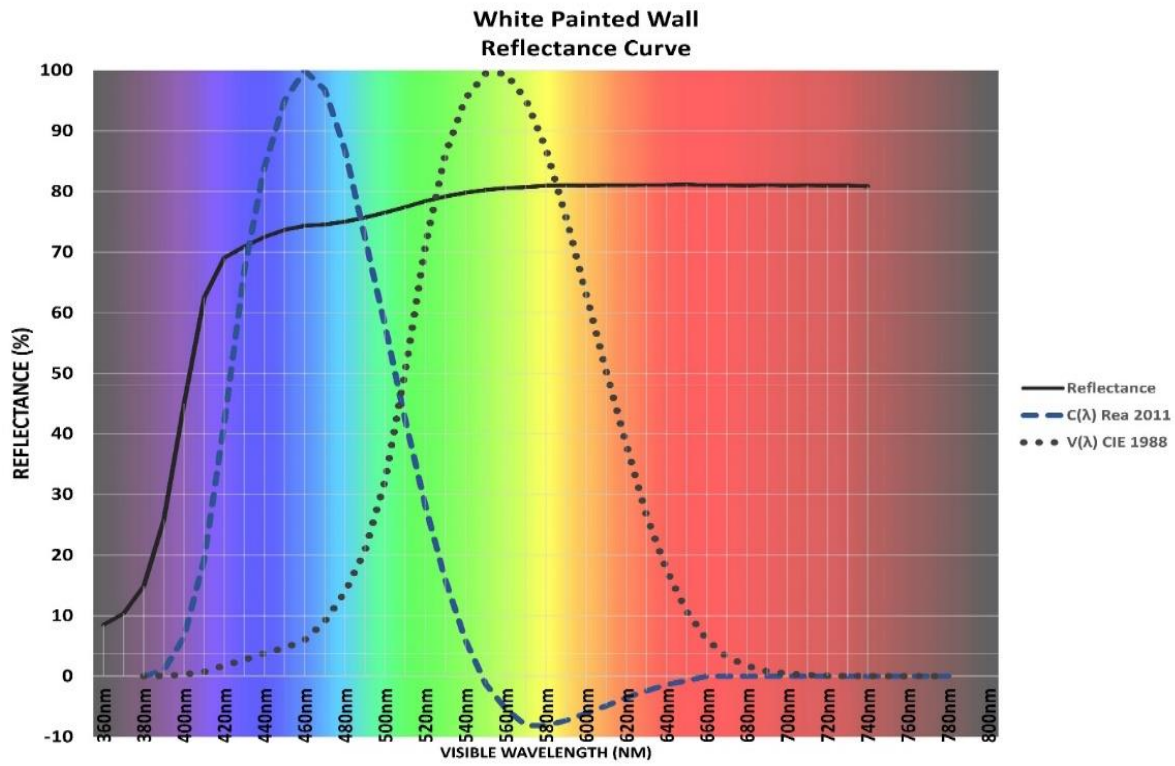
## APPENDIX A

### SURFACE MATERIALS' REFLECTANCE INFORMATION

<b>Floor:</b>  Dark Grey Tiles  	Total Reflectance:	20.06%	Radiance Material definition					
	R <sub>Reflectance</sub>	20.15%	void plastic Dark_grey_floor_tiles					
	G <sub>Reflectance</sub>	18.79%	0					
	B <sub>Reflectance</sub>	17.16%	0					
	Specularity	1.25%	5	0.2015	0.1879	0.1716	0.0125	0.0000
	Roughness	0.0%						

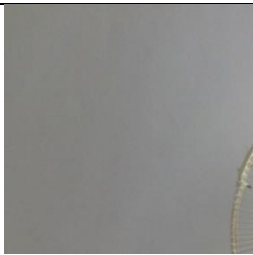


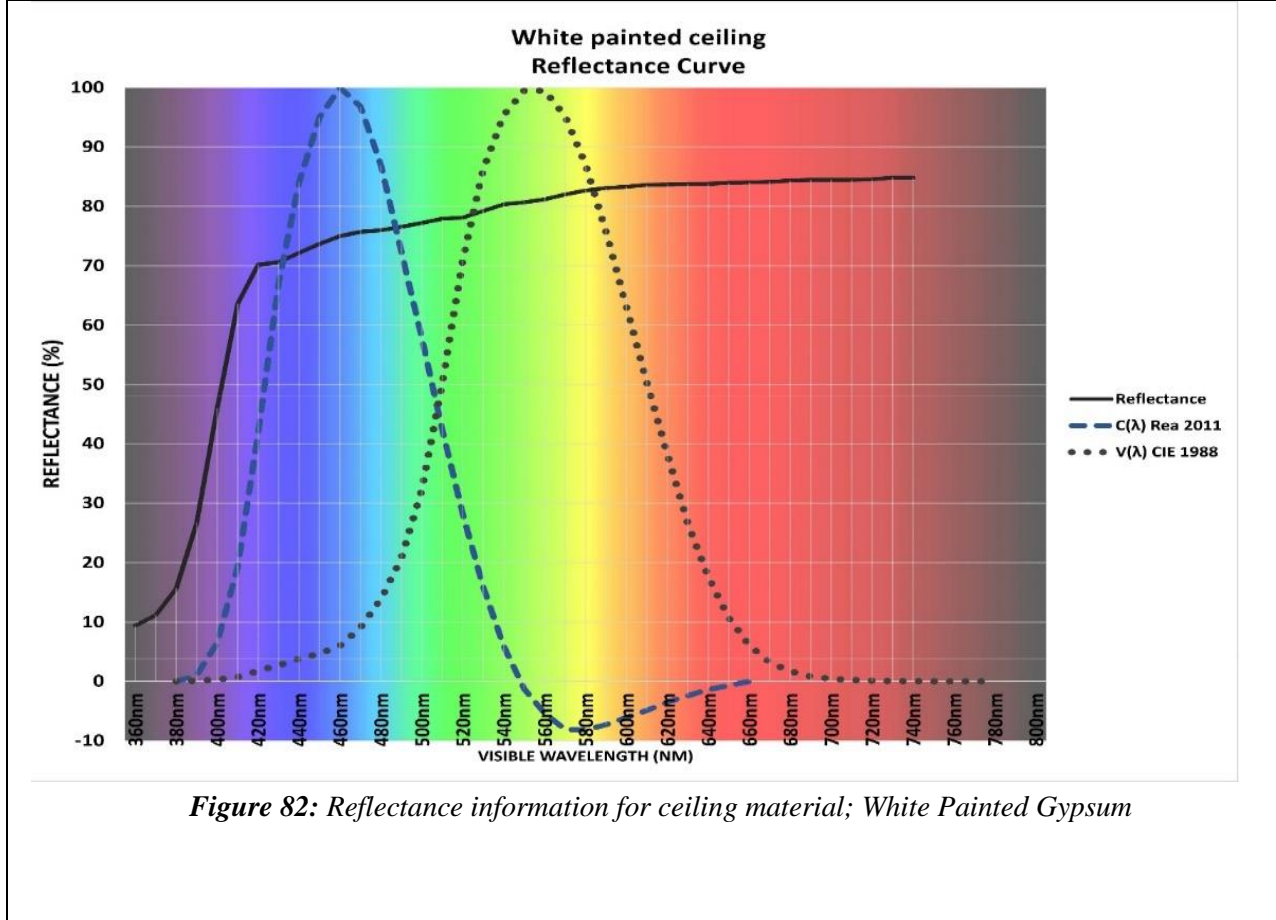
<b>Walls:</b> White Painted Gypsum	Total Reflectance:	79.8%	Radiance Material definition					
	R <sub>Reflectance</sub>	81.43%	void plastic White_painted_corridor_walls					
	G <sub>Reflectance</sub>	79.84%	0					
	B <sub>Reflectance</sub>	71.50%	0					
	Specularity	0.39%	5	0.8143	0.7984	0.7150	0.0039	0.0000
	Roughness	0.0%						



*Figure 81: Reflectance information for wall material; White Painted Gypsum*



<b>Ceiling:</b>  White Painted  Gypsum	Total Reflectance:	82.2%	Radiance Material definition					
	R <sub>Reflectance</sub>	84.62%	void plastic White_painted_room_ceiling					
	G <sub>Reflectance</sub>	82.06%	0					
	B <sub>Reflectance</sub>	72.63%	0					
	Specularity	0.44%	5	0.8462	0.8206	0.7263	0.0044	0.0000
	Roughness	0.0%						
								



<b>Tables:</b> Wood	Total Reflectance:	31.87%	Radiance Material definition			
	R <sub>Reflectance</sub>	46.28%	void plastic Wood_Table			
	G <sub>Reflectance</sub>	26.18%	0			
	B <sub>Reflectance</sub>	10.43%	0			
	Specularity	2.01%	5	0.4628	0.2618	0.1043 0.0201 0.0000
	Roughness	0.0%				

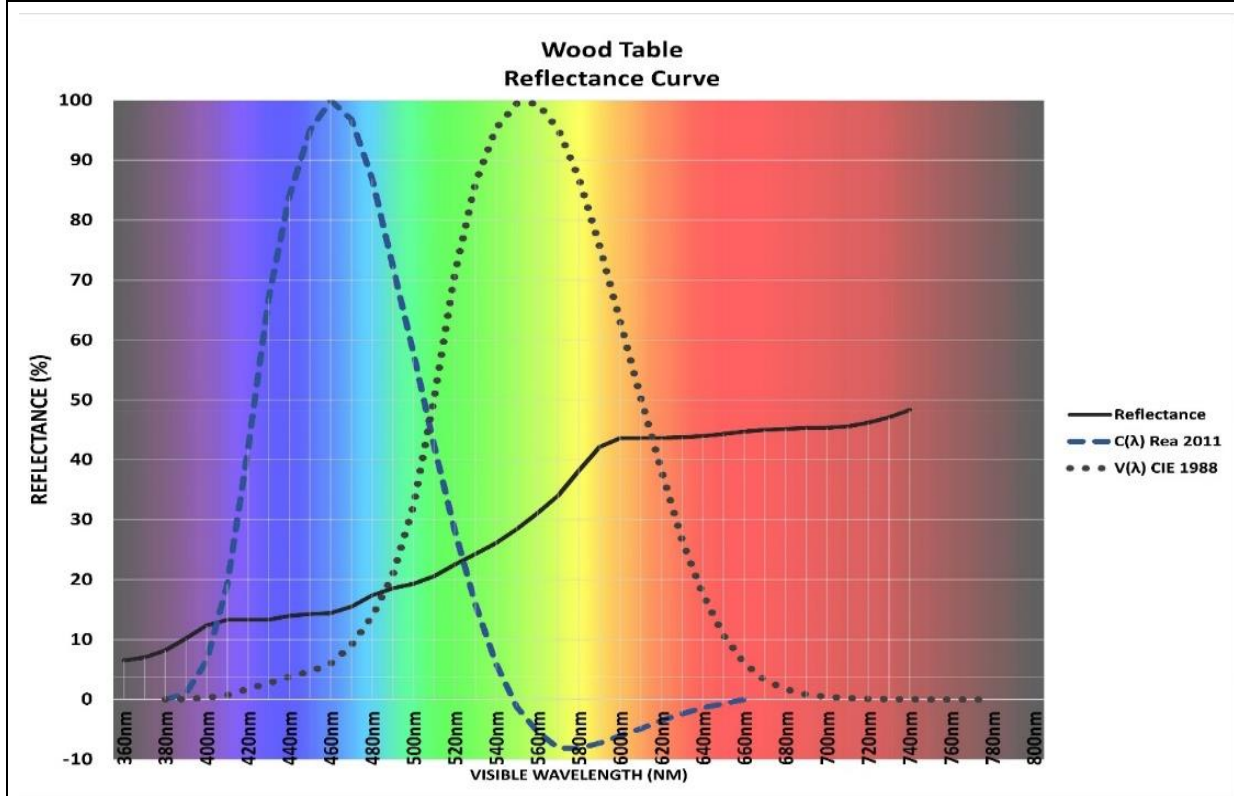

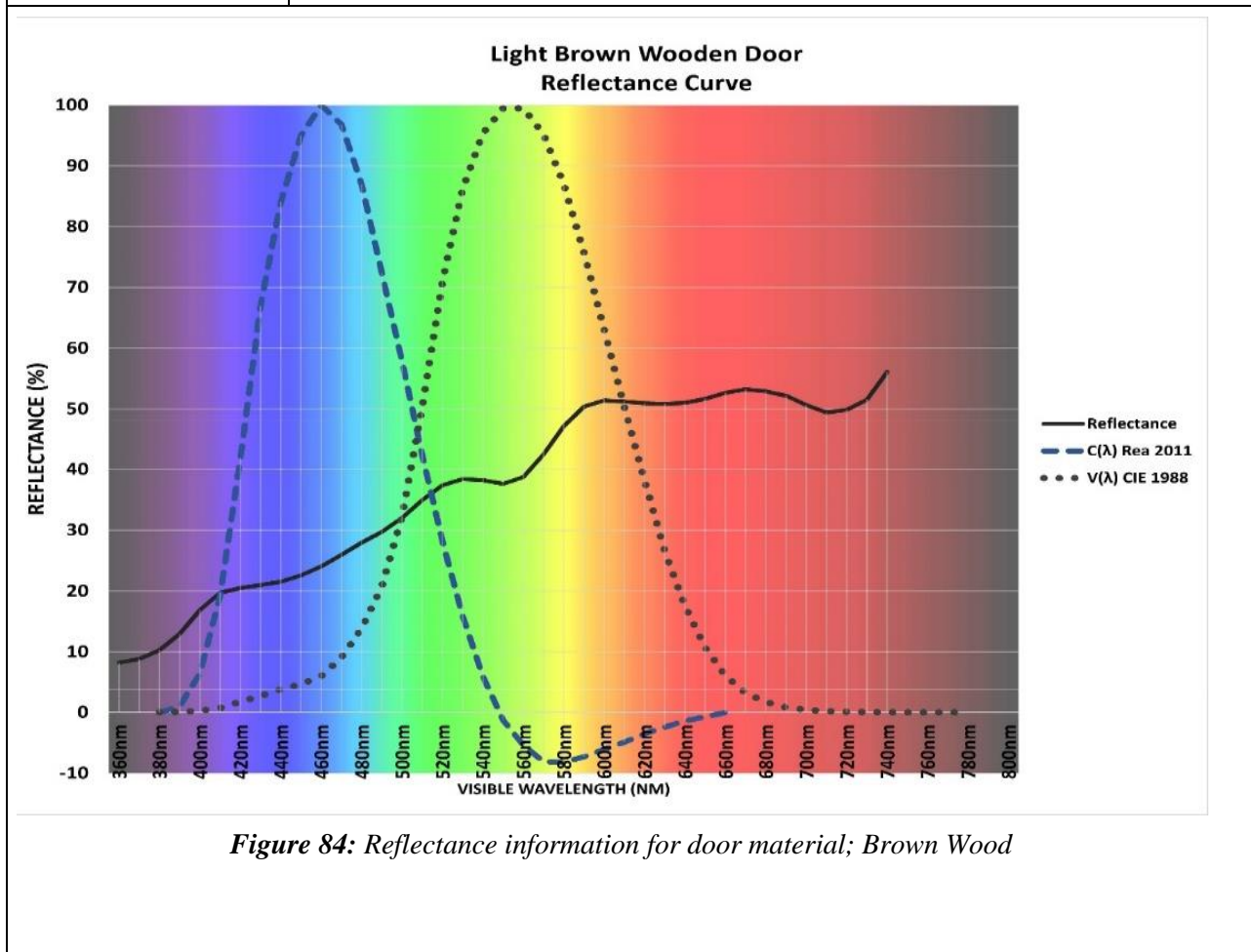

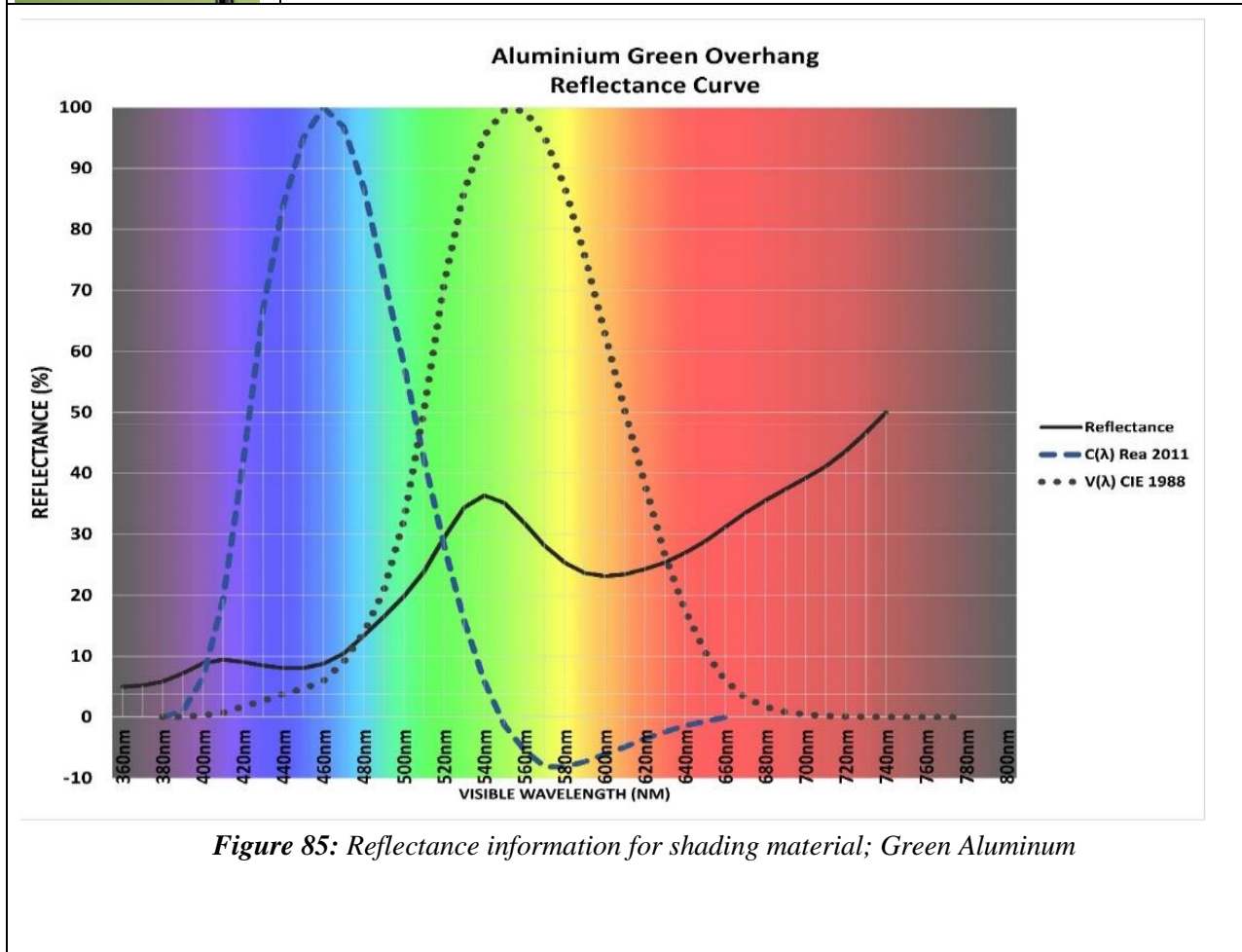


Figure 83: Reflectance information for table material; Wood

<b>Door:</b>  Brown Wood	Total Reflectance:	41.88%	Radiance Material definition					
	R <sub>Reflectance</sub>	52.35%	void plastic Light_brown_wooden_doors					
	G <sub>Reflectance</sub>	38.15%	0					
	B <sub>Reflectance</sub>	19.30%	0					
	Specularity	2.01%	5	0.5235	0.3815	0.1930	0.0201	0.0000
	Roughness	0.0%						



<b>Shading:</b>  Green Aluminum	Total Reflectance:	27.96%	Radiance Material definition					
	R <sub>Reflectance</sub>	22.78%	void plastic Aluminium_green_overhang					
	G <sub>Reflectance</sub>	29.95%	0					
	B <sub>Reflectance</sub>	4.83%	0					
	Specularity	2.10%	5	0.2278	0.2995	0.0483	0.0210	0.0000
	Roughness	0.0%						



**APPENDIX B**  
**UCLF DATA TABLES**

*Table 13: South orientation useful melatonin suppression for the whole space, and total melatonin suppression for point 1 & 3 under clear sky condition.*

South orientation- Clear sky		20-Mar			21-Jun			20-Sep			21-Dec			Average	
		10:00 AM	1:00 PM	5:00 PM	10:00 AM	1:00 PM	5:00 PM	10:00 AM	1:00 PM	5:00 PM	10:00 AM	1:00 PM	5:00 PM		
Optimized Shade	Useful melatonin Suppression	Wall direction	20.5	45.4	43.9	45.0	46.1	51.7	21.2	40.8	47.4	7.3	40.9	33.5	37.0
		Window direction	7.2	21.4	57.7	35.4	28.6	54.0	0.0	21.9	58.0	7.3	7.3	49.3	29.0
		Both directions	13.8	33.4	50.8	40.2	37.3	52.8	10.6	31.3	52.7	7.3	24.1	41.4	33.0
		Point 1	21.9	20.8	57.2	42.0	20.5	60.3	0.0	21.9	57.2	21.9	21.5	50.8	33.0
		Point 3	61.1	57.8	37.5	55.1	58.3	48.8	41.7	60.8	42.1	42.7	62.3	27.5	49.6
Low-E 39%	Useful melatonin Suppression	Wall direction	40.2	44.2	41.4	52.9	58.7	50.9	41.7	46.6	43.5	7.3	34.5	31.5	41.1
		Window direction	36.2	28.2	56.4	47.6	49.9	60.5	7.2	21.4	56.9	7.3	7.3	46.3	35.4
		Both directions	38.2	36.2	48.9	50.3	54.3	55.7	24.4	34.0	50.2	7.3	20.9	38.9	38.3
		Point 1	21.2	19.6	54.6	59.4	41.5	59.1	21.9	20.8	56.3	0.0	0.0	48.3	33.5
		Point 3	57.8	55.1	37.5	48.8	56.3	46.3	60.8	58.7	39.2	43.0	41.3	27.5	47.7
Low-E 53%	Useful melatonin Suppression	Wall direction	46.1	52.4	31.8	51.8	52.0	39.4	40.5	55.7	34.0	50.1	36.6	22.5	42.7
		Window direction	41.9	48.2	48.3	45.7	46.7	54.1	35.6	41.6	48.9	35.2	35.3	37.4	43.2
		Both directions	44.0	50.3	40.1	48.8	49.3	46.8	38.1	48.7	41.5	42.6	35.9	29.9	43.0
		Point 1	63.5	40.3	46.7	58.8	60.6	50.0	21.2	42.0	46.7	63.5	19.6	37.5	45.9
		Point 3	54.2	47.1	27.5	44.6	47.1	35.8	57.2	50.8	27.5	59.8	55.1	17.5	43.7
Low-E 65%	Useful melatonin Suppression	Wall direction	47.3	54.8	35.3	53.6	55.1	43.2	41.2	50.9	36.4	28.7	38.2	25.3	42.5
		Window direction	35.4	48.6	51.0	47.2	48.1	55.9	36.2	42.5	51.6	28.3	28.6	40.4	42.8
		Both directions	41.3	51.7	43.2	50.4	51.6	49.6	38.7	46.7	44.0	28.5	33.4	32.8	42.7
		Point 1	42.7	41.5	50.0	60.3	61.8	53.1	21.5	20.8	50.0	64.6	20.5	42.9	44.1
		Point 3	55.1	50.8	29.2	47.1	50.0	37.5	58.7	53.9	32.5	61.6	58.7	19.2	46.2
LoE 366-NO shade	Useful melatonin Suppression	Wall direction	34.0	49.8	40.0	56.7	58.2	47.2	27.7	46.1	42.2	14.3	34.3	28.5	39.9
		Window direction	36.2	42.5	54.3	48.8	49.3	58.5	7.2	21.3	54.3	21.4	7.3	44.9	37.2
		Both directions	35.1	46.2	47.2	52.8	53.8	52.8	17.4	33.7	48.3	17.9	20.8	36.7	38.5
		Point 1	21.2	20.2	54.3	62.1	41.5	56.3	21.9	21.5	54.3	21.5	0.0	46.7	35.1
		Point 3	57.8	53.9	32.5	51.7	54.8	43.8	61.1	58.3	37.5	62.8	62.9	22.5	50.0

*Table 14: South orientation useful melatonin suppression for the whole space, and total melatonin suppression for point 1 & 3 under overcast sky condition.*

South orientation- Overcast sky		20-Mar			21-Jun			20-Sep			21-Dec			Average	
		10:00 AM	1:00 PM	5:00 PM	10:00 AM	1:00 PM	5:00 PM	10:00 AM	1:00 PM	5:00 PM	10:00 AM	1:00 PM	5:00 PM		
Optimized Shade	Useful melatonin Suppression	Wall direction	43.8	47.7	30.8	48.3	50.9	39.6	44.3	47.7	29.7	33.5	38.9	2.5	38.1
		Window direction	42.3	44.7	46.2	45.2	46.4	54.5	42.8	44.7	45.4	49.3	53.3	3.1	43.1
		Both directions	43.0	46.2	38.5	46.7	48.6	47.0	43.6	46.2	37.6	41.4	46.1	2.8	40.6
		Point 1	54.6	57.2	42.9	57.8	37.9	51.4	54.6	57.5	42.9	46.7	50.0	2.5	46.3
		Point 3	37.5	40.8	24.2	42.1	44.6	32.5	37.5	42.1	22.5	24.2	32.5	2.5	31.9
Low-E 39%	Useful melatonin Suppression	Wall direction	39.6	43.8	27.5	44.0	47.7	35.6	40.4	43.8	25.8	29.2	34.6	2.5	34.5
		Window direction	54.1	56.6	42.2	42.7	44.7	51.3	55.1	42.3	41.7	45.0	49.9	2.5	44.0
		Both directions	46.8	50.2	34.9	43.4	46.2	43.4	47.7	43.0	33.8	37.1	42.3	2.5	39.3
		Point 1	50.8	54.3	38.8	54.6	57.2	47.5	51.4	54.3	37.5	42.1	46.7	2.5	44.8
		Point 3	32.5	37.5	20.8	37.5	42.1	29.2	32.5	37.5	19.2	22.5	27.5	2.5	28.4
Low-E 53%	Useful melatonin Suppression	Wall direction	30.8	35.0	20.3	36.4	39.6	29.2	33.1	35.0	18.6	21.9	26.9	2.5	27.4
		Window direction	46.6	50.6	35.0	51.6	54.2	45.0	49.3	50.9	33.5	36.9	42.5	2.5	41.5
		Both directions	38.7	42.8	27.6	44.0	46.9	37.1	41.2	42.9	26.0	29.4	34.7	2.5	34.5
		Point 1	43.8	47.5	32.5	48.3	51.4	40.4	45.4	47.5	30.8	34.2	38.8	2.5	38.6
		Point 3	24.2	27.5	14.2	27.5	32.5	22.5	24.2	27.5	12.5	14.2	19.2	2.5	20.7
Low-E 65%	Useful melatonin Suppression	Wall direction	34.6	38.9	22.5	39.6	42.4	30.8	35.0	35.8	21.4	24.2	29.7	2.5	29.8
		Window direction	50.3	53.3	37.8	54.5	48.8	46.2	50.9	52.4	36.4	40.8	45.4	2.5	43.3
		Both directions	42.4	46.1	30.1	47.0	45.6	38.5	42.9	44.1	28.9	32.5	37.6	2.5	36.5
		Point 1	46.7	50.0	34.2	51.4	53.4	42.9	47.5	48.3	32.5	37.5	42.9	2.5	40.8
		Point 3	27.5	32.5	14.2	32.5	32.5	22.5	27.5	27.5	14.2	19.2	22.5	2.5	22.9
LoE 366-NO shade	Useful melatonin Suppression	Wall direction	38.9	39.6	26.9	43.8	46.7	35.0	39.6	44.3	24.7	29.2	34.0	2.5	33.8
		Window direction	53.3	54.6	41.7	42.3	44.0	50.6	54.2	42.8	40.8	44.4	49.3	2.5	43.4
		Both directions	46.1	47.1	34.3	43.0	45.4	42.8	46.9	43.6	32.8	36.8	41.6	2.5	38.6
		Point 1	50.0	51.8	37.5	54.6	57.2	47.5	51.4	54.6	37.5	42.1	46.7	2.5	44.4
		Point 3	32.5	32.5	19.2	37.5	39.2	27.5	32.5	37.5	19.2	20.8	27.5	2.5	27.4

*Table 15: East orientation useful melatonin suppression for the whole space, and total melatonin suppression for point 1 & 3 under clear sky condition.*

East orientation- Clear sky		20-Mar			21-Jun			20-Sep			21-Dec			Average	
		10:00 AM	1:00 PM	5:00 PM	10:00 AM	1:00 PM	5:00 PM	10:00 AM	1:00 PM	5:00 PM	10:00 AM	1:00 PM	5:00 PM		
Clear Glass- No Shade	Useful melatonin Suppression	Wall direction	44.0	52.0	43.2	45.4	55.1	48.5	44.0	52.0	43.2	51.2	47.7	28.6	46.2
		Window direction	28.3	47.0	57.8	21.3	48.4	60.4	35.3	47.0	57.3	47.7	59.6	45.6	46.3
		Both directions	36.2	49.5	50.5	33.3	51.8	54.4	39.7	49.5	50.3	49.4	53.6	37.1	46.3
		Point 1	21.2	60.3	53.1	20.8	61.8	57.2	20.5	60.3	51.4	40.6	57.2	38.8	45.2
		Point 3	55.4	47.1	37.5	57.5	50.8	46.3	55.1	47.1	37.5	45.4	42.1	22.5	45.4
Optimized Shade	Useful melatonin Suppression	Wall direction	45.1	39.7	28.6	49.9	43.3	31.4	45.7	39.7	28.1	35.8	34.2	14.2	36.3
		Window direction	59.1	56.1	49.2	46.7	58.2	52.8	59.5	56.1	49.2	52.7	52.4	34.7	52.2
		Both directions	52.1	47.9	38.9	48.3	50.8	42.1	52.6	47.9	38.6	44.3	43.3	24.4	44.3
		Point 1	49.2	45.4	30.8	55.1	49.2	35.8	51.7	45.4	30.8	40.4	39.2	15.8	40.7
		Point 3	42.1	39.2	29.2	46.3	42.5	32.5	43.8	39.2	27.5	32.5	32.5	14.2	35.1
Low-E 39%	Useful melatonin Suppression	Wall direction	50.1	40.3	30.8	52.1	43.2	37.2	48.7	40.0	29.2	42.1	34.0	16.9	38.7
		Window direction	46.7	54.4	49.0	39.9	56.3	52.4	46.3	54.4	48.2	56.7	50.1	35.3	49.1
		Both directions	48.4	47.4	39.9	46.0	49.8	44.8	47.5	47.2	38.7	49.4	42.0	26.1	43.9
		Point 1	40.3	50.8	42.9	39.4	53.1	46.7	39.1	50.0	38.8	57.2	46.7	25.8	44.2
		Point 3	44.6	37.5	27.5	47.1	37.5	32.5	42.9	37.5	27.5	35.8	27.5	14.2	34.3
Low-E 53%	Useful melatonin Suppression	Wall direction	52.9	43.2	33.6	55.0	46.7	39.4	51.9	43.2	33.6	44.5	38.6	19.7	41.9
		Window direction	40.5	56.6	51.4	40.8	58.0	54.4	39.9	56.6	49.9	58.8	53.5	37.8	49.8
		Both directions	46.7	49.9	42.5	47.9	52.3	46.9	45.9	49.9	41.7	51.6	46.1	28.8	45.8
		Point 1	41.5	53.4	43.8	40.6	56.3	50.0	40.3	53.1	42.9	57.8	50.0	29.2	46.6
		Point 3	47.1	37.5	29.2	50.8	42.1	35.8	47.1	37.5	27.5	38.8	32.5	14.2	36.7
Low-E 65%	Useful melatonin Suppression	Wall direction	48.5	47.5	38.3	42.3	51.1	43.2	48.2	47.5	38.3	48.6	43.2	24.2	43.4
		Window direction	41.6	59.2	54.1	42.1	60.2	57.4	41.2	59.2	53.9	46.1	56.3	41.1	51.0
		Both directions	45.0	53.3	46.2	42.2	55.6	50.3	44.7	53.3	46.1	47.4	49.8	32.6	47.2
		Point 1	20.2	56.3	47.5	19.6	58.4	53.4	19.6	56.3	46.7	61.0	53.1	34.2	43.8
		Point 3	50.8	42.1	32.5	53.3	46.3	37.5	50.8	42.1	32.5	42.9	37.5	19.2	40.6



*Table 16: East orientation useful melatonin suppression for the whole space, and total melatonin suppression for point 1 & 3 under overcast sky condition.*

East orientation- Overcast sky			20-Mar			21-Jun			20-Sep			21-Dec			Average
			10:00 AM	1:00 PM	5:00 PM	10:00 AM	1:00 PM	5:00 PM	10:00 AM	1:00 PM	5:00 PM	10:00 AM	1:00 PM	5:00 PM	
Clear Glass- No Shade	Useful melatonin Suppression	Wall direction	41.5	45.1	30.3	46.5	47.9	38.2	42.4	45.1	27.5	30.8	36.1	2.5	36.2
		Window direction	41.6	43.3	44.9	44.8	45.8	53.7	42.0	43.3	44.9	46.6	51.8	3.6	42.2
		Both directions	41.6	44.2	37.6	45.6	46.9	45.9	42.2	44.2	36.2	38.7	43.9	3.1	39.2
		Point 1	54.6	55.5	42.9	57.5	36.7	51.4	54.6	57.2	41.3	43.8	48.3	2.5	45.5
		Point 3	32.5	37.5	22.5	37.5	40.4	29.2	34.2	37.5	19.2	22.5	27.5	2.5	28.6
Optimized Shade	Useful melatonin Suppression	Wall direction	25.8	28.6	14.2	31.4	33.6	23.1	26.9	28.6	13.1	16.9	20.8	2.5	22.1
		Window direction	45.3	49.1	32.4	50.2	52.0	41.9	46.3	49.1	30.8	35.3	40.6	2.5	39.6
		Both directions	35.6	38.8	23.3	40.8	42.8	32.5	36.6	38.8	21.9	26.1	30.7	2.5	30.9
		Point 1	29.2	32.5	15.8	34.2	37.5	27.5	30.8	32.5	15.8	19.2	22.5	2.5	25.0
		Point 3	22.5	24.2	12.5	27.5	29.2	19.2	24.2	24.2	10.8	14.2	17.5	2.5	19.0
Low-E 39%	Useful melatonin Suppression	Wall direction	30.3	33.3	18.6	35.0	37.2	25.3	30.3	33.3	18.1	20.8	25.3	2.5	25.8
		Window direction	46.4	49.8	34.4	51.0	53.6	43.3	46.6	50.7	31.9	36.7	41.7	2.5	40.7
		Both directions	38.3	41.5	26.5	43.0	45.4	34.3	38.5	42.0	25.0	28.8	33.5	2.5	33.3
		Point 1	42.9	46.7	30.8	47.5	48.3	38.8	43.8	47.5	29.2	34.2	38.8	2.5	37.6
		Point 3	22.5	24.2	12.5	27.5	27.5	17.5	22.5	24.2	12.5	14.2	17.5	2.5	18.8
Low-E 53%	Useful melatonin Suppression	Wall direction	31.8	36.1	20.8	37.6	39.3	30.3	33.3	36.1	20.3	22.5	27.5	2.5	28.2
		Window direction	48.8	52.2	36.7	53.7	55.1	46.2	49.9	52.4	35.6	40.0	44.9	2.5	43.1
		Both directions	40.3	44.1	28.8	45.7	47.2	38.2	41.6	44.3	27.9	31.3	36.2	2.5	35.7
		Point 1	46.7	48.3	34.2	50.6	51.8	42.9	47.5	48.3	32.5	34.2	41.3	2.5	40.1
		Point 3	22.5	27.5	14.2	29.2	32.5	22.5	24.2	27.5	12.5	14.2	19.2	2.5	20.7
Low-E 65%	Useful melatonin Suppression	Wall direction	36.1	40.1	25.3	42.1	43.8	33.3	37.6	40.1	22.5	25.8	30.8	2.5	31.7
		Window direction	51.8	54.6	40.6	41.6	42.8	49.2	53.0	54.8	38.6	42.8	47.2	2.5	43.3
		Both directions	43.9	47.4	32.9	41.8	43.3	41.3	45.3	47.5	30.6	34.3	39.0	2.5	37.5
		Point 1	48.3	51.8	37.5	54.6	54.9	46.7	50.6	51.8	35.8	38.8	43.8	2.5	43.1
		Point 3	27.5	32.5	15.8	32.5	35.8	24.2	27.5	32.5	14.2	19.2	22.5	2.5	23.9

*Table 17: North orientation useful melatonin suppression for the whole space, and total melatonin suppression for point 1 & 3 under clear sky condition.*

North orientation- Clear sky		20-Mar			21-Jun			20-Sep			21-Dec			Average	
		10:00 AM	1:00 PM	5:00 PM	10:00 AM	1:00 PM	5:00 PM	10:00 AM	1:00 PM	5:00 PM	10:00 AM	1:00 PM	5:00 PM		
Clear Glass- No Shade	Useful melatonin Suppression	Wall direction	51.2	53.1	51.5	53.9	55.6	41.0	51.5	53.5	52.6	46.5	49.1	30.3	49.1
		Window direction	61.4	47.5	52.7	47.5	48.4	36.1	54.2	47.5	52.8	58.8	60.2	45.6	51.0
		Both directions	56.3	50.3	52.1	50.7	52.0	38.5	52.8	50.5	52.7	52.6	54.7	37.9	50.1
		Point 1	58.8	60.3	58.1	60.6	61.8	21.9	59.1	60.3	59.6	54.3	57.2	42.1	54.5
		Point 3	48.8	48.8	44.6	50.0	53.3	59.6	48.8	50.0	46.3	42.1	46.3	24.2	46.9
Optimized Shade	Useful melatonin Suppression	Wall direction	46.9	49.4	41.7	50.6	52.3	53.4	48.3	50.0	40.8	42.2	44.3	23.6	45.3
		Window direction	58.8	60.2	54.2	60.4	46.9	47.2	59.7	60.2	54.2	55.6	57.7	39.4	54.5
		Both directions	52.8	54.8	47.9	55.5	49.6	50.3	54.0	55.1	47.5	48.9	51.0	31.5	49.9
		Point 1	55.9	56.3	50.0	57.2	59.1	60.6	56.3	56.3	50.0	50.0	53.1	32.5	53.1
		Point 3	43.8	46.3	37.5	46.3	48.8	48.8	46.3	46.3	35.8	37.5	42.1	19.2	41.5
Low-E 39%	Useful melatonin Suppression	Wall direction	38.6	42.2	39.3	42.5	43.5	42.4	40.3	42.2	41.3	33.6	37.4	18.1	38.4
		Window direction	53.7	54.9	51.3	54.9	56.3	47.6	54.1	54.9	52.4	50.4	52.3	33.1	51.3
		Both directions	46.1	48.5	45.3	48.7	49.9	45.0	47.2	48.5	46.8	42.0	44.8	25.6	44.9
		Point 1	49.2	50.0	48.3	52.5	53.1	62.6	50.0	50.0	49.2	42.9	46.7	27.5	48.5
		Point 3	34.2	37.5	32.5	37.5	39.2	50.8	35.8	37.5	32.5	29.2	32.5	14.2	34.4
Low-E 53%	Useful melatonin Suppression	Wall direction	42.9	43.8	41.8	46.0	47.5	44.0	42.9	42.9	44.3	37.9	39.2	21.9	41.3
		Window direction	55.7	57.3	53.4	57.4	58.5	48.7	56.3	56.3	54.1	52.4	54.3	35.8	53.4
		Both directions	49.3	50.5	47.6	51.7	53.0	46.3	49.6	49.6	49.2	45.2	46.8	28.9	47.3
		Point 1	52.5	53.1	51.7	54.3	55.9	64.2	52.5	51.4	52.5	46.7	50.0	32.5	51.4
		Point 3	37.5	40.8	32.5	40.8	42.1	51.7	37.5	37.5	35.8	32.5	37.5	15.8	36.8
Low-E 65%	Useful melatonin Suppression	Wall direction	46.9	47.5	45.4	50.2	51.1	38.9	46.9	48.1	45.4	41.4	43.8	24.2	44.1
		Window direction	58.0	59.2	56.3	59.8	60.9	35.2	58.6	59.3	56.3	55.6	57.3	40.3	54.7
		Both directions	52.5	53.4	50.9	55.0	56.0	37.0	52.8	53.7	50.9	48.5	50.5	32.2	49.4
		Point 1	55.9	56.3	54.2	57.2	58.4	21.2	55.9	56.3	52.5	50.0	53.1	35.8	50.6
		Point 3	42.1	44.6	37.5	46.3	46.3	55.9	43.8	46.3	37.5	37.5	40.8	19.2	41.5

*Table 18: North orientation useful melatonin suppression for the whole space, and total melatonin suppression for point 1 & 3 under Overcast sky condition.*

North orientation- Overcast sky			20-Mar			21-Jun			20-Sep			21-Dec			Average
			10:00 AM	1:00 PM	5:00 PM	10:00 AM	1:00 PM	5:00 PM	10:00 AM	1:00 PM	5:00 PM	10:00 AM	1:00 PM	5:00 PM	
Clear Glass- No Shade	Useful melatonin Suppression	Wall direction	43.8	47.7	30.8	48.3	50.3	39.6	44.0	47.7	29.7	33.5	38.9	2.5	38.1
		Window direction	49.4	44.7	46.0	44.9	46.4	54.5	42.8	44.7	45.4	48.3	52.9	3.1	43.6
		Both directions	46.6	46.2	38.4	46.6	48.3	47.0	43.4	46.2	37.6	40.9	45.9	2.8	40.8
		Point 1	54.6	57.2	42.9	57.8	37.9	51.4	54.6	57.2	42.9	46.7	50.0	2.5	46.3
		Point 3	37.5	40.8	22.5	42.1	42.9	32.5	37.5	40.8	22.5	24.2	32.5	2.5	31.5
Optimized Shade	Useful melatonin Suppression	Wall direction	38.9	42.6	25.8	43.5	45.7	34.4	38.9	43.2	24.2	28.6	33.6	2.5	33.5
		Window direction	53.4	55.9	41.7	49.9	44.1	50.9	54.1	49.0	40.3	44.7	49.3	2.5	44.6
		Both directions	46.2	49.3	33.8	46.7	44.9	42.7	46.5	46.1	32.2	36.7	41.4	2.5	39.1
		Point 1	48.3	51.4	37.5	53.4	54.6	46.7	50.0	51.8	34.2	38.8	43.8	2.5	42.7
		Point 3	32.5	37.5	19.2	37.5	40.8	29.2	32.5	37.5	19.2	22.5	27.5	2.5	28.2
Low-E 39%	Useful melatonin Suppression	Wall direction	30.3	35.0	19.7	36.4	39.6	29.2	33.1	35.0	18.6	19.7	26.9	2.5	27.2
		Window direction	46.0	50.6	34.6	51.6	54.2	45.0	48.3	50.9	33.1	36.4	42.2	2.5	41.3
		Both directions	38.1	42.8	27.2	44.0	46.9	37.1	40.7	42.9	25.8	28.1	34.6	2.5	34.2
		Point 1	41.3	47.5	30.8	48.3	51.4	40.4	43.8	47.5	30.8	30.8	38.8	2.5	37.8
		Point 3	22.5	27.5	14.2	27.5	32.5	22.5	24.2	27.5	12.5	14.2	19.2	2.5	20.6
Low-E 53%	Useful melatonin Suppression	Wall direction	35.8	38.9	22.5	39.6	42.4	30.3	35.0	38.9	21.4	26.4	29.7	2.5	30.3
		Window direction	51.5	53.0	36.9	54.2	48.6	46.2	50.6	53.3	36.1	41.7	45.4	2.5	43.3
		Both directions	43.7	45.9	29.7	46.9	45.5	38.2	42.8	46.1	28.8	34.0	37.6	2.5	36.8
		Point 1	48.3	50.0	34.2	51.4	51.8	42.9	47.5	50.0	32.5	38.8	42.9	2.5	41.1
		Point 3	27.5	32.5	14.2	32.5	32.5	22.5	27.5	32.5	14.2	19.2	22.5	2.5	23.3
Low-E 65%	Useful melatonin Suppression	Wall direction	39.6	42.4	24.2	43.8	45.4	35.0	39.6	42.4	24.7	29.7	33.5	2.5	33.6
		Window direction	54.5	48.3	41.1	42.3	43.7	50.6	54.2	48.8	40.8	46.0	49.3	2.5	43.5
		Both directions	47.0	45.3	32.6	43.0	44.6	42.8	46.9	45.6	32.8	37.8	41.4	2.5	38.5
		Point 1	51.4	53.4	35.8	54.6	54.9	46.7	51.4	53.4	37.5	42.9	46.7	2.5	44.3
		Point 3	32.5	34.2	15.8	37.5	37.5	27.5	32.5	34.2	17.5	22.5	24.2	2.5	26.5

*Table 19: West orientation useful melatonin suppression for the whole space, and total melatonin suppression for point 1 & 3 under clear sky condition.*

West orientation- Clear sky		20-Mar			21-Jun			20-Sep			21-Dec			Average	
		10:00 AM	1:00 PM	5:00 PM	10:00 AM	1:00 PM	5:00 PM	10:00 AM	1:00 PM	5:00 PM	10:00 AM	1:00 PM	5:00 PM		
Clear Glass- No Shade	Useful melatonin Suppression	Wall direction	50.6	37.8	0.0	52.0	58.7	26.6	51.3	37.9	0.0	45.4	39.8	45.1	37.1
		Window direction	53.3	35.3	0.0	47.0	42.5	7.3	46.6	28.2	0.0	57.5	35.9	60.7	34.5
		Both directions	52.0	36.5	0.0	49.5	50.6	16.9	48.9	33.1	0.0	51.5	37.8	52.9	35.8
		Point 1	58.8	20.5	0.0	60.3	41.5	0.0	59.1	20.8	0.0	54.3	21.5	49.2	32.1
		Point 3	46.3	55.1	0.0	48.8	54.8	39.6	47.1	55.1	0.0	37.5	56.3	42.1	40.2
Optimized Shade	Useful melatonin Suppression	Wall direction	33.1	44.0	27.8	36.9	44.3	51.3	34.2	46.3	26.7	25.3	47.2	29.2	37.2
		Window direction	51.9	50.8	21.1	54.3	58.4	47.3	52.4	51.5	14.1	45.6	51.5	51.8	45.9
		Both directions	42.5	47.4	24.4	45.6	51.4	49.3	43.3	48.9	20.4	35.4	49.4	40.5	41.5
		Point 1	37.5	50.0	62.5	42.9	49.2	55.9	40.4	51.7	62.5	30.8	55.6	27.5	47.2
		Point 3	34.2	39.2	21.2	35.8	42.5	48.8	34.2	40.8	21.9	24.2	40.8	29.2	34.4
Low-E 39%	Useful melatonin Suppression	Wall direction	38.6	51.9	7.2	41.5	48.9	36.8	38.9	52.4	0.0	33.6	41.1	33.1	35.3
		Window direction	53.7	45.7	7.2	54.4	45.6	28.2	54.2	45.8	0.0	49.0	46.8	53.4	40.3
		Both directions	46.1	48.8	7.2	48.0	47.2	32.5	46.5	49.1	0.0	41.3	43.9	43.2	37.8
		Point 1	50.0	59.6	64.2	50.0	57.2	21.5	50.0	59.9	20.8	42.9	62.3	37.5	48.0
		Point 3	32.5	44.6	21.9	37.5	42.1	55.1	32.5	46.3	0.0	27.5	47.1	30.8	34.8
Low-E 53%	Useful melatonin Suppression	Wall direction	42.4	53.9	7.2	43.5	52.1	38.4	42.6	54.6	0.0	36.1	43.1	35.8	37.5
		Window direction	55.1	47.1	7.3	56.6	46.7	28.6	56.1	47.3	0.0	50.9	47.8	55.4	41.6
		Both directions	48.7	50.5	7.2	50.0	49.4	33.5	49.3	50.9	0.0	43.5	45.5	45.6	39.5
		Point 1	52.5	61.4	42.0	53.1	60.3	21.9	52.5	61.8	21.2	46.7	63.5	41.3	48.2
		Point 3	37.5	47.1	21.9	37.5	46.3	56.6	37.5	47.1	0.0	29.2	50.0	32.5	36.9
Low-E 65%	Useful melatonin Suppression	Wall direction	46.3	49.2	0.0	47.5	55.6	32.3	47.5	42.6	0.0	39.9	45.4	39.7	37.2
		Window direction	57.8	48.5	0.0	59.5	48.2	21.7	58.0	48.9	0.0	54.2	41.9	57.9	41.4
		Both directions	52.0	48.9	0.0	53.5	51.9	27.0	52.8	45.7	0.0	47.0	43.7	48.8	39.3
		Point 1	54.3	63.0	21.5	56.3	62.1	0.0	55.9	41.5	21.5	50.0	42.7	43.8	42.7
		Point 3	42.1	50.8	0.0	42.1	50.8	59.0	42.1	51.7	0.0	32.5	53.1	37.5	38.5

*Table 20: West orientation useful melatonin suppression for the whole space, and total melatonin suppression for point 1 & 3 under Overcast sky condition.*

West orientation- Overcast sky		20-Mar			21-Jun			20-Sep			21-Dec			Average	
		10:00 AM	1:00 PM	5:00 PM	10:00 AM	1:00 PM	5:00 PM	10:00 AM	1:00 PM	5:00 PM	10:00 AM	1:00 PM	5:00 PM		
Clear Glass- No Shade	Useful melatonin Suppression	Wall direction	41.0	42.6	29.7	46.5	47.9	38.2	42.4	45.1	27.5	30.8	36.1	2.5	35.9
		Window direction	41.6	42.9	44.9	44.8	45.8	53.7	42.0	43.3	44.9	46.6	51.8	3.6	42.1
		Both directions	41.3	42.8	37.3	45.6	46.9	45.9	42.2	44.2	36.2	38.7	43.9	3.1	39.0
		Point 1	54.6	54.9	42.9	57.5	36.7	51.4	54.6	57.2	41.3	43.8	48.3	2.5	45.5
		Point 3	32.5	34.2	20.8	37.5	40.4	29.2	34.2	37.5	19.2	22.5	27.5	2.5	28.2
Optimized Shade	Useful melatonin Suppression	Wall direction	21.9	25.8	12.5	28.6	29.7	19.7	23.6	25.8	12.5	14.2	18.6	2.5	19.6
		Window direction	42.9	45.9	29.7	47.3	49.7	38.6	42.9	47.0	28.6	33.5	38.6	2.5	37.3
		Both directions	32.4	35.8	21.1	37.9	39.7	29.2	33.3	36.4	20.6	23.8	28.6	2.5	28.4
		Point 1	24.2	27.5	14.2	29.2	32.5	22.5	27.5	27.5	14.2	15.8	20.8	2.5	21.5
		Point 3	19.2	24.2	9.2	24.2	25.8	17.5	19.2	24.2	9.2	12.5	14.2	2.5	16.8
Low-E 39%	Useful melatonin Suppression	Wall direction	30.3	35.3	18.6	35.0	37.2	25.3	30.3	33.3	18.1	20.8	25.3	2.5	26.0
		Window direction	46.4	51.1	33.9	51.0	53.0	43.3	47.1	50.4	31.9	36.7	41.7	2.5	40.7
		Both directions	38.3	43.2	26.3	43.0	45.1	34.3	38.7	41.9	25.0	28.8	33.5	2.5	33.4
		Point 1	42.9	48.3	30.8	47.5	48.3	38.8	43.8	47.5	29.2	34.2	38.8	2.5	37.7
		Point 3	22.5	27.5	12.5	27.5	27.5	17.5	22.5	24.2	12.5	14.2	17.5	2.5	19.0
Low-E 53%	Useful melatonin Suppression	Wall direction	31.8	37.9	20.8	37.6	39.6	30.3	33.3	36.1	20.3	22.5	27.5	2.5	28.4
		Window direction	48.8	53.8	36.7	53.7	54.9	46.2	50.4	52.4	35.6	40.0	44.9	2.5	43.3
		Both directions	40.3	45.8	28.8	45.7	47.2	38.2	41.9	44.3	27.9	31.3	36.2	2.5	35.8
		Point 1	46.7	51.4	34.2	50.6	51.8	42.9	47.5	48.3	32.5	34.2	41.3	2.5	40.3
		Point 3	22.5	29.2	14.2	29.2	30.8	22.5	24.2	27.5	12.5	14.2	19.2	2.5	20.7
Low-E 65%	Useful melatonin Suppression	Wall direction	36.1	42.4	25.3	42.1	43.8	33.3	37.6	40.1	22.5	25.8	30.8	2.5	31.9
		Window direction	51.8	41.6	40.6	41.6	42.8	49.2	53.0	55.1	39.2	42.8	47.2	2.5	42.3
		Both directions	43.9	42.0	32.9	41.8	43.3	41.3	45.3	47.6	30.8	34.3	39.0	2.5	37.1
		Point 1	48.3	54.6	37.5	54.6	54.9	46.7	50.6	51.8	35.8	38.8	43.8	2.5	43.3
		Point 3	27.5	32.5	15.8	32.5	35.8	22.5	27.5	32.5	14.2	19.2	22.5	2.5	23.8